Hepatic regeneration counteracts hepatic atrophy following portal vein ligation:

Intrahepatic size regulation in surgical models of simultaneous stimuli

Dissertation

in partial fulfilment of the requirements for the degree of doctor medicinae (Dr. med.)

submitted to the Faculty Council of the School of Medicine at Friedrich Schiller University of Jena

by Weiwei Wei
born on 06.06.1983 in Hubei

Reviewers

1. Prof.Dr.Uta Dahmen, Universitätsklinikum Jena

2. Prof.Dr.Andreas Stallmach, Universitätsklinikum Jena

3. PD.Dr.Jun Li, Universitätsklinikum Hamburg-Eppendorf

Date of the public disputation: 07.11.2017

Table of contents

Abbreviations

ALPPS: Associating Liver Partition and Portal vein ligation for Staged hepatectomy

FLR: Future liver remnant

HABR: hepatic arterial buffer response

PHx: Partial hepatectomy

PVE: portal vein embolization

PVL: Portal vein ligation

Zusammenfassung

Einleitung: Die Leber ist das einzige Organ, was nach der Resektion eines Anteiles, z.B. wegen eines Lebertumors, zur Regeneration fähig ist. Bei der einzeitigen Leberresektion (PHx) wird die erkrankte Leber vollständig entfernt. Dementsprechend ist die 70%-ige Resektion im Kleintier das am häufigsten verwendete experimentelle Modell zur Untersuchung der resektionsinduzierten Leberregeneration. Ist das onkologisch erforderliche Resektionsausmaß so groß, daß die künftige Restleber zu klein für den Patienten ist, wird das zweizeitige Verfahren angewendet. Bei dem zweizeitigen Verfahren wird im ersten Schritt eine Pfortaderokklusion des tumortragenden Leberlappens durchgeführt. Die Pfortaderokklusion führt zur Atrophie des portaldeprivierten Lappens und damit zur Hypertrophie der zukünftigen Restleber. Im zweiten Schritt wird der atrophierte tumortragende Leberanteil entfernt. Häufig wird im ersten Operationsschritt zusätzlich zur Pfortaderligatur (PVL) eine atypische Resektion durchgeführt. In dieser Situation wirken zwei Stimuli gleichzeitig auf den deportalisierten Leberlappen. Es ist jedoch unbekannt, wie der deportalisierte Leberlappen auf den gleichzeitig applizierten Regenerationsreiz antwortet; wie also der Leberlappen im Falle von gegensätzlich wirkenden Stimuli seine Größe reguliert. Deshalb ist ein besseres Verständnis der regulatorischen Prozesse erforderlich, um den Prozess der Größenregulation potenziell an die Bedürfnisse der Patienten anzupassen zu können.

Ziel: Das Ziel dieser Arbeit ist die Untersuchung der intrahepatischen Größenregulation. Zwei Faktoren, die die intrahepatischen Größenregulation beeinflussen, wurden untersucht: der Effekt der interlobären Kollateralbildung zwischen portalisierter und deportalisierter Leber und die Wirkung gegensätzlicher, aber gleichzeitig applizierter Stimuli wie der PVL und der PHx, die auf die deportalisierte Leber einwirken.

Methoden und Ergebnisse: Um ein geeignetes experimentelles System zur Untersuchung dieser spezifischen wissenschaftlichen Fragen zu identifizieren, evaluierten wir die beschriebenen Tiermodelle und verschafften uns einen Überblick über die aktuellen Techniken zur Untersuchung der Leberregeneration. Zusammen mit unseren Kooperationspartnern erarbeiteten wir einen Ablauf zur Generierung und Analyse von computertomographischen Schnittbildern um das lebervenöse System und die Kollateralbildung zu visualisieren.

Um den Effekt der interlobären Kollateralbildung auf die intrahepatische Größenregulation zu untersuchen, entwickelten wir ein „Associating Liver Partition and Portal Vein Ligation for Staged Hepatectomy" (ALPPS) –Modell in der Ratte. Das chirurgische Modell besteht aus

einer erweiterten PVL und der Transektion des medianen Leberlappens vor der nachfolgenden Leberresektion. Die Resektionsflächen wurden durch die Platzierung einer mechanischen Barriere zwischen den zwei getrennten Lappen separiert, um eine Kollateralbildung zu verhindern. Wir bestätigten, dass die Verhinderung der Kollateralbildung die Hypertrophie des künftigen Restleberlappens beschleunigte, und die Atrophie des deportalisierten Leberlappens steigerte.

Um die Wirkung der gegensätzlichen, aber gleichzeitig auf die deportalisierte Leber einwirkenden Stimulus zu untersuchen, haben wir ein weiteres chirurgisches Modell etabliert. Wir kombinierten eine kleine 20%-ige PVL mit einer großen 70%-igen PHx. Trotz des fehlende portalen Zustrom verhinderte der PHx-vermittelte Regenerationsstimulus die Atrophie des deportalisierten Leberlappens durch Induktion der Hepatozytenproliferation. Der portal deprivierte Leberlappen nahm an Größe zu.

Um die Balance zwischen unterschiedlichen starken Regenerations- und Atrophiestimuli zu untersuchen, etablierten wir ein weiteres chirurgisches Modell, bestehend aus einer großen 70%-igen PVL und einer kleinen 20%-iger PHx. Der PHx-induzierte Regenerationsstimulus hemmte die Atrophie des deportalisierten Leberlappens durch Herunterregulierung der hepatischen Apoptose. Es zeigte sich ein inverser Zusammenhang der Apoptoserate mit der Stärke des Regenerationsstimulus: ein großer Resektionsreiz(70%PHx) war mit einer geringen Apoptoserate assoziiert, ein kleiner Resektionreiz(20%PHx) war mit einer höheren Apoptoserate assoziiert, jedoch niedriger als nach alleiniger PVL. In dieser Situation (kleiner Resektionsreiz und großer Atrophiereiz) trug möglicherweise die Bildung extrahepatischer porto-portaler Kollateralen aufgrund der inkompletten portalen Deprivation zur Hemmung der Apoptose und damit zu der niedrigen Apoptoserate bei.

Zusammenfassung: Die Ausbildung porto-portaler Kollateralen reduziert das Ausmaß an Atrophie nach PVL. Wir konnten erstmalig zeigen, dass die Einwirkung gegensätzlicher Stimuli auf den portal deprivierten Leberlappen (simultaner PHx und PV) gleichzeitig zur Proliferation und zur Apoptose von Hepatozyten im diesem Leberlappen führt. Leberregeneration und hepatische Hypertrophie können also trotz portaler Deprivation induziert werden. Das Ausmaß der gleichzeitig durchgeführten Resektion bestimmt die Apoptoserate und damit maßgeblich die Größe des portal deprivierten Leberlappens.

Diese Ergebnisse stellen die weitverbreitete Annahme in Frage, dass der portale Fluss eine wesentliche Rolle bei der Leberregeneration spielt. Als nächster Schritt müssen die molekularen Mechanismen der intrahepatischen Größenregulation weiter untersucht werden.

Summary

Background: The liver is the only organ that can regenerate after partial surgical removal, e.g. because of a tumor. In the one-stage procedure, major partial hepatectomy (PHx) is performed to remove the diseased liver completely. Accordingly, the rodent model of 70%PHx is the most frequently used experimental model to study resection-induced liver regeneration. Once the oncological requirement of liver mass resection is so large that the future remnant liver is too small for the patient, a two-stage procedure is performed. The two-stage procedure consists of portal vein occlusion of the tumor-bearing liver lobe as first step prior to resecting this lobe in the second step. Portal vein occlusion induces atrophy of the deportalized liver lobes and hypertrophy of the future remnant liver. Frequently, atypical resection is performed in addition to portal vein ligation (PVL) in the first stage operation. In this situation, two concurrent stimuli act on the deportalized liver lobe. However, it is not well explored how the liver governs intrahepatic size regulation, especially how the deportalized liver may respond to the concurrent stimuli. Therefore, better understanding of the underlying regulatory processes is needed to potentially modulate the size adaption process according to the need of the patient.

Aim: We put our emphasis on exploring intrahepatic size regulation. Two factors accounting for intrahepatic size regulation were investigated: the effect of inter-lobar collateral formation between portalized and deportalized liver and the effect of a simultaneous regeneration signals imposed on the deportalized liver.

Methods and results: *To identify* an adequate model for the specific scientific questions, we evaluated the existing models and gained an overview about current techniques for studying liver regeneration. We established a CT-based image acquisition and analysis work flow with our cooperation partners to visualize the hepatic venous system and the formation of collaterals.

To explore the effect of inter-lobar collateral formation on intrahepatic size regulation, we developed an "Associating Liver Partition and Portal vein ligation for Staged hepatectomy" (ALPPS) model consisting of major PVL and median lobe transection. Liver transection was secured by placing a mechanical barrier between the two divided lobes to prevent formation of collateral. We confirmed that prevention of collateral formation accelerated hypertrophy of the future remnant liver lobes and augmented atrophy of the deportalized liver lobes.

To investigate the effect of a simultaneous regeneration stimulus acting on the deportalized liver lobe, we developed a novel surgical model consisting of the combination of 20%PVL and 70%PHx. We observed that the PHx-induced regeneration signals prevented atrophy of the deportalized liver lobe by inducing hepatocyte proliferation despite the lack of portal supply. Actually the deportalized liver lobe increased in size.

To investigate the effect of the balance between regeneration stimulus and atrophy stimulus on the deportalized liver, we further evaluated the intrahepatic size regulation using a model of 70%PVL and 20%PHx. We learned that the PHx-induced regeneration stimulus inhibited atrophy of the deportalized liver lobe by down-regulation of hepatic apoptosis, which was inversely correlated to the strength of the regeneration stimulus: a major resection stimulus was associated with a low apoptotic rate; a minor resection stimulus was associated with a higher apoptotic rate, although lower than the apoptotic rate after PVL only. In case of minor PHx and major PVL, the formation of porto-portal collaterals probably contributed to the less pronounced apoptotic rate because of the incomplete portal deprivation.

Conclusions: The formation of porto-portal collaterals decreased the extent of atrophy after PVL. We demonstrated for the first time that hepatocyte proliferation and apoptosis can be induced in the same liver lobe despite portal deprivation. This observation challenges the widespread assumption of the essential role of portal flow in liver regeneration. As a next step, the underlying molecular mechanisms governing the intrahepatic size regulation need to be further explored.

Introduction

The liver plays an important role in many bodily functions spanning from protein synthesis and glucose metabolism to excretion of waste products and detoxification. The liver is the only organ with the capacity to regenerate after death of parenchymal cells or surgical loss of parenchymal mass. The earliest description of liver regeneration can be found in myths from ancient Greece--the well-known legend of "Prometheus". His liver was partly eaten by an eagle during the day and grew back over night so that Prometheus had to suffer the punishment over and over (Hesiod's Theogony, circa 700 B.C.). The liver recovery after partly loss was called "regeneration".

Liver regeneration is needed to compensate for loss of hepatocytes. Loss of hepatocytes may occur due to intoxication, viral infection, and inflammatory processes or due to hepatic surgery. Liver regeneration is playing a crucial role in restoring the number of hepatocytes lost due to such liver injuries. These injuries can directly cause cell damage by inducing dysfunction of cell membranes, interfering with gene expression and protein synthesis or inflammatory reactions.

The surgically most important loss of hepatocytes occurs upon liver resection. The commonly studied rodent model of liver resection– 70% partial hepatectomy (PHx), was firstly introduced by Higgins and Anderson in 1931 (Higgins 1931). The liver underwent compensatory hypertrophy after the removal of liver lobes. The model is still widely used nowadays. In clinical settings, liver resection is mainly performed in oncological surgery to remove primary or secondary liver tumors (Glantzounis et al. 2016, Giglio et al. 2016, Hayashi et al. 2007). After liver resection, the portal flow (per unit liver mass) increases instantly. This hyperperfusion initiates the release of various molecular signals such as cytokines (tumor necrosis factor alpha, interleukin 6) and growth factors (hepatocyte growth factor, epidermal growth factor), resulting in hepatocyte mitosis and proliferation.

Liver regeneration leads to a restoration of liver mass within weeks. In the 70%PHx model in rodents, three of the five liver lobes are surgically removed without causing damage to the remnant two lobes. The remnant liver lobes undergo hypertrophy until the original liver weight is restored. This process takes 5-7 days in small animals such as rats and mice. In humans, normal liver weight is reestablished within 8-15 days (Michalopoulos 2007).

Small and moderate liver resections are well tolerated by the healthy organ without concurrent hepatic disease. However, extended liver resection puts the patient at risk due to an

insufficient mass of the future liver remnant (FLR). The size of the FLR represents the major limitation when planning extended liver resections.

Great efforts in surgical research were placed on developing strategies to accelerate liver regeneration. The key strategy to enhance the size of the FLR is portal vein occlusion. The occlusion of a portal vein induces atrophy of the occluded liver lobe carrying the tumor, while the non-occluded liver lobe undergoes compensatory hypertrophy by liver regeneration (Dimitroulis et al. 2014, Makuuchi et al. 1990). Therefore, portal vein occlusion is widely adopted to enlarge the FLR before extended liver resection (Abdalla et al. 2002).

However, in about 20% of the cases, this strategy fails to achieve curative resection because of tumor progress or insufficient liver regeneration after portal vein occlusion (Lam et al. 2013, Abulkhir et al. 2008). Tumor progress usually occurs in the waiting period (1-3 months) prior to extended liver resection (Hoekstra et al. 2012, Hayashi et al. 2007, Mailey et al. 2009). Insufficient liver regeneration may have several reasons: **insufficient size** or **impaired tissue quality** of the FLR and **collateral formation** between the ligated and the non-ligated liver lobe (Riehle et al. 2011, Stavrou et al. 2012, Wilms et al. 2008).

Limited size of FLR is impairing liver regeneration. There are reports indicating that experimental 90%hepatectomy is mostly fatal (Asencio et al. 2014). It is also well-known that the marginal mass in orthotopic split liver transplantation causes so-called "small for size syndrome" (Dahm et al. 2005, Serenari et al. 2013). The limited size of FLR is presenting a high risk of acute liver failure after operation. It is well known that portal hyperperfusion to the FLR induces severe shear stress in the hepatic sinusoids, which causes damage to sinusoidal endothelial cells and subsequently impairs liver regeneration (Schleimer et al. 2006, Xu et al. 2006).

Impaired tissue quality subsequent to preexistent damage of the liver such as hepatic steatosis, fibrosis, cirrhosis, cholestasis, or damage due to a previous chemotherapy is increasing the risk of insufficient liver regeneration (de Graaf et al. 2009). Therefore a larger future remnant liver mass is required after liver injury compared to healthy liver tissue.

Collateral formation between deprived liver and non-deprived liver was discovered in cases with limited hypertrophy in FLR (van Lienden et al. 2013, Denys et al. 1999). During waiting period after PVL perfusion of the ligated portal veins was observed. This revealed intrahepatic collateral connections between the non-ligated left portal branches and the ligated right branches. This collateral formation was taken as one reason for this limited hypertrophy.

Additional evidence for this view was gained from the observation that an increase in FRL volume was achieved after complete secondary portal vein embolization (PVE).

Accordingly, Schnitzbauer et al. developed a novel surgical technique so called "associating liver partition and portal vein ligation for staged hepatectomy" (ALPPS) to prevent formation of porto-portal collaterals between the FLR and the liver to be resected (Schnitzbauer et al. 2012). The key procedure is liver transection followed by a major PVL of the liver to be resected. Although the procedure is unequivocally of great challenge and carries a certain surgical risk, it is efficient to accelerate liver regeneration of the FLR.

Liver size recovery is due to liver regeneration. After PHx, hypertrophy of remnant liver is due to liver regeneration. It is well known, that regeneration is due to proliferation of hepatocytes and non-parenchymal cells (Michalopoulos 2007, Michalopoulos und DeFrances 1997, Fausto et al. 2006). Once the necessary liver mass size/liver function has been restored, liver regeneration is terminated. After PVL, size increase of contralateral liver lobe and atrophy of deportalized liver lobe occurs. Evidence was also accumulated that hepatic atrophy of portally deprived liver is due to necrosis and apoptosis (Mueller et al. 2003). However, the extent of hepatic atrophy and hypertrophy cannot be reliably predicted. This also leads to an interest in the interaction of liver regeneration and hepatic atrophy.

Recently, some studies focused on **intrahepatic size regulation** in terms of liver regeneration and hepatic atrophy. The balance between hepatocyte proliferation and apoptosis in considered critical for liver homeostasis (Zhou et al. 2015). However, the investigation regarding regulatory processes is limited to the situation of PVL, and the investigations of size regulation are limited to either liver regeneration or lobular atrophy.

It has not been reported how contradictory stimuli govern intrahepatic size regulation in case of simultaneous PVL and PHx. Further research is needed to better understand the regulatory processes. Understanding is not only scientifically interesting, but also important to better modulate liver regeneration to the need of the patients.

Aims

We wanted to better understand intrahepatic liver size regulation after liver resection and portal vein ligation in this study. Therefore, we set three goals:

1. Establish an ALPPS model to explore the role of collateral formation in intrahepatic size regulation;

2. Investigate intrahepatic size regulation in case of concurrent stimuli in a novel surgical model;

3. Assess the balance of liver regeneration and hepatic atrophy governing the intrahepatic size regulation.

For each aim we proposed a hypothesis to be tested in the study.

Hypotheses

1. Transsection of hepatic parenchyma prevents collateral formation and enhances hepatic regeneration.

2. Hepatic atrophy of deportalized liver lobe after PVL can be prevented by a simultaneously applied regeneration stimulus induced by concurrent PHx.

3. Intrahepatic size regulation is governed by the balance of regeneration and atrophy stimuli in case of opposing simultaneously applied stimuli.

- If regeneration stimulus is larger than atrophy stimulus on a given lobe, a size increase of the liver lobe is induced (RS>AS results in size increase);
- If regeneration stimulus is smaller than atrophy stimulus on a given lobe, a size decrease of the liver lobe is induced (RS<AS results in size decrease).

Study design

1. To better understand liver regeneration, a literature work up spanning over the past decades was required. The current knowledge about liver regeneration in animal models was summarized. Special emphasis was put on rodent models and techniques for assessment of liver regeneration up to date. A review paper entitled "*Models and Techniques of Studying Liver Regeneration*" was generated (Wei W, et al, Eur Surg Res 2015)**.**

2. To investigate the effect of hepatic transection on collateral formation, intrahepatic vascular anatomy was visualized and a novel ALPPS model established. This model was used to assess intrahepatic size regulation. A paper entitled "*Establishment of a Rat Model: Associating Liver Partition with Portal Vein Ligation for Staged Hepatectomy*" was published (Wei W, et al, Surgery 2016).

3. To explore intrahepatic size regulation in case of concurrent PHx and PVL, the individual size regulation of each lobe in a surgical model of right PVL+70%PHx was studied. Individual liver size adaptation and the hepatic proliferation index were evaluated. In this experiment, the portal hyper perfusion was also assessed. The manuscript entitled "*Intrahepatic size regulation in a surgical model: "Liver resection induced-liver regeneration" counteracts the local atrophy following simultaneous portal vein ligation*" was published (Wei W, et al, Eur Surg Res 2016)

4. To expand investigation of intrahepatic size regulation, concurrent PHx and PVL of varying extent were combined. The effects of balance between regeneration and atrophy were elucidated by assessing liver size regulation in terms of proliferation index and apoptosis index in different models of concurrent PVL and PHx. The corresponding manuscript entitled *"The regenerative stimulus in the deportalized liver determines hepatic apoptosis to govern the extent of hepatic atrophy"* is submitted to "British Journal of Surgery" (Wei W, et al, Br J Surg. **Under review**).

Manuscripts

Manuscript I

Rodent Models and Imaging Techniques to Study Liver Regeneration

---

Weiwei Wei, Olaf Dirsch, Anna Lawson Mclean, Sara Zafarnia, Michael Schwier and

Uta Dahmen

Authorship

First author

Authors' Contribution

W.Wei and U.Dahmen contributed to conception and design;

W.Wei and U.Dahmen for analysis and interpretation;

W.Wei and A.Mclean for data and references collection;

S.Zafarnia and M.Schwier for providing and assisting the tools for imaging acquisition analysis.

W.Wei and U.Dahmen for writing the article;

O.Dirsch and U.Dahmen for critical revision of the article;

U.Dahmen and O.Dirsch for obtaining funding.

Invited Review

Rodent Models and Imaging Techniques to Study Liver Regeneration

Weiwei Wei[a]   Olaf Dirsch[b]   Anna Lawson Mclean[c]   Sara Zafarnia[d]
Michael Schwier[e]   Uta Dahmen[a]

[a]Department of General, Visceral and Vascular Surgery, and [b]Institute of Pathology, Jena University Hospital, and [c]Faculty of Medicine, Friedrich Schiller University, Jena, [d]Department of Experimental Molecular Imaging, Medical Faculty, RWTH Aachen University, Aachen, and [e]Fraunhofer Institute for Medical Image Computing MEVIS, Bremen, Germany

Key Words

Liver regeneration · Surgical model · Toxic model · Imaging techniques

Abstract

The liver has the unique capability of regeneration from various injuries. Different animal models and in vitro methods are used for studying the processes and mechanisms of liver regeneration. Animal models were established either by administration of hepatotoxic chemicals or by surgical approach. The administration of hepatotoxic chemicals results in the death of liver cells and in subsequent hepatic regeneration and tissue repair. Surgery includes partial hepatectomy and portal vein occlusion or diversion: hepatectomy leads to compensatory regeneration of the remnant liver lobe, whereas portal vein occlusion leads to atrophy of the ipsilateral lobe and to compensatory regeneration of the contralateral lobe. Adaptation of modern radiological imaging technologies to the small size of rodents made the visualization of rodent intrahepatic vascular anatomy possible. Advanced knowledge of the detailed intrahepatic 3D anatomy enabled the establishment of refined surgical techniques. The same technology allows the visualization of hepatic vascular regeneration. The development of modern histological image analysis tools improved the quantitative assessment of hepatic regeneration. Novel image analysis tools enable us to quantify reliably and reproducibly the proliferative rate of hepatocytes using whole-slide scans, thus reducing the sampling error. In this review, the refined rodent models and the newly developed imaging technology to study liver regeneration are summarized. This summary helps to integrate the current knowledge of liver regeneration and promises an enormous increase in hepatological knowledge in the near future.

© 2014 S. Karger AG, Basel

Uta Dahmen
Experimental Transplantation Surgery
Department of General, Visceral and Vascular Surgery,
Jena University Hospital
Drackendorferstrasse 1, DE–07747 Jena (Germany)
E-Mail Uta.Dahmen@med.uni-jena.de

Introduction

The liver is the only organ with the capacity to regenerate after the death of parenchymal cells or the surgical loss of parenchymal mass. The earliest description of liver regeneration can be found in the well-known legend of Prometheus – a myth from ancient Greece. The eagle ate a part of Prometheus' liver and the liver did grow back over night so that the eagle could feed from it the next day. This phenomenon is called 'regeneration'.

Regeneration is clinically important, compensating for any reduction in parenchymal tissue: on the one hand, for patients with acute liver failure due to the death of hepatocytes subsequent to intoxication or viral infection, and on the other hand, for patients with surgical loss of liver mass after tumor resection or living liver donation [1]. Regeneration is also important for patients undergoing portal vein occlusion as a strategy to enhance the future liver remnant volume prior to extended major liver resection.

Liver regeneration after different types of injuries has been studied for many years. Two different types of animal models were developed: administration of toxins and surgical manipulations.

This review is focusing on three issues: first, we want to give an overview of the existing animal models, especially the surgical models in rodents; second, we want to present the new developments in imaging technologies improving the assessment of liver regeneration, and third, we want do highlight the impact of both on system biology of the liver.

Animal Species

Species used for the investigation of liver regeneration include mice, rats, rabbits, dogs, monkeys and pigs. The ultimate choice of the species depends essentially on the scientific problems that researchers intend to solve and also relates to the anatomies and physiological specifics. The use of large animals such as pigs and monkeys is usually limited to very specific research [2, 3], such as surgical-technical issues and the radiological follow-up of volume recovery within the same animal. Surgical-technical questions are easier to address in a large animal due to the comparable size of the liver. For the same reason, imaging of large animals is of advantage compared to small rodents. However, the experimental costs and efforts are much higher including the practical work load for animal care. Availability of reagents for in vitro work is still limited. Administrative issues such as obtaining approval from the authorities are far more complicated because of the related ethical conflict, especially when primates are involved [4].

Small animals such as mice and rats are widely used because they are easy to manage. Abundant reagents are available covering all scientific topics. Furthermore, a variety of strains, especially genetically altered mouse strains, are available allowing the study of specific molecular pathways [5].

However, up to now, delicate surgical questions have not been addressed in small animals due to the lack of knowledge regarding the detailed intrahepatic vascular anatomy of the rodent liver. With the adaptation of clinical imaging technology to small animals, visualization of rodent intrahepatic anatomy became possible allowing the development of refined surgical techniques as well as assessing volume recovery and vascular regeneration.

Toxin Injury Models

Toxin injury models are induced by the administration of hepatotoxic chemicals, which cause damage to hepatocytes and result in the death of hepatic parenchymal cells. Toxin

Table 1. The most common hepatotoxic chemicals in rodent models

Chemicals	Species	Dose	Mechanism	Location of injury	Time course	Initiation of regeneration
Carbon tetrachloride	rat mouse	0.1 ml/kg BW [6, 7]	enhances free radicals and activates Kupffer cells releasing inflammatory factors	pericentral necrosis	within 24 h	within 48 h
D-Galactosamine	rat mouse	0.5–3 g/kg BW [12] 0.7–1.5 g/kg BW [11, 13, 14]	causes intracellular deficiency in uridine metabolites	random pattern	within 24h	within 48h
Acetaminophen	rat mouse	750–1,500 mg/kg BW [16, 17] 300–500 mg/kg BW [18–20]	enhances free radicals and activates Kupffer cells releasing inflammatory factors	pericentral necrosis	within 3 h peak at 18 h	within 48 h
Thioacetamide	rat mouse	200–500 mg/kg BW [24, 26, 27] 100–200 mg/kg BW [28, 29]	increases the production of toxic reactive metabolites and reactive oxygen species	pericentral necrosis	peak at 24 h	within 24 h
Ethanol	rat mouse	4–6 g/kg BW [32–37]	increases the production of reactive oxygen species and the infiltration of inflammatory cells	no necrosis	–	within 48 h after PHx

Figures in brackets are reference numbers. BW = Body weight.

models are widely used because the initiation of regeneration requires only a single administration of the toxic compound (table 1). These hepatotoxic chemicals can directly cause cell injury by damaging cell membranes, interfering with gene expression and protein synthesis or inflammatory reactions. Therefore, models of acute liver failure associated with a high mortality are induced by a relative overdose of various hepatotoxins. Underlying cellular events causing acute liver failure include centrilobular necrosis, apoptosis, inflammatory response and insufficient parenchymal cell proliferation.

Carbon tetrachloride (CCl_4) is a typical exogenous toxin that can induce acute and chronic liver injuries. CCl_4 acts on cytochrome P450 to produce markedly elevated free peroxide radicals, which causes injury or necrosis due to lipid peroxidation of the hepatocyte membranes [6–9]. Necrosis occurs predominantly in the pericentral region of the liver lobule. Regeneration in the CCl_4-induced rat model was associated with delayed DNA synthesis and mitotic activity in the rat compared to the partial hepatectomy (PHx) model as reported by Rozga et al. [10].

CCl_4 has been used extensively in the pharmacological research of drugs preventing liver damage. In contrast to the PHx model, the disadvantage of CCl_4-induced liver injury and regeneration is its complexity, since hepatocyte damage is accompanied by inflammation and immune reaction. The intense inflammatory response is thought to affect both the onset and duration of the liver regenerative response [11]. Thus, the processes of liver injury and tissue repair are closely interwoven, which makes the investigation more difficult.

D-Galactosamine is considered to cause intracellular deficiency in uridine metabolites, inducing acute liver injury [12–15]. The acute liver injury by D-galactosamine is associated with waste accumulation, systemic inflammation and impaired regeneration [16]. D-Galactosamine also induces hepatocyte apoptosis when administered in combination with lipopolysaccharide, by blocking gene translation or transcription [17]. The kinetics of liver regeneration after D-galactosamine-induced liver injury is similar to that after CCl_4-induced liver regeneration. Therefore, D-galactosamine is used more frequently for the induction of fulminant liver failure than for the investigation of liver regeneration.

Acetaminophen has also been adopted to induce acute liver injuries. After an overdose, acetaminophen is metabolized by the cytochrome P450 leading to a toxic accumulation of

N-acetyl-benzoquinone imine [18, 19]. Subsequently, it leads to the formation of free radicals and the activation of Kupffer cells, which cause centrilobular apoptosis and necrosis [8]. Proinflammatory cytokines and the innate immune system were considered to mediate the acetaminophen-induced liver injuries [20–22]. The course of regeneration after acetaminophen-induced injury is similar to that in the CCl_4 model.

Thioacetamide is a hepatotoxin conventionally used for the induction of acute and chronic liver injuries. Along the cytochrome P450-dependent pathway, thioacetamide is converted to thioacetamide sulfoxide and subsequently to thioacetamide disulfoxide, a toxic reactive metabolite [23]. These reactive metabolites remarkably increase the production of reactive oxygen species causing oxidative stress and acute centrilobular liver necrosis [23, 24]. According to the specific purpose, single or repeated administration of thioacetamide can induce acute hepatic failure and hepatic cirrhosis in the rodent model [25–28]. Liver injuries induced by thioacetamide are characterized by acute centrilobular liver necrosis and the gradual accumulation of fibroblast-like cells in the periportal area [29]. Necrosis developed and peaked at 24 h of intoxication, and a synchronous proliferative response was immediately initiated, reaching a peak of DNA synthesis at 48 h [26].

Hepatotoxic ethanol-induced liver injury has been studied extensively because alcoholic liver disease is becoming a major global health concern [30]. Ethanol damages hepatocyte mitochondrial functions and produces oxidative stress, which probably plays a critical role in hepatic injury; activation and infiltration of inflammatory cells are involved in this process as well [31, 32]. Some investigators also reported that acute exposure of ethanol was associated with increased gut permeability, which caused the normal bacterial flora and toxins to enter general and hepatic circulation [33, 34]. Liver injury induced by ethanol is characterized by steatosis, hepatitis, fibrosis and cirrhosis [35, 36]. Its severity is related to the frequency, dose and duration of ethanol consumption. Studies have shown that chronic ethanol exposure delays the induction of hepatocyte DNA synthesis in response to PHx [37, 38]. Regeneration was observed within 48 h after PHx instead of 24 h [39]. However, Ding et al. [35] reported that acute ethanol pre-exposure promotes liver regeneration in mice within 12 h after PHx by activating aldehyde dehydrogenase 2.

Anatomy

Detailed knowledge of liver lobar and vascular anatomy is essential for experimental hepatobiliary surgical manipulations. The anatomy of the mouse liver is very similar to that of the rat liver. There are only subtle differences in the proportion of each lobe in relation to the whole liver [40]. One significant characteristic of the mouse liver is that the gall bladder is located in the fossa between the left median lobe (LML) and the right median lobe (RML), connecting with the falciform ligament, whereas the rat has no gall bladder at all. With respect to texture, the mouse liver is softer and more fragile than the rat liver.

Lobar Anatomy

The rat liver mass contains four main parts: the ML (comprising 38% of the liver mass), the left lateral lobe (LLL, 30%), the right lobe (RL, 22%) and the caudate lobe (CL, 8%). The paracaval portion, which encircles the inferior vena cava, accounts for approximately 2% of the liver mass. The ML can be divided into two parts: the RML and the LML. The RL, located on the right lateral vena cava, consists of one pyramidal-shaped right inferior lobe and one round-shaped right superior lobe. The CL is divided into the superior CL/anterior CL and inferior CL/posterior CL [40–42].
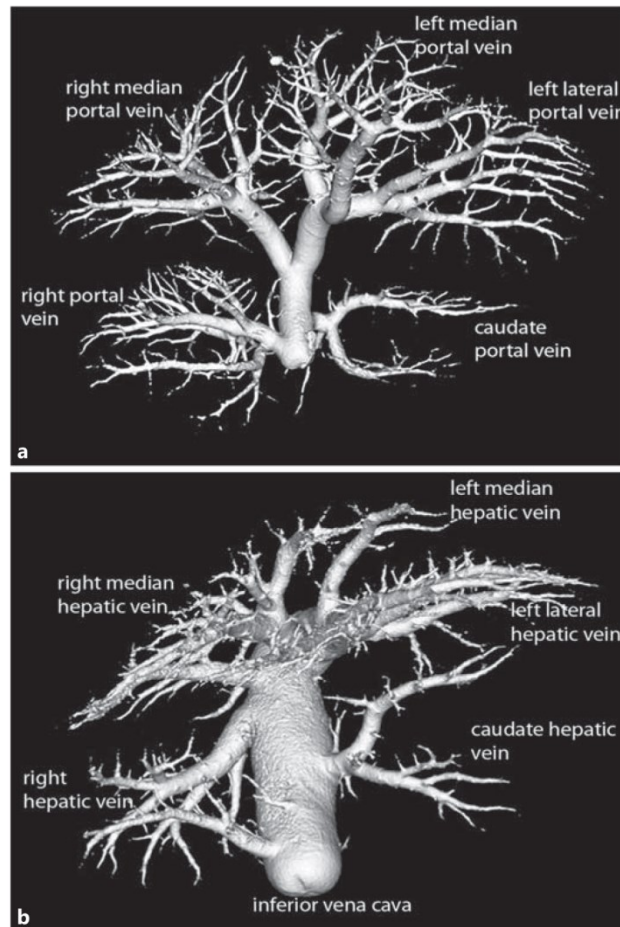
Fig. 1. The portal venous tree (**a**) and the hepatic venous tree (**b**). The right portal vein supplies a large portion of the paracaval liver; the left lateral hepatic vein disembogues into the left median hepatic vein. The hepatic venous drainage of the ML is similar to that of the human liver: right median, middle median and left median hepatic vein.

Vascular Anatomy

Each lobe of the rat liver has its own pedicle containing a portal triad [40, 42]. Each portal triad consists of a branch of the portal vein (supplying the liver with nutrient-rich blood from the intestine), a branch of the hepatic artery (supplying the liver with highly oxygenated blood) and a bile ductule (draining bile from the liver to the intestine). The blood, which comes from the portal vein and the hepatic artery, converges through the sinusoids and drains into the central venules located in the center of the liver lobule. Based on corrosion casts and on a detailed analysis of µCT scans and MRI scans of the intrahepatic vascular tree, anatomical details influencing experimental hepatobiliary surgery were revealed in our laboratory.

Portal Vein Anatomy

The left median portal vein shares a common trunk with the left lateral portal vein. The right portal vein supplies a large portion of the paracaval liver leading to a potentially compromised portal vein supply when resecting the RL (fig. 1a).

Hepatic Vein Anatomy

The left lateral hepatic vein disembogues into the left median hepatic vein leading to a potentially compromised hepatic venous drainage when resecting the LLL (30% PHx). The

hepatic venous drainage of the ML is very similar to the human liver with three veins: the right median hepatic vein, the middle median hepatic vein and the left median hepatic vein. This is of utmost importance when considering the resection of the RML or LML (fig. 1b).

Anatomies of other species are different from those of rodents. The rabbit liver is divided into 3 cranial lobes (LLL, ML and RL, total 80%) and 1 separated CL, which is clearly distinguished; the dog liver consists of 7 lobes: the LLL, LML, RML, papillary lobe and quadrate lobe are supplied by the left portal vein (70%), while the RL and CL are supplied by the right portal vein; the pig liver consists of 4 lobes: the LLL (20–25%), LML, RML and RL. The lobar volume distribution is similar to that of the human liver [5].

Surgical Models

Currently, three surgical models are commonly used to study liver regeneration: PHx models, portal branch occlusion models and portosystemic shunt models.

PHx Models

The PHx model is the most widely used surgical model and was first established by Higgins and Anderson in 1931. After the removal of nearly 70% of the liver mass, the remnant liver lobes underwent compensatory growth until reaching the original liver weight. Various surgical modifications have been introduced since then.

The extent of the liver mass reduction can be varied by selecting the liver lobes that are to be resected. There are more than 10 variations of hepatectomy according to the amount of the resected liver mass in relation to the whole liver, such as 5, 10, 20, 30, 40, 50, 60, 70, 80, 90, 95 and even 97%. 70% PHx (also called 2/3 PHx by some authors) is the most frequently used model for studying liver regeneration. The LLL and ML were removed by putting ligations around the pedicles of the respective liver lobe. The 90% PHx (resection of the LLL, ML and RL) animal model was explored for understanding fulminant hepatic failure [43, 44]. With the improvement in anatomic knowledge and surgical technique, 90% PHx became a nonlethal rodent model [41]. Furthermore, a change in the lobe resection technique has been proposed in our laboratory involving the resection of the LLL, ML, right inferior lobe and CL leaving the right superior lobe untouched [45]. Therefore, 95% PHx (resection of all liver lobes but the inferior CL) and 97% PHx (resection of all liver lobes) were subsequently considered as models for fulminant hepatic failure. Histomorphology of the insufficient remnant liver is characterized by massive fatty change, congestion, apoptosis and centrilobular necrosis, with little evidence of regeneration. Acute liver failure induced by this surgical approach is not reversible. It does not provide a therapeutic window which allows investigating and assessing a given treatment of liver failure.

The extent of additional injury to the remnant liver depends on the surgical technique. To date, 3 main principally different techniques have been reported. (1) The mass ligation technique, which is achieved by putting a ligation on the pedicle of the respective liver lobe [43, 44, 46]. Using this technique for 90% PHx carries a high risk of causing outflow obstruction or massive bleeding. (2) The vessel-oriented technique, which Kubota et al. [47] introduced in 1997. In their study, ligation of the portal vein and hepatic artery was performed prior to ligation of the respective hepatic vein with a piercing suture, and then, the individual liver lobe was resected without the risk of bleeding and compressing the inferior vena cava. However, ligation of the pedicle causes ischemia and necrosis of the stump and the paracaval liver. (3) The precise vessel-oriented, parenchyma-preserving technique, which was optimized by Madrahimov et al. [41] in 2006. A mosquito clamp instead of preliminary ligation of the portal vein and hepatic artery was placed on the pedicle of the liver lobe, positioning

piercing sutures proximal to the clamp in number and location according to the vascular anatomy of the individual liver lobe before removing the liver lobe and the clamp. When applied properly, this technique has a very low risk of outflow obstruction and ischemia of the stump or paracaval liver. The advantage of this parenchyma-preserving technique increases when increasing the resecting liver mass. Besides, the resection procedure can be performed in a precise, reproducible and safe manner. It can be controlled better than a soft suture line when defining the resection plane on the liver lobe. Consequently, maximal success and minimal hemodynamic complications can be achieved. The following suggestions help to master this technique: (1) to prevent outflow obstruction, the ligature and clamp must not be placed too close to the cava because that might cause partial outflow obstruction of the vena cava; 3 mm is a recommended distance. (2) To prevent ischemia of the stump, especially of the RLs, the suture must be placed in close proximity to the clamp. (3) To prevent hemorrhages of the remnant stumps, some overlap between all piercing sutures should be accomplished. In the mouse model, we suggest a cholecystectomy before the resection of the ML.

Kinetics of Regeneration after PHx

It is generally accepted that the initiation of liver regeneration after PHx can be precisely timed – it starts within few minutes after resection. Hepatocytes in the periportal region begin to proliferate after 14–16 h in the rat model [40, 48], while those in the pericentral region begin to proliferate 36–48 h after PHx [49]. The DNA synthesis reaches its peak at 24 h in rats, but in mice, both the start and the peak of DNA replication are about 20 h later [46, 48]. The sinusoidal endothelial cells enter the S-phase of the cell cycle even later, after the hepatocytes [49]. Once the necessary functional mass has been restored, liver cell proliferation is terminated. The process of liver regeneration upon PHx has been exhaustively analyzed. However, the PHx model on a healthy liver cannot mimic the pathological situations in human liver diseases, which involve chronic viral hepatitis, alcoholic liver disease and nonalcoholic fatty liver disease. Therefore, in the modes of steatotic liver and hepatitis, regeneration after PHx has recently drawn increasing attention. There is substantial evidence that the proliferative response after PHx is significantly delayed and reduced in rats and mice with hepatic steatosis and chronic viral hepatitis [50–54]. Although the underlying mechanism remains uncertain, impaired liver regeneration was believed to be associated with mitochondrial dysfunction and interruption of signaling pathways [53, 55, 56].

Portal Branch Occlusion Models

Occlusion of the portal branch can be achieved by ligation and embolization. Portal vein embolization is a radiological procedure, which is mainly done in large animals [57, 58]. Ligation requires open surgery and is frequently performed in rodents. The effect of portal vein occlusion is well known. The ligation of a portal branch induces atrophy of the portally ligated liver lobe(s), while the portally supplied liver lobes undergo compensatory growth [59–61]. This finding is of great clinical relevance and was translated into a surgical therapeutic concept: portal vein occlusion as a strategy to enlarge the future liver remnant prior to extended liver resection.

The extent of liver mass reduction can vary by selecting the lobar portal vein branches to be ligated. In 1920, Rous and Larimore [62] demonstrated that the extent of atrophy of the portally ligated liver lobe was related to the size of the ligated lobe. Portal branch ligation (PBL) is usually performed on right portal branches (1/4 PBL), the left portal branch (1/3 PBL) and the left portal branch + median portal branches (2/3 PBL) in rats.

The extent of additional injury to the liver depends on the surgical technique and the extent of the portally ligated liver lobe. The injury to the liver may increase in case of rough dissection before ligation which may probably cause subtle damage to the branches of the

hepatic artery and bile duct. The PBL model became highly reproducible after re-evaluation in 1986 by Rozga et al. [63]. They optimized the operative technique by proposing the use of an operating microscope to minimize the surgical trauma. With this technique, the rat model showed a highly reproducible extent of atrophy in the portally deprived lobe(s) and of compensatory hyperplasia in nonligated lobes. However, necrosis formation within the portally ligated lobe occurs when the lobe size increases.

Kinetics of Regeneration after PBL

As compared to the PHx model, the PBL model incorporates two opposite processes in one animal: atrophy in the ligated lobe(s) and hypertrophy in the nonligated lobes. The early stage of reduction in the portally deprived lobe(s) mainly relates to necrosis and apoptosis of parenchymal hepatic cells. Previous studies have explored the kinetics of the liver weight of the deprived lobe(s) and of necrosis in the corresponding lobe(s) [60, 61, 63]. In 70% PBL, the weight of ligated lobe(s) decreased within a few hours after PBL when necrosis was hardly observed. Little necrosis covering up to 5% and apoptosis were observed in ligated lobe(s) 24 h after PBL when the weight had decreased to about 70% of its initial value. At 48 h, only 50% of the original liver volume and a maximum of 24% necrosis could be found. After 3 days, resorption of necrosis started and was almost completed within the next day. The reduction in liver cell volume, the contraction of the vascular system and the collapse of the bile ducts may play a major role in the later phase of atrophy, and the ligated lobe(s) shrink to nearly 15% of their original size within 2 weeks. Currently, there is a controversy concerning the intensity of the proliferative response in nonligated lobes. In the study of Weinbren and Tarsh [64], regeneration after PBL was considered to be initiated in the same time frame as after PHx. The proliferating cell nuclear antigen (PCNA) protein level was significantly elevated in nonligated lobes 1–3 days after PBL [2, 60, 63]. We have similar results for the 70% PBL model, but interestingly, we observed delayed and subtle regeneration after 20% PBL in rats with a maximal bromine-deoxyuridine (BrdU) labeling rate of 2% on postoperative day 3.

The relative total liver weight in the PBL groups is maintained throughout the whole remodeling phase despite the ongoing atrophy in the ligated lobe and the ongoing proliferation in the nonligated lobes. There is no good explanation of the mechanism leading to the balance between the two contradictory progresses. Further research is necessary to identify the underlying processes.

A combined model of right PBL and 70% PHx (rPBL + 70% PHx) has been established in our group. The prominent novelty of this model is the induction of concurrent contradictory stimuli on the portally deprived RL – atrophy and regeneration. The regulatory response of the RL is interesting: the portally deprived RL increases its size slightly, but significantly, by a moderate regenerative response. In contrast, the nonligated CL increases to around 4.5-fold of its original size within 7 days (unpublished data). This finding is of considerable scientific and potential therapeutic relevance and may motivate further hypothesis-driven research in the field of liver regeneration and regulation of intrahepatic size.

Portosystemic Shunt Models

The portosystemic shunt model was first introduced by Nicholas Eck in 1877. In his work, completely diverting portocaval anastomosis was performed in dogs, which became known as the 'Eck fistula'. He proposed that this surgical technique was potentially suitable to treat portal hypertension-related 'mechanical ascites' in human beings. Subsequently, numerous portocaval shunt models have been developed in dogs, pigs, rabbits and rats [65–69]. Various surgical strategies have been refined and employed to study portosystemic shunt models since the last century, for instance, side-to-side shunts and end-to-side shunts [67, 70–72].

A portosystemic shunt causes deprivation of the portal flow and impairment of the liver. The main feature is the alteration of liver morphology, including hepatocyte atrophy, fatty infiltration, deglycogenation, and others [69]. These alterations are considered to be caused by the diversion of the hepatotrophic substances in portal venous blood.

Portosystemic shunt models are especially suitable for studying the hepatotrophic effect of the portal vein blood supply. However, the surgical technique of these shunts, in particular vascular anastomosis, is technically challenging.

An interesting animal model to study the effects of portosystemic shunts on liver regeneration is the congenital portosystemic shunt dog [65]. The congenital portosystemic shunt dog presents with liver hypoplasia associated with hepatic insufficiency. Liver regeneration can be induced to enlarge the liver size when the congenital shunting vessel is closed. This model can be used to study liver regeneration by closing or reducing the shunt.

Assessment Techniques

The assessment of liver regeneration and its kinetics has been limited to observations obtained at defined time points in different animals. By harvesting the liver of individual animals, the liver lobe can be weighed, measured and subjected to histological examination for the evaluation of liver regeneration in terms of weight and volume recovery and proliferation index.

Liver Weight Recovery

Certainly, we can weigh the excised liver and acquire all weight data representing the kinetics of liver regeneration at defined time points by killing the subjects. It is widely accepted that the weight of the remnant liver at 24 and 72 h reaches 45 and 70% of the original liver weight, respectively, after a 70% PHx in the rat [40], and approximately 90% on day 7. Investigators also assess the liver weight recovery based on the liver lobe to body weight ratio using the formula: liver weight recovery (%) = weight of individual liver lobes/body weight · 100 (%), which indicates the hypertrophy or atrophy of different liver lobes [46, 73, 74]. Liver weight is widely adopted for the assessment of liver regeneration because it is an easy method, but it cannot indicate the proliferation kinetics of hepatocytes.

Liver Volume Recovery

The liver volume can be assessed using physical principles. The liver has to be immersed in water, and the volume of water which is replaced by the organ has to be determined. However, the accuracy and precision of such an approach is limited.

With the development of μCT and MRI technology, radiological imaging can be used to assess liver volume recovery and vascular regeneration. However, small animal imaging facilities are still rare and may influence the decision about the choice of technology. When using the μCT, the desired resolution and required X-ray dose have to be outweighed, especially when considering repeated in vivo scans. Using the MRI technology eliminates the radiation dose problem, but it also has the lowest availability within the imaging devices.

Simple volume determination requires imaging of the native or contrasted liver and can be performed ex vivo on explanted livers and in vivo in the living animal. In vivo imaging allows longitudinal studies of hepatic growth. Liver volume recovery can be assessed repeatedly in the same animal over time. Besides saving the animals, it also reduces inter-animal variation.

The calculation of the volume is based on manual or automated segmentation of the liver on all images. Previous investigators have described their studies on liver regeneration using

a rodent model with 70% PHx. Contiguous slices at individual time points showed that the liver volume recovered up to 93% between 7 and 14 days [40, 75]. Recently, Szijarto and colleagues [76] have studied hepatic volumetric recovery in an 80% PVL rat model using the nanoscan PET/MRI technique. In their study, the rats' livers maintained their liver volume by a balance of atrophy in ligated lobes and hypertrophy in nonligated lobes throughout the entire experiment.

Another technique for the assessment of liver volume recovery is by calculating the territories of either the portal venous or the hepatic venous tree. This technology has been introduced into clinical practice and even allows the calculation of territories at risk of outflow obstruction [1, 77]. Today, this technology is also applicable in small animal CT scans of sufficient quality. However, it requires some experience to reach the required level of resolution of the vascular tree to allow these calculations. Visualization of the vascular tree obviously requires the use of a contrast agent. The selection of contrast agents is an important issue. Currently, several different contrast agents are available on the market and are based on different formulations. Contrast agents for in vivo CT imaging include Iomeron (iomeprol), AuroVist and ExiTron, which are used for the identification of suitable in vivo vascular imaging applications [78]. AuroVist might be the best suited for anatomical investigations of the vascular network. Iomeprol is used to enhance attenuation differences between normal and pathological tissues; its high extravasation level can be adopted for perfusion analysis. ExiTron is advised to be used in longitudinal monitoring with repeated injections, and Primovist (Gd-EOB-DTPA) is a new hepatocyte-specific contrast agent for MRI of the liver. Compared to extracellular contrast agents, Primovist shows a partial specific uptake by hepatocytes followed by a subsequent biliary excretion [79, 80].

High-quality imaging requires a bit of experience because the circulation time of the contrast agent is different than that in the clinical situation due to the much higher heart rate of small animals. This technology has the potential to assess vascular regeneration and volume recovery with respect to intrahepatic vascular geometry, potentially providing an explanation for the sometimes observed inhomogeneously distributed proliferative response. However, the application of contrast media may lead to severe, even lethal, cardiovascular side effects. Hepatic elimination time may hamper repeated imaging if scheduled in time intervals below 24 h [78].

For ex vivo imaging, polymers such as Microfil and Batson kit 17 are used. Injection of polymers requires reaching the optimal viscosity of the material, which is related to the mixture of components and the time point after preparation. However, if technical problems can be overcome, the results are very convincing. Figure 2 shows the explanted liver after 90% PHx (resection of the LLL, ML and RL) and the 3D reconstruction of the portal venous tree based on portal Microfil injection 0 h and 2 weeks after the operation (unpublished data). The 3D reconstruction of the vascular tree can be based on a defined threshold (Imalytics Preclinical, Philips Research, Aachen, Germany), as used in figure 1. It can also be done based on a semi-automatic liver and vessel segmentation using a dedicated software program from Fraunhofer MEVIS, Bremen, Germany. Using a series of processes, the volume calculation of the dependent hepatic territory can be achieved [81]. The crucial steps performed are: liver segmentation, vessel segmentation and an analysis of vessel structure. Based on those previous steps, a model-based approximation of hepatic territories is performed. The result of the image processing and analysis steps is a 3D reconstruction of the vasculature as well as of the hepatic territories. Based on this reconstruction, the volume for the individual territories is determined. A 3D visualization of the vasculature and the hepatic territories is available as well. Volume calculation revealed a 4.4-fold volume difference from 1.978 ml immediately after resection to 8.725 ml 14 days after resection. Vascular regeneration becomes clearly visible and demonstrated that the paracaval liver contributed significantly
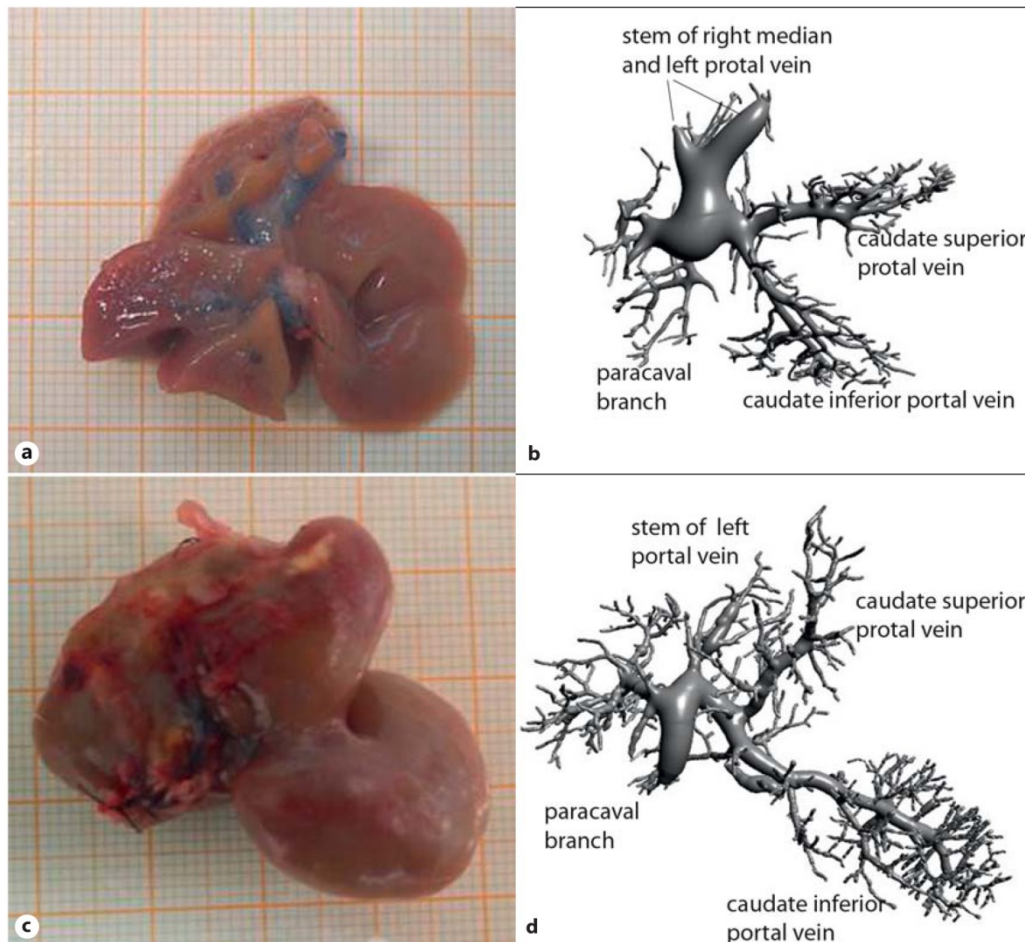
Fig. 2. Macroscopic appearance of a remnant liver after 90% PHx on day 0 (**a**) and on day 14 (**c**). 3D reconstruction of a hepatic portal vein from a Microfil CT scan after 90% PHx on day 0 (**b**) and on day 14 (**d**).

to volume recovery after a 90% liver resection. This finding supports the fact that the vessel-oriented resection technique with ligation of the portal triad of the RL prior to resection leads to the observed necrosis of the paracaval liver and reduces the regenerative potential of the remnant liver.

Proliferation Rate

The first histological parameter used to quantify liver regeneration was the mitotic index. The mitotic index was determined by calculating the proportion of the mitotic figures on at least 5 random high-power fields (×400) of the hematoxylin and eosin-stained section, expressed as the rate of cells undergoing mitosis in percentage.

Today, the identification of proliferating cells is facilitated by the visualization of nucleoside analogues incorporated into the newly synthesized DNA such as tritiated thymidine or BrdU. Tritiated (radioactive) thymidine can be similarly incorporated into the synthesized DNA. Afterwards, the radioactivity of the proliferating cell can be measured by autoradiography or scintillation. BrdU is a synthetic nucleoside and an analogue of thymidine. It can be
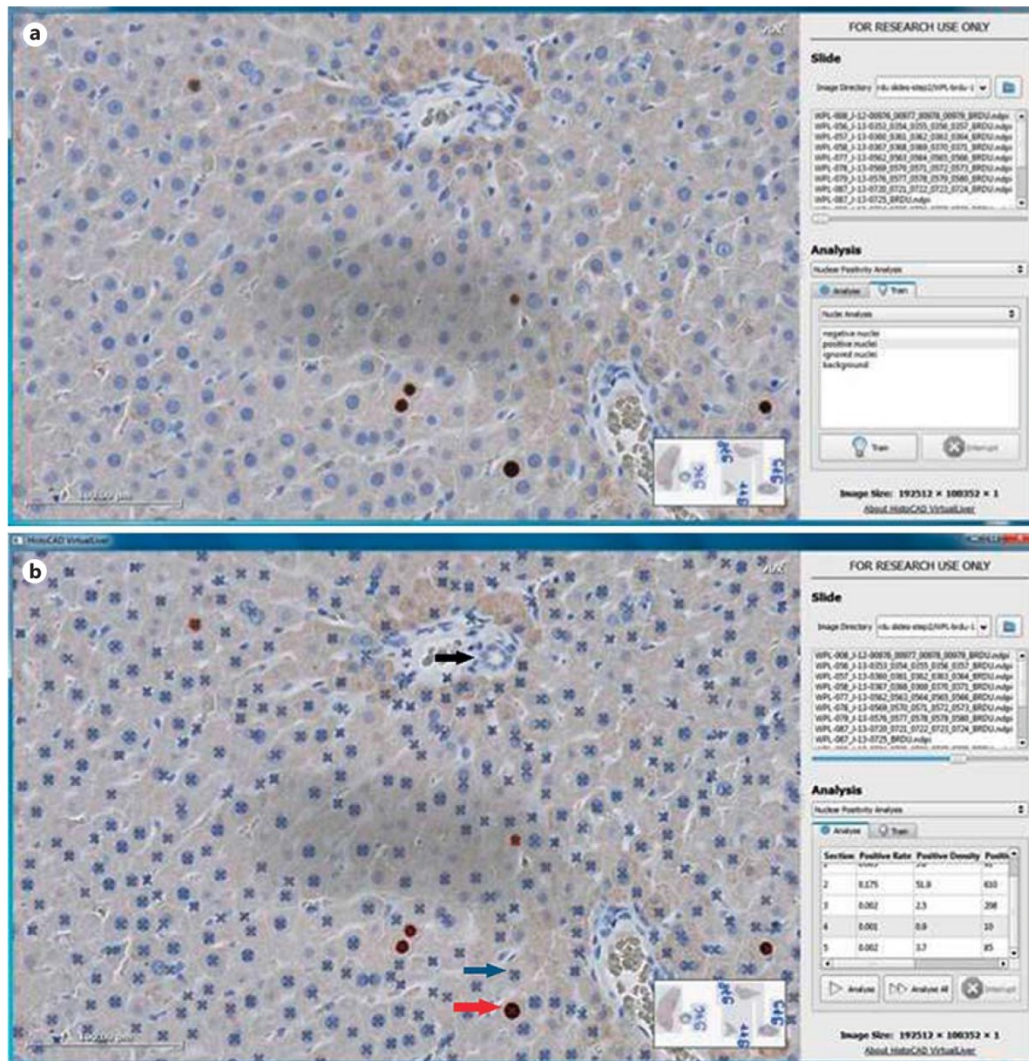
Fig. 3. The menu of the 'HistoCAD VirtualLiver' program. **a** Training procedure. **b** Analysis procedure. After the training procedure, BrdU-negative hepatocyte nuclei (with a blue cross indicated by the blue arrow) and BrdU-positive hepatocyte nuclei (with a red cross indicated by the red arrow) in the whole slide are identified, while the red blood cells and epithelial cells of bile duct are classified as nuclei to be 'ignored' (without a cross indicated by the black arrow).

incorporated into the newly synthesized DNA, substituting thymidine during DNA replication [82, 83].

Proliferating cells can also be identified by immunohistochemical visualization of cell cycle-associated proteins such as Ki-67 or PCNA. Antigen Ki-67 is a nuclear protein that is strictly associated with cellular proliferation [84]. The expression of Ki-67 protein is present during all active phases of the cell cycle. Therefore, it is an excellent marker to determine the growth fraction of hepatocytes. PCNA was originally identified as an antigen that is expressed in the nuclei of cells during the DNA synthesis phase of the cell cycle and played an important role in initiating cell proliferation.

The proliferation index can be assessed according to the quantitative analysis of positively staining hepatocytes. In the past, this was a very tedious approach, since cells were counted manually. The development of image analysis facilitated the process [85] but could not alleviate the sample size problem. Currently, whole-slide scanners are developed which allow the digitalization of several tissue sections on one slice. Accordingly, a novel technique was adapted to analyze whole-slide scans. The software 'HistoCAD VirtualLiver' (Fraunhofer MEVIS) is an accurate and highly efficient tool to perform quantitative analysis of histological sections [86, 87]. One application was developed specifically to quantify nuclear staining as needed for the analysis of the proliferation index. This tool enabled to reduce the sampling error since large tissue samples with more than 30,000 hepatocytes can be analyzed. By means of a simple 'training' process, including picking a few representative samples from morphological structures (e.g., color, roundness and size features), it can automatically identify unstained (negative) hepatocyte nuclei, stained (positive) hepatocyte nuclei and other nonhepatocyte nuclei (fig. 3). This application allows the quantitative analysis of batches of sections via a highly efficient and accurate classification of differentially stained cell nuclei.

Systems Biology

Systems biology is an emerging approach applied to study the hepatic biology as a whole [88]. Particularly in the past few years, systems biology was used to understand the fundamental biology associated with drug-induced liver injury, in which hepatic regeneration was inclusive.

The purpose is best expressed in the following citation from Sauer et al. [89]: 'The reductionist approach has successfully identified most of the components and many of the interactions but, unfortunately, offers no convincing concepts or methods to understand how system properties emerge (...) the pluralism of causes and effects in biological networks are better addressed by observing, through quantitative measures, multiple components simultaneously and by rigorous data integration with mathematical models.'

This approach is applied worldwide to study the hepatic biology, in particular, the fundamental biology of liver toxicity in drug-induced liver injury models. Various measurement and visualization technologies are employed in the systems biology approach. The global biological information and the interaction information of the drug-induced liver injury models were quantified and integrated, and the dynamical changes in the drug-induced liver injury models were recorded as well. After a complex computation, the hepatic biology could be modeled through computational and modeling tools. This model can be used for the understanding and prediction of detailed processes during liver injury and liver regeneration [88].

The Virtual Liver Network represents a major research investment by the German Government focusing on work at the 'bleeding edge' of systems biology and systems medicine. This major multidisciplinary research program is dedicated to developing a whole-organ model of the human liver, representing its central physiological functions under normal and pathological conditions. Numerous models of the geometry of the hepatic vascular tree [90], of liver regeneration [91], liver perfusion [92] and liver metabolism have already been developed during the ongoing integrative process. The development of these models is highly dependent on the availability of imaging data on all scales: CT images for the organ scale, whole-slide scans for the lobular level and confocal imaging for the sublobular level. An integrated model allowing the prediction and validation of cell alignment along microvessels as order principle to restore tissue architecture in liver regeneration after CCl_4 intoxication is already available [93]. This model is currently being extended to incorporate the regenerative process after liver resection [94, 95]. The final aim is a model that is composed of a larger battery of interconnected submodels representing liver anatomy and physiology, integrating processes across hierarchical levels in space, time and structural organization.

KARGER

Conclusion

The liver has the amazing capability of regeneration after injury and hepatectomy. Liver regeneration is both a clinically important process and a scientifically great model to study regenerative growth.

Rodent models are well suited to investigate the multifaceted process of liver regeneration. The selection of the resection technique has to be adapted to the experimental purpose. We recommend the precise vessel-oriented parenchyma-preserving technique when exploring regeneration after extended 90% PHx.

Modern radiological imaging technologies enabled the visualization of rodent hepatic vascular anatomy as a prerequisite for the development of delicate surgical resection techniques. Histological image analysis tools applicable in whole-slide scans enabled to reduce the sampling error since large tissue samples can be analyzed.

The system biology approach as applied in the BMBF (German Federal Ministry of Education and Research)-funded Virtual Liver Network aims to integrate data from different sources into one scale spanning model. The combination of these novel technologies promises an enormous increase in knowledge in the near future.

References

1 Donati M, Stavrou GA, Oldhafer KJ: Current position of ALPPS in the surgical landscape of CRLM treatment proposals. World J Gastroenterol 2013;19:6548–6554.
2 Gaglio PJ, Liu H, Dash S, Cheng S, Dunne B, Ratterree M, Baskin G, Blanchard J, Bohm R Jr, Theise ND, LaBrecque D: Liver regeneration investigated in a non-human primate model *(Macaca mulatta)*. J Hepatol 2002;37:625–632.
3 Krupski G, Broring DC, Wittkugel O, Muller L, Nicolas V, Rogiers X, Adam G, Bucheler E: Formation of portal venous collaterals after ligation of the portal vein for induction of liver regeneration. Rofo 2002;174:1281–1284.
4 Mortensen KE, Revhaug A: Liver regeneration in surgical animal models – a historical perspective and clinical implications. Eur Surg Res 2011;46:1–18.
5 Huisman F, van Lienden KP, Damude S, Hoekstra LT, van Gulik TM: A review of animal models for portal vein embolization. J Surg Res 2014;191:179–188.
6 Khan RA, Khan MR, Sahreen S: CCl$_4$-induced hepatotoxicity: protective effect of rutin on p53, CYP2E1 and the antioxidative status in rat. BMC Complement Altern Med 2012;12:178.
7 Palmes D, Spiegel HU: Animal models of liver regeneration. Biomaterials 2004;25:1601–1611.
8 Bruccoleri A, Gallucci R, Germolec DR, Blackshear P, Simeonova P, Thurman RG, Luster MI: Induction of early-immediate genes by tumor necrosis factor alpha contribute to liver repair following chemical-induced hepatotoxicity. Hepatology 1997;25:133–141.
9 Liu KX, Kato Y, Yamazaki M, Higuchi O, Nakamura T, Sugiyama Y: Decrease in the hepatic clearance of hepatocyte growth factor in carbon tetrachloride-intoxicated rats. Hepatology 1993;17:651–660.
10 Rozga J, Foss A, Alumets J, Ahren B, Jeppsson B, Bengmark S: Liver cirrhosis in rats: regeneration and assessment of the role of phenobarbital. J Surg Res 1991;51:329–335.
11 Michalopoulos GK: Liver regeneration. J Cell Physiol 2007;213:286–300.
12 Rahman TM, Hodgson HJ: Animal models of acute hepatic failure. Int J Exp Pathol 2000;81:145–157.
13 Keppler D, Lesch R, Reutter W, Decker K: Experimental hepatitis induced by D-galactosamine. Exp Mol Pathol 1968;9:279–290.
14 Baumgartner D, LaPlante-O'Neill PM, Sutherland DE, Najarian JS: Effects of intrasplenic injection of hepatocytes, hepatocyte fragments and hepatocyte culture supernatants on D-galactosamine-induced liver failure in rats. Eur Surg Res 1983;15:129–135.
15 Koniaris LG, Zimmers-Koniaris T, Hsiao EC, Chavin K, Sitzmann JV, Farber JM: Cytokine-responsive gene-2/IFN-inducible protein-10 expression in multiple models of liver and bile duct injury suggests a role in tissue regeneration. J Immunol 2001;167:399–406.
16 Mao SA, Glorioso JM, Nyberg SL: Liver regeneration. Transl Res 2014;163:352–362.
17 Matsuda H, Ninomiya K, Morikawa T, Yoshikawa M: Inhibitory effect and action mechanism of sesquiterpenes from Zedoariae Rhizoma on D-galactosamine/lipopolysaccharide-induced liver injury. Bioorg Med Chem Lett 1998;8:339–344.

Wei et al.: Rodent Models and Imaging Techniques to Study Liver Regeneration

18   Zieve L, Anderson WR, Dozeman R, Draves K, Lyftogt C: Acetaminophen liver injury: sequential changes in two biochemical indices of regeneration and their relationship to histologic alterations. J Lab Clin Med 1985;105: 619–624.

19   Leonard TB, Morgan DG, Dent JG: Ranitidine-acetaminophen interaction: effects on acetaminophen-induced hepatotoxicity in Fischer 344 rats. Hepatology 1985;5:480–487.

20   Fisher JE, McKenzie TJ, Lillegard JB, Yu Y, Juskewitch JE, Nedredal GI, Brunn GJ, Yi ES, Malhi H, Smyrk TC, Nyberg SL: Role of Kupffer cells and Toll-like receptor 4 in acetaminophen-induced acute liver failure. J Surg Res 2013;180:147–155.

21   Shah N, Montes de Oca M, Jover-Cobos M, Tanamoto K, Muroi M, Sugiyama K, Davies NA, Mookerjee RP, Dhar DK, Jalan R: Role of Toll-like receptor 4 in mediating multiorgan dysfunction in mice with acetaminophen induced acute liver failure. Liver Transpl 2013;19:751–761.

22   Gardner CR, Laskin JD, Dambach DM, Sacco M, Durham SK, Bruno MK, Cohen SD, Gordon MK, Gerecke DR, Zhou P, Laskin DL: Reduced hepatotoxicity of acetaminophen in mice lacking inducible nitric oxide synthase: potential role of tumor necrosis factor-alpha and interleukin-10. Toxicol Appl Pharmacol 2002;184:27–36.

23   Koen YM, Sarma D, Hajovsky H, Galeva NA, Williams TD, Staudinger JL, Hanzlik RP: Protein targets of thioacetamide metabolites in rat hepatocytes. Chem Res Toxicol 2013;26:564–574.

24   Pallottini V, Martini C, Bassi AM, Romano P, Nanni G, Trentalance A: Rat HMGCoA reductase activation in thioacetamide-induced liver injury is related to an increased reactive oxygen species content. J Hepatol 2006;44: 368–374.

25   Honda H, Ikejima K, Hirose M, Yoshikawa M, Lang T, Enomoto N, Kitamura T, Takei Y, Sato N: Leptin is required for fibrogenic responses induced by thioacetamide in the murine liver. Hepatology 2002;36:12–21.

26   Bautista M, Del Rio MA, Benedi J, Sanchez-Reus MI, Morales-Gonzalez JA, Tellez-Lopez AM, Lopez-Orozco M: Effect of dichloromethylene diphosphonate on liver regeneration following thioacetamide-induced necrosis in rats. World J Hepatol 2013;5:379–386.

27   Traber PG, Chou H, Zomer E, Hong F, Klyosov A, Fiel MI, Friedman SL: Regression of fibrosis and reversal of cirrhosis in rats by galectin inhibitors in thioacetamide-induced liver disease. PLoS One 2013;8:e75361.

28   Yang YL, Li JJ, Ji R, Wei YY, Chen J, Dou KF, Wang YY: Abnormal chloride homeostasis in the substancia nigra pars reticulata contributes to locomotor deficiency in a model of acute liver injury. PLoS One 2013;8:e65194.

29   Kim JH, Jeong YJ, Hong JM, Kim HR, Kang JS, Lee WJ, Hwang YI: Chronic vitamin C insufficiency aggravated thioacetamide-induced liver fibrosis in gulo-knockout mice. Free Radic Biol Med 2014;67:81–90.

30   Mathews S, Xu M, Wang H, Bertola A, Gao B: Animals models of gastrointestinal and liver diseases. Animal models of alcohol-induced liver disease: pathophysiology, translational relevance, and challenges. Am J Physiol Gastrointest Liver Physiol 2014;306:G819–G823.

31   Gao B, Bataller R: Alcoholic liver disease: pathogenesis and new therapeutic targets. Gastroenterology 2011; 141:1572–1585.

32   Vidhya A, Renjugopal V, Indira M: Impact of thiamine supplementation in the reversal of ethanol induced toxicity in rats. Indian J Physiol Pharmacol 2013;57:406–417.

33   Enomoto N, Ikejima K, Yamashina S, Hirose M, Shimizu H, Kitamura T, Takei Y, Sato AN, Thurman RG: Kupffer cell sensitization by alcohol involves increased permeability to gut-derived endotoxin. Alcohol Clin Exp Res 2001;25:51S–54S.

34   Rao R: Endotoxemia and gut barrier dysfunction in alcoholic liver disease. Hepatology 2009;50:638–644.

35   Ding X, Beier JI, Baldauf KJ, Jokinen JD, Zhong H, Arteel GE: Acute ethanol preexposure promotes liver regeneration after partial hepatectomy in mice by activating ALDH2. Am J Physiol Gastrointest Liver Physiol 2014; 306:G37–G47.

36   He S, Rehman H, Shi Y, Krishnasamy Y, Lemasters JJ, Schnellmann RG, Zhong Z: Suramin decreases injury and improves regeneration of ethanol-induced steatotic partial liver grafts. J Pharmacol Exp Ther 2013;344:417–425.

37   Koteish A, Yang S, Lin H, Huang J, Diehl AM: Ethanol induces redox-sensitive cell-cycle inhibitors and inhibits liver regeneration after partial hepatectomy. Alcohol Clin Exp Res 2002;26:1710–1718.

38   Zhang BH, Hornsfield BP, Farrell GC: Chronic ethanol administration to rats decreases receptor-operated mobilization of intracellular ionic calcium in cultured hepatocytes and inhibits 1,4,5-inositol trisphosphate production: relevance to impaired liver regeneration. J Clin Invest 1996;98:1237–1244.

39   Diehl AM, Thorgeirsson SS, Steer CJ: Ethanol inhibits liver regeneration in rats without reducing transcripts of key protooncogenes. Gastroenterology 1990;99:1105–1112.

40   Martins PN, Theruvath TP, Neuhaus P: Rodent models of partial hepatectomies. Liver Int 2008;28:3–11.

41   Madrahimov N, Dirsch O, Broelsch C, Dahmen U: Marginal hepatectomy in the rat: from anatomy to surgery. Ann Surg 2006;244:89–98.

42   Martins PN, Neuhaus P: Surgical anatomy of the liver, hepatic vasculature and bile ducts in the rat. Liver Int 2007;27:384–392.

43   Weinbren K, Woodward E: Delayed incorporation of ^{32}P from orthophosphate into deoxyribonucleic acid of rat liver after subtotal hepatectomy. Br J Exp Pathol 1964;45:442–449.

44   Gaub J, Iversen J: Rat liver regeneration after 90% partial hepatectomy. Hepatology 1984;4:902–904.

45   Deng M, Huang H, Jin H, Dirsch O, Dahmen U: The anti-proliferative side effects of AEE788, a tyrosine kinase inhibitor blocking both EGF- and VEGF-receptor, are liver-size-dependent after partial hepatectomy in rats. Invest New Drugs 2011;29:593–606.

Wei et al.: Rodent Models and Imaging Techniques to Study Liver Regeneration

46 Mitchell C, Willenbring H: A reproducible and well-tolerated method for 2/3 partial hepatectomy in mice. Nat Protoc 2008;3:1167–1170.

47 Kubota T, Takabe K, Yang M, Sekido H, Endo I, Ichikawa Y, Togo S, Shimada H: Minimum sizes for remnant and transplanted livers in rats. J Hepatobiliary Pancreat Surg 1997;4:398–404.

48 Fausto N: Liver regeneration. J Hepatol 2000;32:19–31.

49 Ota S, Suzuki S, Sakaguchi T, Baba S, Mitsuoka H, Nakamura S, Konno H: Significance of morphological alteration by portal vein branch ligation in endotoxin-induced liver injury after partial hepatectomy. Liver Int 2007;27:1076–1085.

50 Abshagen K, Mertens F, Eipel C, Vollmar B: Limited therapeutic efficacy of thrombopoietin on the regeneration of steatotic livers. Int J Clin Exp Pathol 2013;6:1759–1769.

51 Marsman HA, de Graaf W, Heger M, van Golen RF, Ten Kate FJ, Bennink R, van Gulik TM: Hepatic regeneration and functional recovery following partial liver resection in an experimental model of hepatic steatosis treated with omega-3 fatty acids. Br J Surg 2013;100:674–683.

52 Itoh T, Miyajima A: Liver regeneration by stem/progenitor cells. Hepatology 2014;59:1617–1626.

53 Park ES, Park YK, Shin CY, Park SH, Ahn SH, Kim DH, Lim KH, Kwon SY, Kim KP, Yang SI, Seong BL, Kim KH: Hepatitis B virus inhibits liver regeneration via epigenetic regulation of urokinase-type plasminogen activator. Hepatology 2013;58:762–776.

54 Quetier I, Brezillon N, Duriez M, Massinet H, Giang E, Ahodantin J, Lamant C, Brunelle MN, Soussan P, Kremsdorf D: Hepatitis B virus HBx protein impairs liver regeneration through enhanced expression of IL-6 in transgenic mice. J Hepatol 2013;59:285–291.

55 Chavin KD, Yang S, Lin HZ, Chatham J, Chacko VP, Hoek JB, Walajtys-Rode E, Rashid A, Chen CH, Huang CC, Wu TC, Lane MD, Diehl AM: Obesity induces expression of uncoupling protein-2 in hepatocytes and promotes liver ATP depletion. J Biol Chem 1999;274:5692–5700.

56 Torbenson M, Yang SQ, Liu HZ, Huang J, Gage W, Diehl AM: STAT-3 overexpression and p21 up-regulation accompany impaired regeneration of fatty livers. Am J Pathol 2002;161:155–161.

57 Wilms C, Mueller L, Lenk C, Wittkugel O, Helmke K, Krupski-Berdien G, Rogiers X, Broering DC: Comparative study of portal vein embolization versus portal vein ligation for induction of hypertrophy of the future liver remnant using a mini-pig model. Ann Surg 2008;247:825–834.

58 van den Esschert JW, van Lienden KP, Alles LK, van Wijk AC, Heger M, Roelofs JJ, van Gulik TM: Liver regeneration after portal vein embolization using absorbable and permanent embolization materials in a rabbit model. Ann Surg 2012;255:311–318.

59 Tashiro S: Mechanism of liver regeneration after liver resection and portal vein embolization (ligation) is different? J Hepatobiliary Pancreat Surg 2009;16:292–299.

60 Gock M, Eipel C, Linnebacher M, Klar E, Vollmar B: Impact of portal branch ligation on tissue regeneration, microcirculatory response and microarchitecture in portal blood-deprived and undeprived liver tissue. Microvasc Res 2011;81:274–280.

61 Lambotte L, Li B, Leclercq I, Sempoux C, Saliez A, Horsmans Y: The compensatory hyperplasia (liver regeneration) following ligation of a portal branch is initiated before the atrophy of the deprived lobes. J Hepatol 2000;32:940–945.

62 Rous P, Larimore LD: Relation of the portal blood to liver maintenance: a demonstration of liver atrophy conditional on compensation. J Exp Med 1920;31:609–632.

63 Rozga J, Jeppsson B, Bengmark S: Portal branch ligation in the rat. Reevaluation of a model. Am J Pathol 1986;125:300–308.

64 Weinbren K, Tarsh E: The mitotic response in the rat liver after different regenerative stimuli. Br J Exp Pathol 1964;45:475–480.

65 Tivers MS, Lipscomb VJ, Smith KC, Wheeler-Jones CP, House AK: Markers of hepatic regeneration associated with surgical attenuation of congenital portosystemic shunts in dogs. Vet J 2014;200:305–311.

66 Ladurner R, Schenk M, Margreiter R, Offner F, Konigsrainer A: Influence of portosystemic shunt on liver regeneration after hepatic resection in pigs. HPB Surg 2009;2009:835965.

67 Aller MA, Martinez V, Corcuera MT, Benito J, Traver E, Gomez-Aguado F, Vergara P, Arias J: Liver impairment after portacaval shunt in the rat: the loss of protective role of mast cells? Acta Histochem 2012;114:301–310.

68 Garcia C, Gine E, Aller MA, Revuelta E, Arias JL, Vara E, Arias J: Multiple organ inflammatory response to portosystemic shunt in the rat. Cytokine 2011;56:680–687.

69 Starzl TE, Porter KA, Francavilla A: The Eck fistula in animals and humans. Curr Probl Surg 1983;20:687–752.

70 Klarik Z, Toth E, Kiss F, Miko I, Furka I, Nemeth N: A modified microsurgical model for end-to-side selective portacaval shunt in the rat. Intraoperative microcirculatory investigations. Acta Cir Bras 2013;28:625–631.

71 Erlik D, Barzilai A, Shramek A: Porto-renal shunt: a new technic for porto-systemic anastomosis in portal hypertension. Ann Surg 1964;159:72–78.

72 Warren WD, Zeppa R, Fomon JJ: Selective trans-splenic decompression of gastroesophageal varices by distal splenorenal shunt. Ann Surg 1967;166:437–455.

73 Alwayn IP, Verbesey JE, Kim S, Roy R, Arsenault DA, Greene AK, Novak K, Laforme A, Lee S, Moses MA, Puder M: A critical role for matrix metalloproteinases in liver regeneration. J Surg Res 2008;145:192–198.

74 Sugimoto T, Yamada T, Iwata H, Sekino T, Matsumoto S, Ishida N, Manabe H, Kimura M, Takemura H: Two-stage portal vein ligation facilitates liver regeneration in rats. Eur Surg Res 2009;42:181–188.

113

75   Garbow JR, Kataoka M, Flye MW: MRI measurement of liver regeneration in mice following partial hepa-
      tectomy. Magn Reson Med 2004;52:177–180.
76   Fulop A, Szijarto A, Harsanyi L, Budai A, Pekli D, Korsos D, Horvath I, Kovacs N, Karlinger K, Mathe D, Szigeti
      K: Demonstration of metabolic and cellular effects of portal vein ligation using multi-modal PET/MRI measure-
      ments in healthy rat liver. PLoS One 2014;9:e90760.
77   Radtke A, Sotiropoulos GC, Molmenti EP, Sgourakis G, Schroeder T, Beckebaum S, Peitgen HO, Cicinnati VR,
      Broelsch CE, Broering DC, Malago M: Transhilar passage in right graft live donor liver transplantation: intra-
      hilar anatomy and its impact on operative strategy. Am J Transplant 2012;12:718–727.
78   Nebuloni L, Kuhn GA, Muller R: A comparative analysis of water-soluble and blood-pool contrast agents for in
      vivo vascular imaging with micro-CT. Acad Radiol 2013;20:1247–1255.
79   Ringe KI, Husarik DB, Gupta RT, Boll DT, Merkle EM: Hepatobiliary transit times of gadoxetate disodium
      (Primovist®) for protocol optimization of comprehensive MR imaging of the biliary system – what is normal?
      Eur J Radiol 2011;79:201–205.
80   Wu J, Li H, Lin Y, Chen Z, Zhong Q, Gao H, Fu L, Sandrasegaran K: Value of gadoxetate biliary transit time in
      determining hepatocyte function. Abdom Imaging 2014, Epub ahead of print.
81   Selle D, Preim B, Schenk A, Peitgen HO: Analysis of vasculature for liver surgical planning. IEEE Trans Med
      Imaging 2002;21:1344–1357.
82   de Graaf W, Bennink RJ, Heger M, Maas A, de Bruin K, van Gulik TM: Quantitative assessment of hepatic
      function during liver regeneration in a standardized rat model. J Nucl Med 2011;52:294–302.
83   Lehner B, Sandner B, Marschallinger J, Lehner C, Furtner T, Couillard-Despres S, Rivera FJ, Brockhoff G, Bauer
      HC, Weidner N, Aigner L: The dark side of BrdU in neural stem cell biology: detrimental effects on cell cycle,
      differentiation and survival. Cell Tissue Res 2011;345:313–328.
84   Bullwinkel J, Baron-Luhr B, Ludemann A, Wohlenberg C, Gerdes J, Scholzen T: Ki-67 protein is associated with
      ribosomal RNA transcription in quiescent and proliferating cells. J Cell Physiol 2006;206:624–635.
85   Deng M, Dirsch O, Sun J, Huang H, Sehestedt C, Homeyer A, Schenk A, Dahmen U: Limited correlation between
      conventional pathologist and automatic computer-assisted quantification of hepatic steatosis due to difference
      between event-based and surface-based analysis. IEEE J Biomed Health Inform 2013;18:1473–1477.
86   Homeyer A, Schenk A, Dahmen U, Dirsch O, Huang H, Hahn HK: A comparison of sampling strategies for histo-
      logical image analysis. J Pathol Inform 2011;2:S11.
87   Homeyer A, Schenk A, Arlt J, Dahmen U, Dirsch O, Hahn HK: Practical quantification of necrosis in histological
      whole-slide images. Comput Med Imaging Graph 2013;37:313–322.
88   Wang K, Lee I, Carlson G, Hood L, Galas D: Systems biology and the discovery of diagnostic biomarkers. Dis
      Markers 2010;28:199–207.
89   Sauer U, Heinemann M, Zamboni N: Genetics. Getting closer to the whole picture. Science 2007;316:550–551.
90   Schwen LO, Krauss M, Niederalt C, Gremse F, Kiessling F, Schenk A, Preusser T, Kuepfer L: Spatio-temporal
      simulation of first pass drug perfusion in the liver. PLoS Comput Biol 2014;10:e1003499.
91   Hohme S, Hengstler JG, Brulport M, Schafer M, Bauer A, Gebhardt R, Drasdo D: Mathematical modelling of liver
      regeneration after intoxication with CCl(4). Chem Biol Interact 2007;168:74–93.
92   Ricken T, Dahmen U, Dirsch O: A biphasic model for sinusoidal liver perfusion remodeling after outflow
      obstruction. Biomech Model Mechanobiol 2010;9:435–450.
93   Hoehme S, Brulport M, Bauer A, Bedawy E, Schormann W, Hermes M, Puppe V, Gebhardt R, Zellmer S, Schwarz
      M, Bockamp E, Timmel T, Hengstler JG, Drasdo D: Prediction and validation of cell alignment along micro
      vessels as order principle to restore tissue architecture in liver regeneration. Proc Natl Acad Sci USA 2010;
      107:10371–10376.
94   Hohmann N, Weiwei W, Dahmen U, Dirsch O, Deutsch A, Voss-Bohme A: How does a single cell know when the
      liver has reached its correct size? PLoS One 2014;9:e93207.
95   Periwal V, Gaillard JR, Needleman L, Doria C: Mathematical model of liver regeneration in human live donors.
      J Cell Physiol 2014;229:599–606.

Manuscript II

Establishment of a Rat Model: Associating Liver Partition with Portal Vein Ligation for Staged Hepatectomy

---

Weiwei Wei, Tianjiao Zhang, Sara Zafarnia, Andrea Schenk, Chichi Xie, Chunyi Kan, Olaf Dirsch, Utz Settmacher and Uta Dahmen

Authorship

First author

Authors' Contribution

W.Wei, O.Dirsch and U.Dahmen contributed to conception and design;

W.Wei, T.Zhang, C.Kan and U.Dahmen for analysis and interpretation;

W.Wei, C.Xie, S.Zafarnia and A.Schenk for data collection and image-reconstruction;

W.Wei and T.Zhang for writing the article;

O.Dirsch, U.Settmacher and U.Dahmen for critical revision of the article;

U.Dahmen and O.Dirsch for obtaining funding.

Establishment of a rat model: Associating liver partition with portal vein ligation for staged hepatectomy

Weiwei Wei, MS,[a] Tianjiao Zhang, MD,[a] Sara Zafarnia, MS,[b] Andrea Schenk, PhD,[c] Chichi Xie, MS,[a] Chunyi Kan, MS,[a] Olaf Dirsch, MD,[d] Utz Settmacher, MD,[a] and Uta Dahmen, MD,[a] *Jena, Aachen, Bremen and Chemnitz, Germany*

Background. *We adapted the anatomically oriented parenchyma-preserving resection technique for associating liver partition with portal vein ligation (PVL) for staged hepatectomy (ALPPS) in rats and examined the role of revascularization in intrahepatic size regulation.*

Methods. *We performed the procedures based on anatomic study. The ALPPS procedure consisted of a 70% PVL (occluding the left median, left lateral, and right lobes), parenchymal transection (median lobe) and partial (10%) hepatectomy (PHx; caudate lobe). The transection effect was evaluated by measuring the extent of hepatic atrophy or regeneration of individual liver lobes in the ALPPS and control groups (70% PVL and 10% PHx without transection). The survival rates after stage II resection and collateral formation within the portal vein system was examined.*

Results. *Anatomic study revealed a close spatial relationship between the demarcation line and the middle median hepatic vein. This enabled placing the transection plane without injuring the hepatic vein. Transection was achieved via stepwise clamping, followed by 2–3 parenchyma-preserving piercing sutures on both sides of the clamp. Ligated liver lobes atrophy was significantly enhanced after ALPPS compared with the control group. In contrast, both a significantly greater relative weight of the regenerated lobe and proliferation index on the first postoperative day were observed. All animals tolerated stage II-resection without complications. Portoportal collaterals were only observed in the control group.*

Conclusion. *We developed an anatomically precise technique for parenchymal transection. The lack of a dense vascular network between the portalized and deportalized lobes may play an important role in accelerating regeneration and atrophy augmentation. (Surgery 2016;159:1299-307.)*

From the Experimental Transplantation Surgery, Department of General, Visceral and Vascular Surgery,[a] Jena University Hospital, Jena; Department of Experimental Molecular Imaging,[b] RWTH Aachen University, Aachen; Fraunhofer Institute for Medical Image Computing MEVIS,[c] Bremen; Institute of Pathology,[d] Chemnitz Hospital, Chemnitz, Germany

MANY PRIMARY AND SECONDARY LIVER TUMORS are unresectable via a single-stage hepatectomy because of the insufficient mass of the putative future liver remnant (FLR). Surgical strategies were developed to increase the FLR volume before an extended hepatectomy and enhance the feasibility of curative resection. Portal vein ligation (PVL) or portal vein

embolization was conventionally adopted in primarily nonresectable liver tumors because this technique induces atrophy of the ipsilateral lobe and a compensatory hypertrophy of the contralateral lobe.[1-5] Another strategy for bilobar liver malignancies is a two-staged hepatectomy, in which atypical resection of tumors on the FLR is performed with or without portal vein occlusion in the first stage, followed by an extended second-stage hepatectomy.[6-9] These surgical strategies enhanced the curative resectability rate, but the long interval between the 2 stages precluded some cases from undergoing the second stage.[10-12] Recent reviews of the current literature revealed that approximately 15–23% patients failed to reach an R0 resection during the second stage of surgery, because of the insufficient FLR hypertrophy or tumor progression.[13,14]

Associating liver partition with PVL for staged hepatectomy (ALPPS) is an emerging surgical

strategy to induce the accelerated FLR hypertrophy and reduce posthepatectomy liver failure.[15] PVL in the first stage is combined with liver transection, followed by liver resection in the second stage. Accelerated liver regeneration in the FLR resulted in a sufficient hypertrophy within days. This technique raised great interest in the field of hepatobiliary surgery worldwide despite its challenging nature,[16-19] and different variants were developed to cover the surgical needs of individual patients.[20,21]

However, open questions of the effect and outcome of ALPPS remain. Clinical reports reveal that ALPPS is associated with high morbidity and mortality.[22-24] The pathophysiologic mechanism underlying the accelerated liver regeneration of the FLR and the enhanced atrophy of the portally deprived lobe are not clear, calling for further investigations in small animals. These investigations are facilitated by the development of highly reproducible safe surgical models. The present study adapted the anatomically oriented parenchyma-preserving liver resection technique for liver partition in rats. This paper investigated the vascular anatomy of the median liver lobe, the surgical procedure, and the effect of parenchymal transection on intrahepatic size regulation.

METHODS

Animal source and management. Animal experiments were performed in inbred male Lewis Rats (Charles River, Sulzfeld, Germany) aged 9–10 weeks (body weight 250–300 g). Rats were fed a laboratory diet with water and rat chow available ad libitum until organ harvest. All procedures and housing of the animals were performed according to current German regulations and guidelines for animal welfare and international principles of laboratory animal care. The Thüringer Landesamt für Verbraucherschutz, Thuringia, Germany, approved the protocols (Approval Number: 02–042/10).

Experimental design. One group of rats (n = 6) was used for the anatomic study. Explanted livers filled with a contrast polymer were subjected to μCT scanning, 3-dimensional (3D) reconstruction and subsequent qualitative analysis.

A second group of rats (n = 10) was used to establish the surgical procedure for liver partition. The delicate parenchyma-preserving piercing suture technique was used.

A third group of rats (N = 53) was used to assess the effect of hepatic transection. Rats were subjected to PVL ligation with transection (ALPPS) and PVL without transection (control group) to

investigate the liver lobe weight adjustments and hepatocyte proliferation index (PI). Animals were sacrificed at different time points (1, 2, 3, and 7 days; n = 5 per group per time point, 40 rats in total). An additional groups of rats underwent extended liver resection after stage I (n = 5) to examine the safety and feasibility for stage II. The hepatic and portal venous tree was visualized detecting the formation of portoportal collaterals immediately and 7 days after surgery (n = 2 per group per time point, 8 rats in total).

Perioperative care. All surgical interventions were performed during the daytime under inhalation 3% isoflurane mixed with pure oxygen at a flow rate of 0.5 L/min (Penlon Sigma Delta Vaporizer, Penlon Limited, Abingdon, UK) in a dedicated S1 operating room. Animals were subjected to laparotomy via a transverse upper-abdominal incision. The mobilization and dissection of portal veins were performed with care under an operating microscope (Zeiss, Jena, Germany; original magnification, ×10-25). Animals were allowed to recover on a heating pad after surgery and received analgesic treatment with buprenorphine (0.05 mg/kg body weight; Temgesic, Essex Pharma GmbH, Munich, Germany) every 24 hours for a maximum of 2 days after surgery. Daily monitoring was performed and body weights were recorded.

Imaging techniques. Contrasting of the vascular tree of normal liver was achieved via the injection of a silicone radiopaque contrast agent (Microfil, Flow Tech, Inc., Carver, MA) into hepatic and portal veins. The livers were explanted and subjected to μCT-scanning (TomoScope Duo CT, CT Imaging GmbH, Erlangen, Germany) and 3D-reconstruction (Imalytics Preclinical, Philips Research, Aachen, Germany).[25,26] An experienced microsurgeon and an imaging specialist further analyzed the vascular spatial distribution and corresponding hepatic territories using software (HepaVision, Fraunhofer MEVIS, Bremen, Germany).

Surgical procedures. *Stage I. PVL*: Occlusion of 70% of the liver mass was achieved via ligation of the portal vein feeding the left median, left lateral, and right lobes.

Parenchymal transection: Hepatic transection was performed via placement of a clamp stepwise along the transection plane, which was marked left of the demarcation line on the median lobe following left PVL. Special attention was paid to spare the middle median hepatic vein and maintain a minimal distance of 5 mm from the vena cava. A line of 2–3 piercing sutures was placed on

both sides of the clamp before transection of the median lobe in between both suture lines.

Partial hepatectomy: The ligation of the lobar pedicle caudate lobe was removed to simulate an atypical resection in clinical practice. Control group animals received only PVL and partial hepatectomy (PHx).

Stage II. Extended liver resection: Animals were subjected to relaparotomy 2 days after stage I. A 70% PHx was performed via removal of all deportalized liver lobes using the parenchyma preserving piercing suture technique, and only the right median lobe remained. Animals were observed for 7 days after stage II hepatectomy.

Visualization of the vascular tree. Rats were subjected to imaging (μCT and 3D-reconstruction) after injection of a Microfil contrast polymer into portal and hepatic veins. The portal and hepatic vascular trees after surgery were identified.

Liver explantation, liver weight determination, and sampling. One hour before harvest, 5-bromo-2-deoxyuridine (BrdU, Sigma-Aldrich, St Louis, MO) was injected intravenously (50 mg/kg body weight) to reveal hepatocellular proliferation. Blood was collected into serum tubes (serum Z/1.2 mL, monovette, SARSTEDT, Nümbrecht, Germany) via puncture of infrahepatic vena cava. Animals were humanely killed via exsanguination under anesthesia on postoperative days 1, 2, 3, and 7. Serum was stored at -20°C until measurement of serum levels of aspartate aminotransferase and alanine aminotransferase was performed using an automated chemical analyzer (Bayer Advia 1650, Leverkusen, Germany). All hepatic vessels and ligaments were mobilized for whole liver explantation. Individual liver lobes were weighed to calculate the liver weight/body weight ratio using the following formula: liver weight of individual lobe (g)/body weight (g)*100%. Five additional rats were subjected to laparotomy to obtain normal values of liver weights and normal range of liver enzymes.

Histologic staining. Liver tissues from right and left median lobe were fixed in 4.5% buffered formalin for 48 hours. Sections (4 μm thick) were cut after paraffin embedding and mounted on slides. Slides were stained with hematoxylin and eosin for routine histologic examination. All slides were digitalized using a slide scanner (Nano-zoomer, Hamamatsu Electronic Press Co., Ltd, Lwata, Japan).

Immunohistochemistry. Sections were deparaffinized and rehydrated, and antigen retrieval was performed. The sections were incubated with a 1:50 monoclonal anti-BrdU antibody (Dako, Hamburg, Germany) at 37°C for 1 hour followed by an alkaline phosphatase–labeled secondary antimouse antibody (Power Vision, Immunovision Technologies, Springdale, AZ) for 1 hour at room temperature. Color reaction was performed using DAB (Dako, Hamburg, Germany) for 10 minutes. The sections were counterstained with Mayer's hemalaun (Merck, Darmstadt, Germany) for 10 seconds, and cover slipped. Whole slides scanning was performed using the same Hamamatsu slide scanner. The PI is expressed as the fraction of proliferating hepatocyte nuclei to the total number of hepatocyte nuclei (accurate to 0.1%) as described previously.[25]

Statistical analysis. Quantitative data are expressed as mean values with standard deviation and analyzed using Sigmaplot 13.0 (Statcon, Witzenhausen, Germany). Differences between 2 groups were compared using Student's *t* test.

RESULTS

Vascular and territorial anatomy of rat median lobe. The median lobe is supplied by 2 portal veins and drained by 3 hepatic veins (Fig 1, *A* and *B*). The vascular territories of the right and left median portal veins and the 3 hepatic veins were clearly separated without any visible collaterals in all animals. Notably, the territory of the left median portal vein was larger in all animals, and the right portal venous territory was smaller than suggested by the anatomic fissure between the right and left median lobes (Fig 1, *C*). We concluded that the transection plane may only be performed between the middle median hepatic vein and left median portal vein (Fig 1, *D*).

Surgical considerations for the anatomically oriented parenchyma-preserving technique for liver partition. The most difficult part of the ALPPS procedure is the parenchymal transection. The transection consists of 3 steps: identification and maintenance of the transection plane, parenchymal transection, and determination of the end point of the resection plane toward the vena cava.

Identification of the transection plane was achieved by ligating the left portal vein. A demarcation would emerge between right and left median portal vein after ligation of the left portal vein (Fig 2, *A*). Examination of the hepatic vein territories revealed that the demarcation line was also near the left median and middle median hepatic veins. The space for transection in between these branches of portal vein and hepatic veins was small. Marking the resection plane using an electrocoagulator immediately after ligating the portal
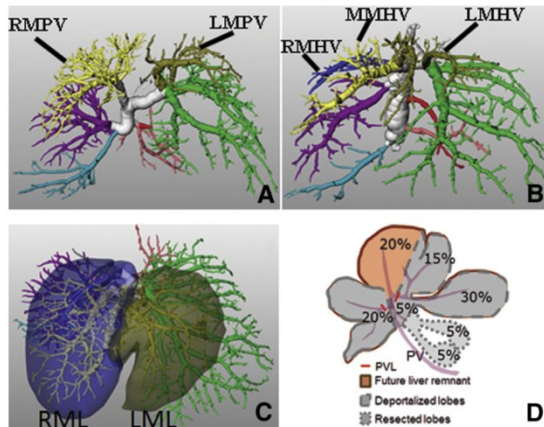
Fig 1. Vascular anatomy of a native rat and the schematic of the ALPPS model. (*A*) Portal vascular tree. (*B*) Hepatic vascular tree. (*C*) Territory of RML/LML. (*D*) Schematic of ALPPS model. *ALPPS,* Associating liver partition with portal vein ligation for staged hepatectomy; *LMHV,* left median hepatic vein; *LML,* left median lobe; *LMPV,* left median portal vein; *MMHV,* middle median hepatic vein; *RMHV,* right median hepatic vein; *RML,* right median lobe; *RMPV,* right median portal vein; *PV,* portal vein.
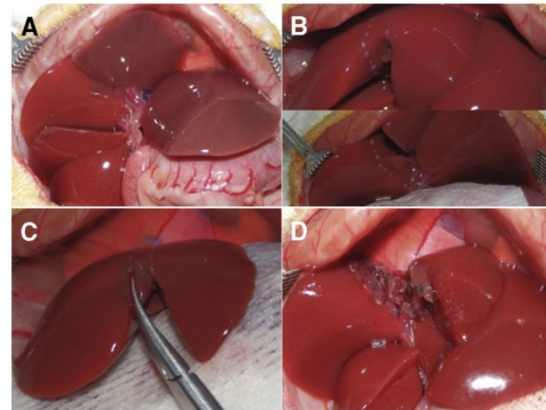

Fig 2. Surgical procedures of ALPPS. (*A*) Demarcation emerged after PVL of LLL, LML and RL. (*B*) The transection plane on ML is slightly left of the demarcation line. (*C*) Gradual transection of the ML along the mark line using clamp. (*D*) Piercing sutures on both sides for hemostasis. *ALPPS,* Associating liver partition with portal vein ligation for staged hepatectomy; *LLL,* left lateral lobe; *LML,* left median lobe; *ML,* median lobe; *PVL,* portal vein ligation; *RL,* right lobe.

vein in cases where the demarcation line was difficult to identify during transection greatly facilitated maintenance of the transection plane. The transection plane was marked on the diaphragmatic and visceral surfaces of the median lobe (Fig 2, *B*).

The transection should be performed in steps to achieve a precise transection of the hepatic parenchyma. A mosquito clamp was placed along the marked transection plane and was moved stepwise toward the vena cava (Fig 2, *C*). The hepatic parenchyma was sectioned carefully after piercing sutures were placed near the clamp, and the clamp was released (Fig 2, *D*).

Defining the end of the resection plane was more difficult because there is no landmark to indicate the immediate vicinity of the main hepatic veins. This decision remains a purely surgical intraoperative decision supported by solid knowledge of the 3D vascular anatomy obtained from qualitative analysis of previous 3D reconstructions. The anatomic study and our experience suggest the maintenance of a minimal distance of 5 mm from the vena cava to avoid injury from the confluence of the left and middle median hepatic vein and thereby massive hemorrhage.

Surgical stress. The procedure was well-tolerated without any loss of animals. Relative body weight loss reached 7.6% ± 0.9% 4 days after

ALPPS and 7.1% ± 1.1% on day 3 in the control group, which reflects the similar severity of the 2 procedures (Fig 3, *A*). Hepatocellular damage as measured by liver enzyme release on the first day after ALPPS was significantly higher than the control group (Fig 3, *B* and *C*; aspartate aminotransferase: 23.69 ± 8.73 vs 13.23 ± 4.90 μmol/L [P = .048]; alanine aminotransferase: 15.55 ± 5.62 vs 6.95 ± 3.81 μmol/L [P = .022]).

Effects of ALPPS on intrahepatic size regulation. The intrahepatic size regulation study revealed that the hepatic atrophy of the ligated left median lobe was significantly more pronounced in the ALPPS than control group (Fig 4, *A*, liver weight reduction up to 48.20 ± 3.40% vs 65.50 ± 4.10% [P < .001]). In contrast, the weight of the regenerating right median lobe was significantly greater in the ALPPS group than the control group (Fig 4, *B*; 2.53 ± 0.17-fold vs 2.31 ± 0.11-fold of original size [P = .04]).

Liver regeneration of the right median lobe was accelerated in the ALPPS group compared with the group without transection (Fig 4, *C* and *D*). The PI in the ALPPS group peaked on the first postoperative day (PI = 15.4 ± 0.9%) and decreased sharply to 2.5 ± 0.4% on the following day. However, a significantly lower proliferative response was observed on the first postoperative day in the control group (PI = 8.6 ± 2.9%; P = .009), and higher PI was observed on the second day (6.1 ± 1.9%; P = .004 vs ALPPS).
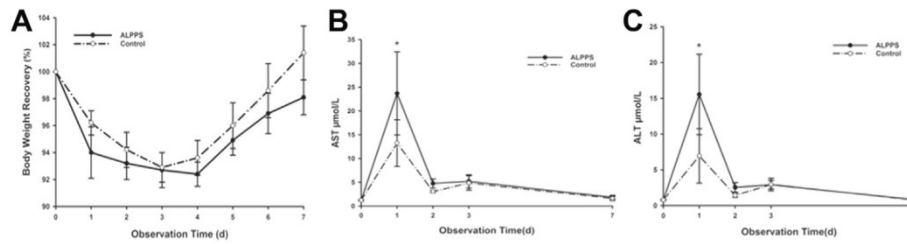
Fig 3. Changes in body weight (*A*) and liver enzymes (*B*, *C*) after surgery. Hepatic injury was indicated by the release of liver enzymes, which was more pronounced on the first day after ALPPS compared with the control group (AST: *P = .048, ALT: *P = .022). *ALPPS*, Associating liver partition with portal vein ligation for staged hepatectomy; *ALT*, alanine aminotransferase; *AST*, aspartate aminotransferase. SI conversion factors: To convert AST and ALT to U/L, divide values by 0.0167.
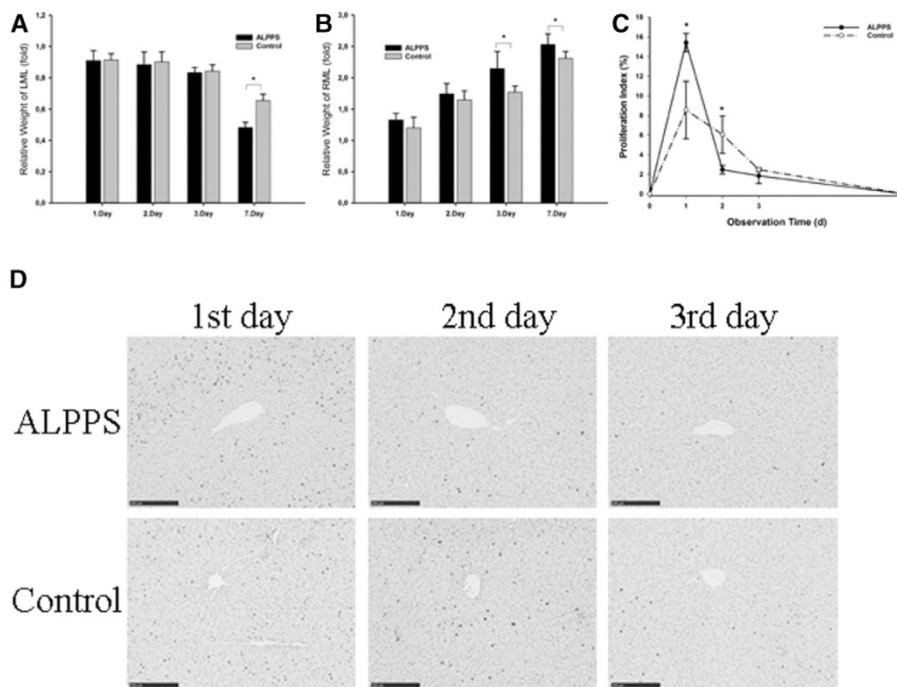

Fig 4. Liver size regulation (*A*, *B*) and assessment of liver proliferation after surgery (*C*, *D*). ALPPS induced a greater extent of atrophy in LML (*A*) and accelerated liver regeneration in RML (*B*) compared with the control group 7 days after surgery (*P < .001). *C*, Proliferation index in the ALPPS group was higher on day 1 and lower on day 2 compared with the control group (*P = .009 and .004, respectively). *D*, Periportal proliferation in the ALPPS group was significant on the first day and remarkably lower thereafter. In contrast, only moderate proliferation was observed in the control group on the first and second days after surgery. *ALPPS*, Associating liver partition with portal vein ligation for staged hepatectomy; *LML*, left median lobe; *RML*, right median lobe. Stain: 5-bromo-2-deoxyuridine (BrdU); original magnification, ×100.

Outcome of the survival experiment. The most attractive advantage of ALPPS is the accelerated liver regeneration after PVL and liver transection, which allows the resection of all diseased lobes after a short interval. We performed the stage II resection on the second day after ALPPS in this model. The second procedure was well-tolerated. Resection of all deportalized lobes (70% PHx) resulted in a 1-week survival rate of 100%. The animals experienced a maximal body weight loss of 10.9%, which occurred on the second day after stage I. Animals began to regain body weight on day 4 after stage I (Fig 5). Stage II hepatectomy did further promote regeneration of the remnant liver, as expected. The weight of the right median lobe increased 1.75 ± 0.16-fold after the stage I
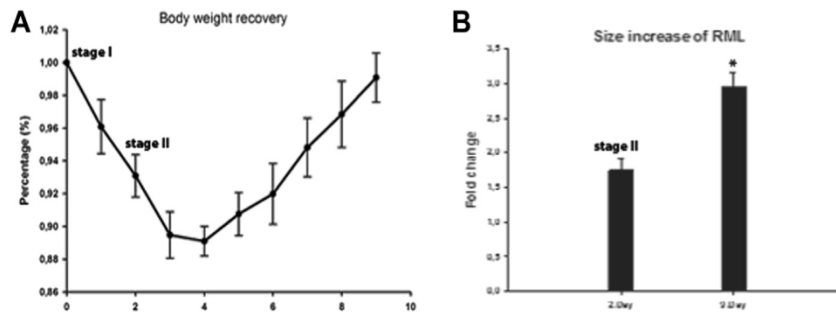
Fig 5. Body weight and RML recovery during the complete surgery. (*A*) Loss of body weight occurred after both stages but began to recover on day 4 after the first surgery. (*B*) Liver weight of RML by harvest day increased significantly owing to stage II hepatectomy (**P* < .001 vs second day). *RML*, Right median lobe.

procedure and totally of 2.94 ± 0.21-fold after stage II hepatectomy (*P* < .001).

Visualization of the vascular trees. Visualization of the vascular tree immediately and 7 days after the procedure revealed the morphologic changes of hepatic and portal venous trees (Fig 6, *A* and *D*). A clear separation of right and left median portal veins was observed after transection (Fig 6, *B* and *C*). In contrast after PVL ligation without transection a dense network of portoportal collaterals developed and could be visualized in the explanted livers (Fig 6, *E* and *F*).

DISCUSSION

ALPPS model: Intrahepatic size regulation is an attractive issue. An understanding of intrahepatic size regulation in animal models allows the optimization of clinical surgical strategies to enhance the size of the future remnant liver. ALPPS is a complex surgical strategy for the induction of substantial hypertrophy in the future remnant liver and pronounced atrophy in the diseased part of the liver. We developed a delicate surgical technique for liver partition in a rat ALPPS model and explored the role of revascularization for intrahepatic size regulation.

Anatomically based surgical technique facilitates the completion of ALPPS in rats safely and easily. Hepatic transection should aim to minimize damage to the remaining hepatic parenchyma. The transection plane must be determined precisely to avoid compromising the middle median hepatic vein. We achieved this result by inferring the detailed anatomic knowledge of vascular spatial distribution on the demarcation line observed after PVL. The demarcation line is located in the subtle invisible space between middle median hepatic vein and left median portal vein. The transection plane is placed slightly left to the demarcation line to remain in between the 2

vascular trees. An anatomically based parenchyma-preserving piercing suture technique is needed for an atraumatic transection of the hepatic parenchyma. We achieved this transection via the placement of 1 Mosquito clamp stepwise toward the vena cava followed by the placement of several piercing sutures near the clamp as previously reported.[26] This technique was safe and effective in causing minimal damage to the remnant liver and minimal hemorrhage in stages I and II.

Role of revascularization. We observed for the first time that the ALPPS procedure enhanced liver regeneration and augmented the extent of hepatic atrophy compared with PVL without transection. Two explanations can be envisioned. First, portal revascularization may explain the delayed time course of regeneration and lower liver weight recovery after PVL without transection.[27] We visualized the formation of a dense network of vascular collaterals between the portally deprived left median lobe and the portally supplied right median lobe when performing PVL without hepatic transection. In contrast, we did not detect any portal collateral between the portally supplied lobe and the portally deprived lobe after transection the median lobe in the ALPPS procedure. Second, the lack of portal blood supply caused a more pronounced atrophy, that is, a greater loss of liver mass, which potentially led to a greater regenerative stimulus in the portally supplied liver lobes.

Novel insights from different variants of ALPPS model. Four different experimental models of ALPPS were reported in the last 2 years (Table).[28-31] These models share a common transection of the median lobe, but differ in the selection of the FLR, the extent of PVL and the extent of an additional PHx. This diversity resembles the clinically observed diversity that is needed to consider the individual clinical needs of a given
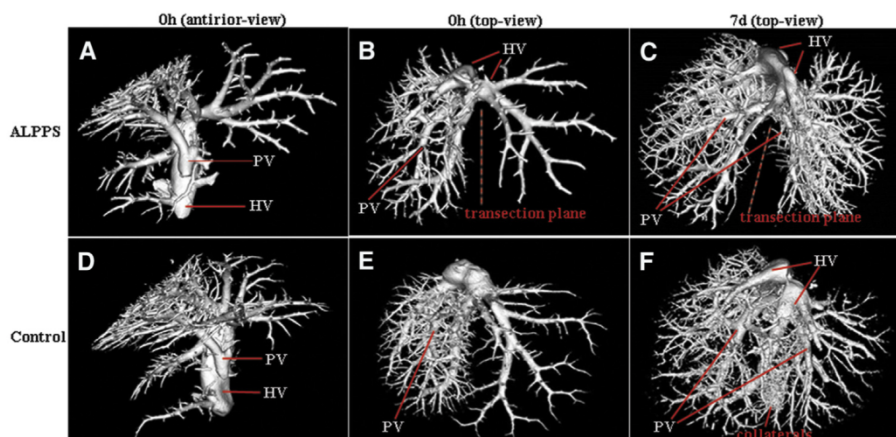
Fig 6. The portal and hepatic vascular trees were visualized immediately and 7 days after surgery. The anterior view of vascular trees (*A*, *D*) confirmed the integrity of the hepatic vein (HV) and properly performed portal vein ligation (PVL). The top view of vascular trees revealed that there were no vascular collaterals immediately (*B*) or 7 days after ALPPS (*C*) because of parenchymal transection, and the portal collaterals were not demonstrated immediately after surgery (*E*), but clearly visible on the seventh day in the control group (*F*). *ALPPS*, Associating liver partition with portal vein ligation for staged hepatectomy; *PV,* portal vein.

patient. The mouse model of Schlegel et al[28] consisted of a 55% PVL and a 30% PHx in the first stage followed by a stage II resection of the ligated lobes. In contrast, the rat models of Yao et al,[29] Dhar et al,[31] and Almau Trenard et al[30] consisted of an 80% PVL via ligation of all lobes, except the right median lobe. Neither an additional PHx nor a second stage was performed in their studies. Our study combined a 70% PVL and 10% PHx in stage I and examined the outcome of the stage II resection.

The results achieved using the different models differ in the regeneration kinetic of the future remnant liver. The proliferative period in the mouse model began on the first postoperative day and extended over 4 days to reach the maximum late on postoperative day 4. Hepatocyte proliferation in mice normally begin on postoperative day 2.[32] However, the authors did not comment on this unusual finding. In contrast, Yao et al[29] and Dhar et al[31] subjected rats to PVL with transection but without additional hepatectomy and observed a proliferation peak on the second day, which is observed after classic PVL.[33] Although the total liver mass reduction (80% of liver mass) is similar in our model and other studies, the peak of PI occurred on postoperative day 1, as observed after the classic 70% PHx. Subsequently, the increase in FLR in the present study was slightly higher than other rat models. The differences in proliferative kinetics suggest that even small differences in the ratio

between the extent of PVL and PHx (55% PVL+ 30% PHx vs 80% PVL + 0% PHx vs 70% PVL vs 10% PHx) may produce a substantial effect on the time course of intrahepatic size regulation. Whether the additional PHx in the stage I accelerates the initiation of hepatocyte proliferation is not clear.

Current molecular studies are limited to investigation of select gene and protein expression in a given model, but these studies do not yield conclusive results. Schlegel et al[28] suggested that putative circulating growth factors are crucial for rapid liver growth. Yao et al[29] investigated the up-regulated expression of growth factors and cytokines (tumor necrosis factor-α, interlekin-6). Dhar et al[31] examined 29 cytokines/chemokines and suggested that CINC-1 plays crucial role in ALPPS.

In conclusion, an improved understanding requires the assessment of size regulation across different surgical variations. Exploration of the pathophysiologic mechanisms underlying intrahepatic size regulation will improve our understanding of liver regeneration and contribute to the performance of safer ALPPS.

Table. Variants of ALPPS models

Year	Authors	Species	PVL	Transection technique	PHx in stage I	PHx in stage II	Loss of liver mass	Atrophy of ligated lobe on day 7	Future remnant liver lobe	Fold increase on day 7	Proliferation
2014	Schlegel et al[28]	Mouse	RML RL CL	Bipolar forceps	LLL (30%)	Ligated lobes	85% totally (55% PVL + 30% PHx)	NA	LML (15%)	4-fold	Peaked on day 4
2014	Yao et al[29]	Rat	LLL LML RL CL	Microscopic Tweezers + ligation	—	—	80% PVL	NA	RML (20%)	2.5-fold	Peaked on day 2
2014	Almau Trenard et al[30]	Rat	LLL LML RL CL	U-stich sutures	—	—	80% PVL	Reduction to 35.2%	RML (20%)	2-fold	NA
2015	Dhar et al[31]	Rat	LLL LML RL CL	Pringle maneuver + sutures	—	—	80% PVL	NA	RML (20%)	2-fold	Peaked on day 2
2015	Wei et al	Rat	LLL LML RL	Mosquito's clamp + piercing suture	CL (10%)	Ligated lobes	80% totally (70% PVL + 10% PHx)	Reduction to 48.2%	RML (20%)	2.53-fold	Peaked on day 1

ALPPS, Associating liver partition with portal vein ligation for staged hepatectomy; *CL*, caudate lobe; *LLL*, left lateral lobe; *LML*, left median lobe; *PHx*, partial hepatectomy; *PVL*, portal vein ligation; *RL*, right lobe; *RML*, right median lobe; *NA*, not applicable.

REFERENCES

1. Bax HR, Mansens BJ, Schalm L. Atrophy of the liver after occlusion of the bile ducts or portal vein and compensatory hypertrophy of the unoccluded portion and its clinical importance. Gastroenterology 1956;31:131-55.
2. Honjo I, Suzuki T, Ozawa K, Takasan H, Kitamura O. Ligation of a branch of the portal vein for carcinoma of the liver. Am J Surg 1975;130:296-302.
3. Nagino M, Kamiya J, Kanai M, Uesaka K, Sano T, Yamamoto H, et al. Right trisegment portal vein embolization for biliary tract carcinoma: technique and clinical utility. Surgery 2000;127:155-60.
4. Ribero D, Abdalla EK, Madoff DC, Donadon M, Loyer EM, Vauthey JN. Portal vein embolization before major hepatectomy and its effects on regeneration, resectability and outcome. Br J Surg 2007;94:1386-94.
5. Abdalla EK. Portal vein embolization (prior to major hepatectomy) effects on regeneration, resectability, and outcome. J Surg Oncol 2010;102:960-7.
6. Adam R, Laurent A, Azoulay D, Castaing D, Bismuth H. Two-stage hepatectomy: A planned strategy to treat irresectable liver tumors. Ann Surg 2000;232:777-85.
7. Jaeck D, Oussoultzoglou E, Rosso E, Greget M, Weber JC, Bachellier P. A two-stage hepatectomy procedure combined with portal vein embolization to achieve curative resection for initially unresectable multiple and bilobar colorectal liver metastases. Ann Surg 2004;240:1037-49.
8. Narita M, Oussoultzoglou E, Bachellier P, Rosso E, Pessaux P, Jaeck D. Two-stage hepatectomy procedure to treat initially unresectable multiple bilobar colorectal liver metastases: technical aspects. Dig Surg 2011;28:121-6.
9. Clavien PA, Petrowsky H, DeOliveira ML, Graf R. Strategies for safer liver surgery and partial liver transplantation. N Engl J Med 2007;356:1545-59.
10. Tsai S, Marques HP, de Jong MC, Mira P, Ribeiro V, Choti MA, et al. Two-stage strategy for patients with extensive bilateral colorectal liver metastases. HPB (Oxford) 2010;12:262-9.
11. Wicherts DA, Miller R, de Haas RJ, Bitsakou G, Vibert E, Veilhan LA, et al. Long-term results of two-stage hepatectomy for irresectable colorectal cancer liver metastases. Ann Surg 2008;248:994-1005.
12. Yang C, Rahbari NN, Mees ST, Schaab F, Koch M, Weitz J, et al. Staged resection of bilobar colorectal liver metastases: surgical strategies. Langenbecks Arch Surg 2015;400:633-40.
13. Lam VW, Laurence JM, Johnston E, Hollands MJ, Pleass HC, Richardson AJ. A systematic review of two-stage hepatectomy in patients with initially unresectable colorectal liver metastases. HPB (Oxford) 2013;15:483-91.
14. Abulkhir A, Limongelli P, Healey AJ, Damrah O, Tait P, Jackson J, et al. Preoperative portal vein embolization for major liver resection: a meta-analysis. Ann Surg 2008;247:49-57.
15. Schnitzbauer AA, Lang SA, Goessmann H, Nadalin S, Baumgart J, Farkas SA, et al. Right portal vein ligation combined with in situ splitting induces rapid left lateral liver lobe hypertrophy enabling 2-staged extended right hepatic resection in small-for-size settings. Ann Surg 2012;255:405-14.
16. Knoefel WT, Gabor I, Rehders A, Alexander A, Krausch M, Schulte Am EJ, et al. In situ liver transection with portal vein ligation for rapid growth of the future liver remnant in two-stage liver resection. Br J Surg 2013;100:388-94.

17. Li J, Girotti P, Konigsrainer I, Ladurner R, Konigsrainer A, Nadalin S. ALPPS in Right Trisectionectomy: a Safe Procedure to Avoid Postoperative Liver Failure? J Gastrointest Surg 2013;17:956-61.
18. Donati M, Stavrou GA, Basile F, Gruttadauria S, Niehaus KJ, Oldhafer KJ. Combination of in situ split and portal ligation: lights and shadows of a new surgical procedure. Ann Surg 2012;256:e11-2.
19. Sala S, Ardiles V, Ulla M, Alvarez F, Pekolj J, de Santibanes E. Our initial experience with ALPPS technique: encouraging results. Updates Surg 2012;64:167-72.
20. Kokudo N, Shindoh J. How can we safely climb the ALPPS? Updates Surg 2013;65:175-7.
21. Gauzolino R, Castagnet M, Blanleuil ML, Richer JP. The ALPPS technique for bilateral colorectal metastases: three "variations on a theme" Updates Surg 2013;65:141-8.
22. Capussotti L, Muratore A, Baracchi F, Lelong B, Ferrero A, Regge D, et al. Portal vein ligation as an efficient method of increasing the future liver remnant volume in the surgical treatment of colorectal metastases. Arch Surg 2008;143:978-82.
23. Schadde E, Ardiles V, Robles-Campos R, Malago M, Machado M, Hernandez-Alejandro R, et al. Early Survival and Safety of ALPPS: First Report of the International ALPPS Registry. Ann Surg 2014;260:829-38.
24. Schadde E, Ardiles V, Slankamenac K, Tschuor C, Sergeant G, Amacker N, et al. ALPPS offers a better chance of complete resection in patients with primarily unresectable liver tumors compared with conventional-staged hepatectomies: results of a multicenter analysis. World J Surg 2014;38:1510-9.
25. Homeyer A, Schenk A, Dahmen U, Dirsch O, Huang H, Hahn HK. A comparison of sampling strategies for histological image analysis. J Pathol Inform 2011;2:S11.
26. Madrahimov N, Dirsch O, Broelsch C, Dahmen U. Marginal hepatectomy in the rat: from anatomy to surgery. Ann Surg 2006;244:89-98.
27. Bertens KA, Hawel J, Lung K, Buac S, Pineda-Solis K, Hernandez-Alejandro R. ALPPS: Challenging the concept of unresectability - A systematic review. Int J Surg 2014;13C:280-7.
28. Schlegel A, Lesurtel M, Melloul E, Limani P, Tschuor C, Graf R, et al. ALPPS: From Human to Mice Highlighting Accelerated and Novel Mechanisms of Liver Regeneration. Ann Surg 2014;260:839-47.
29. Yao L, Li C, Ge X, Wang H, Xu K, Zhang A, et al. Establishment of a rat model of portal vein ligation combined with in situ splitting. PLoS One 2014;9:e105511.
30. Almau Trenard HM, Moulin LE, Padin JM, Stringa P, Gondolesi GE, Barros SP. Development of an experimental model of portal vein ligation associated with parenchymal transection (ALPPS) in rats. Cir Esp 2014;92:676-81.
31. Dhar DK, Mohammad GH, Vyas S, Broering DC, Malago M. A novel rat model of liver regeneration: possible role of cytokine induced neutrophil chemoattractant-1 in augmented liver regeneration. Ann Surg Innov Res 2015;9:11.
32. Fausto N, Campbell JS, Riehle KJ. Liver regeneration. J Hepatol 2012;57:692-4.
33. Furrer K, Tian Y, Pfammatter T, Jochum W, El Badry AM, Graf R, et al. Selective portal vein embolization and ligation trigger different regenerative responses in the rat liver. Hepatology 2008;47:1615-23.

Manuscript III

Intrahepatic Size Regulation in a Surgical Model: Liver Resection-Induced Liver Regeneration Counteracts the Local Atrophy following Simultaneous Portal Vein Ligation

Running title: hypertrophy of portal deprived liver lobe after liver resection

---

Weiwei Wei, Tianjiao Zhang, Haoshu Fang, Olaf Dirsch, Andrea Schenk, André Homeyer, Felix Gremse, Sara Zafarnia, Utz Settmacher and Uta Dahmen

Authorship

First author

Authors' Contribution

W.Wei, O.Dirsch and U.Dahmen contributed to conception and design;

W.Wei, A.Schenk and U.Dahmen for analysis and interpretation;

W.Wei, T.Zhang and H.Fang for data collection and writing the article;

A.Homeyer for providing the analysis tool Histokat;

S. Zafarnia and F. Gremse for CT-imaging;

O.Dirsch, U.Settmacher and U.Dahmen for critical revision of the article;

U.Dahmen, O.Dirsch and A.Schenk for obtaining funding.

European Surgical Research

Technical Note

Intrahepatic Size Regulation in a Surgical Model: Liver Resection-Induced Liver Regeneration Counteracts the Local Atrophy following Simultaneous Portal Vein Ligation

Weiwei Wei[a]   Tianjiao Zhang[a]   Haoshu Fang[a, e]   Olaf Dirsch[b]
Andrea Schenk[c]   André Homeyer[c]   Felix Gremse[d]   Sara Zafarnia[d]
Utz Settmacher[a]   Uta Dahmen[a]

[a]Department of General, Visceral and Vascular Surgery, Jena University Hospital, Jena,
[b]Institute of Pathology, Chemnitz Hospital, Chemnitz, [c]Fraunhofer Institute for Medical
Image Computing MEVIS, Bremen, and [d]Department of Experimental Molecular Imaging,
RWTH Aachen University, Aachen, Germany; [e]Department of Pathophysiology, Anhui
Medical University, Hefei, China

Key Words

Intrahepatic size regulation · Liver regeneration · Partial hepatectomy ·
Portal hyperperfusion · Right portal vein ligation

Abstract

Background/Aim: Liver size regulation is based on the balance between hepatic regeneration and atrophy. To achieve a better understanding of intrahepatic size regulation, we explored the size regulation of a portally deprived liver lobe on a liver subjected to concurrent portal vein ligation (PVL) and partial hepatectomy (PHx). ***Materials and Methods:*** Using a surgical rat model consisting of right PVL (rPVL) plus 70% PHx, we evaluated the size regulation of liver lobes 1, 2, 3, and 7 days after the operation in terms of liver weight and hepatocyte proliferation. Portal hyperperfusion was confirmed by measuring portal flow. The portal vascular tree was visualized by injection of a contrast agent followed by CT imaging of explanted livers. Control groups consisted of 70% PHx, rPVL, and sham operation. ***Results:*** The size of the ligated right lobe increased to 1.4-fold on postoperative day 7 when subjected to rPVL + 70% PHx. The right lobe increased to 3-fold when subjected to 70% PHx alone and decreased to 0.3-fold when subjected to rPVL only. The small but significant increase in liver weight after the combined procedure was accompanied by a low proliferative response. In contrast, hepatocyte proliferation was undetectable in the right lobe undergoing atrophy after PVL only. The caudate lobe in the rPVL + 70% PHx group increased to 4.6-fold, which is significantly more than in the other groups. This increase in liver weight was paralleled by

Uta Dahmen, MD
Department of General, Visceral and Vascular Surgery
Experimental Transplantation Surgery, Jena University Hospital
Drackendorferstrasse 1, DE–07747 Jena (Germany)
E-Mail Uta.Dahmen @ med.uni-jena.de

KARGER

persisting portal hyperperfusion and a prolonged proliferative phase of 3 days. **Conclusions:** A discontinued portal blood supply does not always result in atrophy of the ligated lobe. The concurrent regenerative stimulus induced by 70% PHx seemed to counteract the local atrophy after a simultaneously performed rPVL, leading to a low but prolonged regenerative response of the portally deprived liver lobe. This observation supports the conclusion that portal flow is not necessary for liver regeneration. The persisting portal hyperperfusion may be crucial for the specific kinetics of prolonged liver regeneration after rPVL + 70% PHx in the portally supplied caudate lobe. Both observations deserve more attention regarding the underlying mechanism in further studies.   © 2016 S. Karger AG, Basel

Introduction

Liver regeneration is a clinically important phenomenon. Regeneration is needed to compensate for surgical loss of liver mass after extended resection due to hepatic tumours or living liver donation. However, the risk of acute liver failure is increased after extended hepatectomy in cases of insufficient volume of the future liver remnant (FLR) [1]. Therefore, the size of the FLR is the limiting factor when performing major liver resections.

A number of strategies have been developed in order to increase the size of the FLR. Already in 1920, Rous and Larimore [2] observed that selective occlusion of a branch of the portal vein resulted in atrophy of the ipsilateral lobe and hyperplasia of the contralateral lobe. Portal vein ligation (PVL) and portal vein embolization were subsequently applied to enhance the FLR in patients prior to performing extended critical liver resection.

A normal liver maintains a relatively constant liver size. Previous studies about PVL/ portal vein embolization showed that the relative size of the whole liver is maintained by a balance between atrophy of portally deprived lobes and hypertrophy of portally supplied lobes [2–4]. It seems that this intrahepatic size regulation is achieved on the basis of hepatic regeneration and atrophy. However, it remains unclear how regenerative and atrophic stimuli govern liver size regulation. Considering that the putative primary change to the remnant liver lobes is an alteration in portal flow, it appears that portal venous blood flow plays an important role in the regulation of hepatic regeneration and liver size. It is an argument that either the quantity or the quality of portal perfusion is a decisive factor. Thus, hemodynamic and metabolic load hypotheses were proposed to explain the process of liver regeneration and liver size regulation. The hemodynamic hypothesis refers to the shear stress (portal hyperperfusion) in the hepatic sinusoids, while the metabolic load hypothesis refers to the metabolic demands (concentration of metabolites) imposed on the liver [5, 6].

The contralateral lobe regenerates when receiving a regenerative stimulus due to liver resection or PVL, whereas the ipsilateral lobe undergoes atrophy when receiving an atrophic stimulus induced by PVL. Current experimental studies are limited to the situation where the liver lobe is subjected to one manipulation, either leading to regeneration or leading to atrophy. However, simultaneous PVL and atypical resection of the contralateral lobe is performed in the clinical setting to meet the clinical needs of a given patient [7]. In this case, intrahepatic size regulation is an important clinical issue.

We hypothesized that the regenerating stimulus may override the atrophic stimulus to cover the metabolic demand of the small liver remnant. We developed a surgical model in rats providing concurrent atrophic and proliferative stimuli to the same liver lobe for investigation of lobar and total liver size regulation. Seventy percent partial hepatectomy (70% PHx) was performed to induce regeneration, whereas right PVL (rPVL) was performed to induce atrophy.

127

Wei et al.: Intrahepatic Size Regulation in a Surgical Model: Liver Resection-Induced Liver Regeneration Counteracts the Local Atrophy following Simultaneous PVL

Materials and Methods

Experimental Design

Ninety-six rats were divided randomly into four groups: (1) rPVL + 70% PHx: ligation of the right portal vein in combination with resection of the left lateral and median lobe for investigating size regulation of the right lobe, inflicting regenerative and atrophic stimuli on the right lobe; (2) 70% PHx: resection of the left lateral and median lobe as a positive control to induce regeneration of the right lobe, with only a regenerative stimulus imposed on the remnant lobe; (3) rPVL: ligation of the right portal vein as a negative control to induce atrophy of the right lobe, exerting atrophy on the right lobe, and (4) sham: sham operation as a normal control. Animals from each group were sacrificed at 4 observation time points [postoperative day (POD) 1, 2, 3, or 7; n = 6/group/time point] to investigate the kinetics of hepatic size regulation. Group size calculation was performed following the formula: n = 1 + 2$C(s/d)^2$ (n = 5.3 in our case) [8].

Animals

The animal experiments were performed on inbred male Lewis rats (Charles River, Sulzfeld, Germany) aged 9–10 weeks (body weight 250–300 g). The rats were fed a laboratory diet with water and rat chow available ad libitum throughout the observation period, and they were kept under constant environmental conditions with a 12-hour light-dark cycle in a conventional animal facility using environmentally enriched type IV cages for groups of 2–3 rats.

Ethics Statement

All procedures, experiments, and the housing of the animals adhered to current German regulations and guidelines for animal welfare and to international principles of laboratory animal care, following the ARRIVE Guidelines Checklist as well. The Thüringer Landesamt für Verbraucherschutz, Thuringia, Germany, approved the protocols (approval No. 02-042/10).

Surgical Procedures

All surgical interventions were performed in the daytime under inhalation of 3% isoflurane mixed with pure oxygen at a flow rate of 0.5 litres/min (isoflurane vaporizer; Sigma Delta, UK) in a dedicated S1 operating room. All rats were subjected to laparotomy via a transverse upper abdominal incision. To minimize the proliferative response of ischemic tissue in the stump, the blood supply to the left lateral and median lobe was ligated before 70% PHx. For liver resection, a precise, vessel-oriented, parenchyma-preserving surgical technique was used [9]. rPVL was carefully performed using a 7-0 suture (Prolene; Ethicon, Inc., USA) under an operating microscope (Zeiss, Oberkochen, Germany; magnification ×10–25) to avoid damaging the hepatic artery and bile duct. A colour alteration from light red to dark red was considered as an indicator of portal deprivation. Sham operation involved laparotomy and gentle manipulation as well as dissection of the hepatoduodenal ligament without ligating any vessels. After completing the procedure, the animals were allowed to recover on a heating pad. All animals received analgesic treatment with buprenorphine (0.05 mg/kg body weight, Temgesic; Essex Pharma GmbH, Munich, Germany) every 24 h for a maximum of 2 days after surgery. Daily monitoring was performed and body weights were recorded.

One hour before harvest, 5-bromo-2′-deoxyuridine (BrdU; Sigma-Aldrich, St. Louis, Mo., USA) was injected intravenously via a penile vein (50 mg/kg body weight) to assess hepatocellular proliferation. Portal blood flow was monitored prior to and at all the designated observation time points after rPVL + 70% PHx using a small animal research flowmeter (T106; Transonic Systems, Inc., Ithaca, N.Y., USA). Blood was collected from the infrahepatic vena cava for analysis of liver enzymes. Animals were sacrificed by exsanguination under anaesthesia on POD 1, 2, 3, or 7. The livers were explanted and photo documented. The remnant liver as well as each individual liver lobe was weighed for calculating liver lobe weight recovery. All liver lobes were collected for histological analysis. The four explanted liver lobes [right superior lobe (RSL), right inferior lobe (RIL), caudate superior lobe (CSL), and caudate inferior lobe (CIL)] were marked with tissue colour (Seven Color Kit; Polysciences, Inc., Warrington, Pa., USA) for liver lobe-specific assessment of proliferation.

Portal Flow

Portal blood flow was recorded using a specific Doppler ultrasound probe (CM4; Transonic Systems). The probe was placed gently around the portal vein after having freed the vessel from surrounding tissue. The portal perfusion rate was calculated to determine the extent of hyperperfusion in the portally perfused

Wei et al.: Intrahepatic Size Regulation in a Surgical Model: Liver Resection-Induced Liver Regeneration Counteracts the Local Atrophy following Simultaneous PVL

remnant caudate lobe. It was calculated using the following formula: portal perfusion rate (ml/min/g) = portal flow (ml/min)/weight of portally perfused remnant liver lobes (g).

Body Weight Recovery

The rats were weighed daily. The data were used for plotting a normalized body weight curve. Body weight recovery was calculated using the formula: body weight recovery = body weight at present/body weight at day 0 × 100%.

Liver Enzymes

Blood was taken via puncture of the inferior vena cava using serum tubes (serum Z/1.2 ml, Monovette; Sarstedt, Nümbrecht, Germany). Serum was stored at −20°C until measuring serum levels of aspartate transaminase (AST) and alanine transaminase (ALT) using an automated chemical analyser (Bayer Advia 1650; Bayer, Leverkusen, Germany).

Macroscopic Appearance

The explanted livers were cleaned and placed on a finely calibrated paper in the same position. The primary evaluation was performed by comparison of macroscopic images from all rats.

Liver Weight Adaptation

Liver weight adaptation (hyperplasia or atrophy) was assessed based on the weight of the individual liver lobes in respect to the body weight on day 0. Results are presented as right liver lobe-to-body weight ratio (LBWR) and caudate LBWR. The following formula was used: LBWR = weight of total liver (or individual liver lobe)/body weight on day 0 × 100%.

Relative liver weight adaptation was calculated by dividing the individual LBWR of the experimental group by the individual LBWR of the sham group at a given observation time point and is expressed as fold change. The following formula was used: relative liver weight adaptation$_{exp.}$ = LBWR of experimental group/LBWR of sham group at a given observation time point.

For the sham group, the LBWR at a given POD was divided by the LBWR on day 0. The LBWR on day 0 was obtained from 6 normal animals which were sacrificed and the livers of which were explanted and dissected into the respective liver lobes (POD 0). The following formula was used: relative liver weight adaptation$_{sham}$ = LBWR at a given observation time point/LBWR on day 0.

Haematoxylin-Eosin Staining

Liver tissue from each liver lobe was fixed in 4.5% buffered formalin for 48 h. Sections, 4-μm thick, were cut after paraffin embedding. Sections from all four liver lobes were placed on one slide. Thereafter, the slides were stained with haematoxylin-eosin (HE) for routine histological examination. All 4 sections were arranged on one glass slide, allowing simultaneous staining to ensure the same staining quality. All slides were digitalized using a slide scanner (Nanozoomer; Hamamatsu Electronic Press Co., Ltd., Iwata, Japan). Morphological analysis focussed on the detection of single-cell necrosis, confluent necrosis, and sinusoidal dilatation as often-reported effects of PVL, as well as on the detection of signs indicative of hepatic outflow obstruction [5, 6].

Immunohistochemistry (BrdU Staining)

Slides were subjected to BrdU staining for evaluation of hepatocyte proliferation. The staining procedure was based on a modified protocol by Sigma-Aldrich [10]. Whole-slide scans were performed using the same Hamamatsu slide scanner as mentioned above.

Assessment of the Proliferation Index

Proliferation was assessed in the portally deprived liver lobes (RSL and RIL) in comparison to the portally supplied liver lobes (CSL and CIL). The proliferation was separately quantified for all 4 tissue sections on the slide, using the Histokat software (Fraunhofer MEVIS, Bremen, Germany). The algorithm for nucleus detection is based on the method described by Homeyer et al. [11]. The software automatically identifies unstained (negative) hepatocyte nuclei, stained (positive) hepatocyte nuclei, and other non-hepatocyte nuclei based on colour, roundness, and size features. The resulting proliferation index – that is, the fraction of proliferating hepatocyte nuclei to the total number of hepatocyte nuclei – is expressed as percentage (accurate to 0.1%; see online suppl. table S1; for all online suppl. material, see www.karger.com/doi/10.1159/000446875).

Visualization of Portal Blood Supply

An additional 3 animals were subjected to this imaging study. The portal blood supply to the remnant liver was visualized, using an imaging approach immediately and 7 days after rPVL + 70% PHx, as well as the portal vascular tree before operation. Contrasting the vascular tree was achieved by injecting a silicone radiopaque contrast agent (Microfil; Flow Tech, Inc., Carver, Mass., USA) into the portal vein. Subsequently, the explanted livers were subjected to formalin fixation, and the specimens were scanned using the scan protocol HQD-6565-390-90 with 720 projections (approx. 1,032 × 1,012 pixels) during one full rotation with a scanning time of 90 s per subscan (TomoScope Duo CT; CT Imaging GmbH, Erlangen, Germany). Three-dimensional renderings were performed using the Imalytics Preclinical Software [12]. The scans resulted in voxel image representations of the specimens at an isotropic resolution of 70 μm. The LiverAnalyzer (Fraunhofer MEVIS) was used for further segmentation and visualization.

Statistical Analysis

The data, expressed as means ± standard deviations, were analysed using Sigmaplot 10.0 (Statcon, Witzenhausen, Germany). Differences between paired groups were analysed using the two-tailed paired-samples Student t test, and multiple groups were compared using one-way independent ANOVA. Differences were considered significant if a p value of <0.05 was obtained.
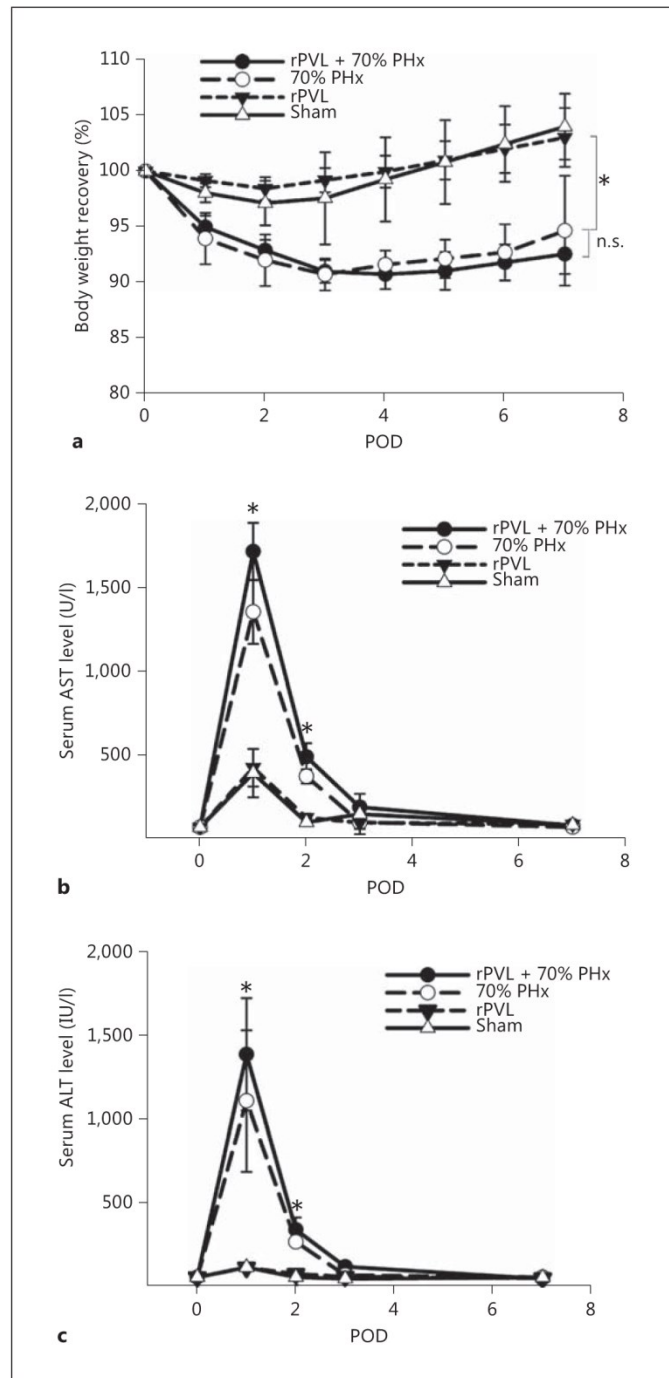
Results

The rPVL + 70% PHx Model Is a Stable and Reliable Model for Studying Intrahepatic Liver Size Regulation

All animals tolerated the procedure well. Surgical stress to the animals, as assessed by body weight loss and recovery, was similar in the sham and rPVL groups as well as in the two PHx groups (fig. 1a). As expected, resection was associated with a higher body weight loss, more severe hepatic damage in terms of liver enzymes, and a prolonged body weight recovery period compared to the sham and ligation-only groups. Additional rPVL did not exert additional stress on the liver-resected animals. Body weight recovery started in all groups by POD 3. Animals subjected to rPVL and sham operation reached their starting weight within 5 days, whereas animals subjected to 70% PHx or rPVL + 70% PHx had delayed body weight recovery and reached about 95% within the observation time of 1 week (94.7 ± 4.9 and 92.5 ± 1.8%, respectively, p > 0.05).

Hepatic damage, as indicated by the release of liver enzymes, was also similar in the two PHx groups (fig. 1b, c). However, as expected, liver resection was associated with higher hepatic damage compared to rPVL on POD 1 and POD 2 (p < 0.05). The levels of liver enzymes in all groups decreased to the normal range within 3 days without any difference between groups on POD 3 (p > 0.05), corresponding to the initiation of body weight recovery.

Liver Resection-Induced Liver Regeneration Counteracts the Local Atrophy following Simultaneous PVL

Portal vein deprivation leads to liver atrophy. We observed that rPVL caused a substantial loss of weight in the portally deprived liver lobe (reduction to nearly 30% of the original weight on POD 7). We did not find any obvious change in hepatic histomorphology in either of the portally ligated right lobes – neither after rPVL nor after rPVL + 70% PHx. We did not see any single-cell necrosis, confluent necrosis, or sinusoidal dilatation in the ligated lobes. However, we observed a low proliferative activity indicated by rarely occurring BrdU-positive hepatocytes. 70% PHx caused an increase in liver weight (around 3-fold), as expected (fig. 2, 3a). Abundant mitotic figures were seen especially on POD 1, reflecting a high proliferative activity, as also seen in BrdU staining.

130

Wei et al.: Intrahepatic Size Regulation in a Surgical Model: Liver Resection-Induced
Liver Regeneration Counteracts the Local Atrophy following Simultaneous PVL

Fig. 1. a Body weight recovery curve during the time of observation. Body weight recovery was faster in the rPVL and sham groups than in the rPVL + 70% PHx and 70% PHx groups. There was no significant difference between the 70% PHx and rPVL + 70% PHx groups (n.s., p > 0.05; n = 6 animals/group/time point). **b, c** AST (**b**) and ALT (**c**) release after the different surgical interventions at all observation time points. In the rPVL + 70% PHx and 70% PHx groups, surgery caused significantly more damage than in the rPVL and sham groups. The levels of AST and ALT were significantly higher in the rPVL + 70% PHx and 70% PHx groups on POD 1 and POD 2 (* p < 0.05; n = 6 animals/group/time point). n.s. = Not significant.

Portal vein deprivation did not prevent liver regeneration, but it altered the kinetics of hepatocyte proliferation. Interestingly, the right lobe did not undergo atrophy after rPVL + 70% PHx but increased to about 1.4-fold of the original size after 7 days. This increase was accompanied by a slight and delayed increase in proliferation index of up to 5%, which was
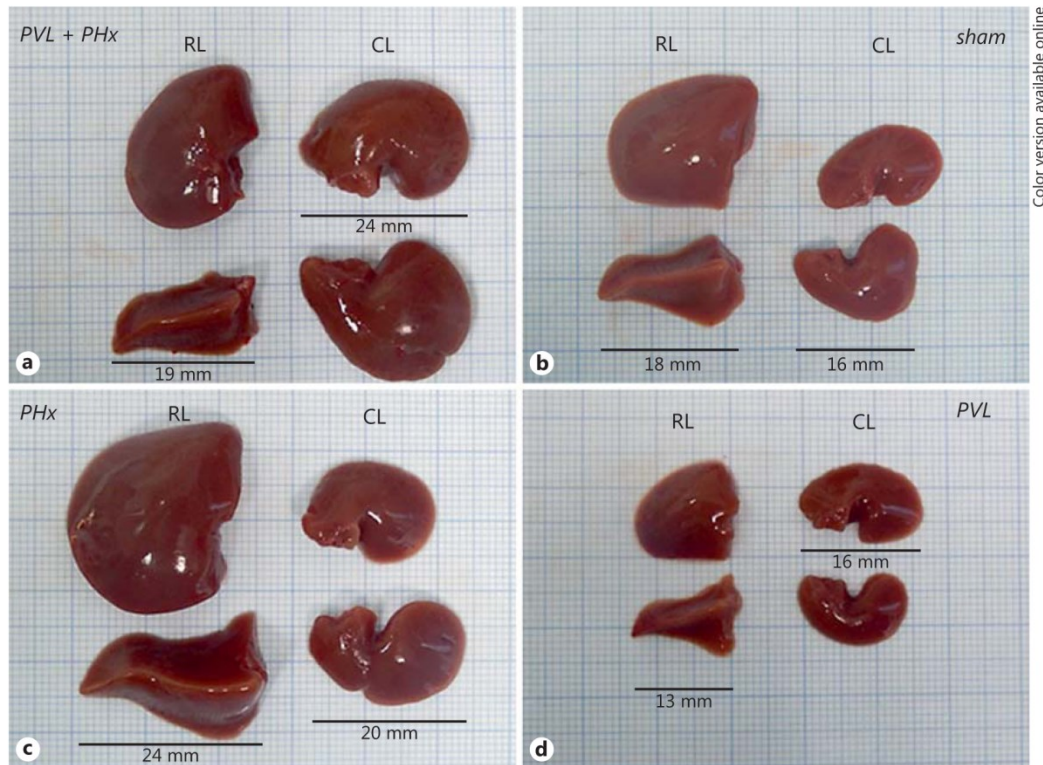
Fig. 2. Macroscopic appearance of the relevant liver lobes 7 days after surgery. The portally ligated right lobe (RL) increased slightly and the portally supplied caudate lobe (CL) increased remarkably in the rPVL + 70% PHx group (**a**) compared with the normal control group (**b**). After 70% PHx, all the remnant liver lobes increased remarkably in size (**c**). The RL decreased remarkably in size in the rPVL group (**d**). Scale: minimal grid = 1 × 1 × 1 mm. Representative pictures from one of the 6 animals of each group.

noted on POD 2, later and on a lower level than after PHx. Hepatocyte proliferation after 70% PHx reached nearly 30% on POD 1 and declined thereafter (fig. 3b). These observations support the conclusion that portal flow is not necessary for liver regeneration but influences the kinetics of hepatocyte proliferation.

Lack of atrophy or the slight increase in size cannot be attributed to the formation of portoportal collaterals. The portal venous tree was visualized in normal animals and at 2 time points after rPVL + 70% PHx: immediately and 7 days after the operation (fig. 4). In normal animals, the right portal vein and the caudate portal vein appeared as expected as two distinct vessels without any collaterals. Immediately after the combined procedure, the caudate portal vein was clearly visible, whereas the ligated right portal vein was not contrasted and did not appear on the CT image or the reconstructed vascular tree. On POD 7, the caudate portal vein appeared elongated, whereas the right portal vein was still invisible. No collaterals were visualized either between the right lobe and the caudate lobe or between the right lobe and the paracaval liver portion. The small portal vessels supplying the paracaval liver and the stumps also elongated in parallel with the increase in stump volume.
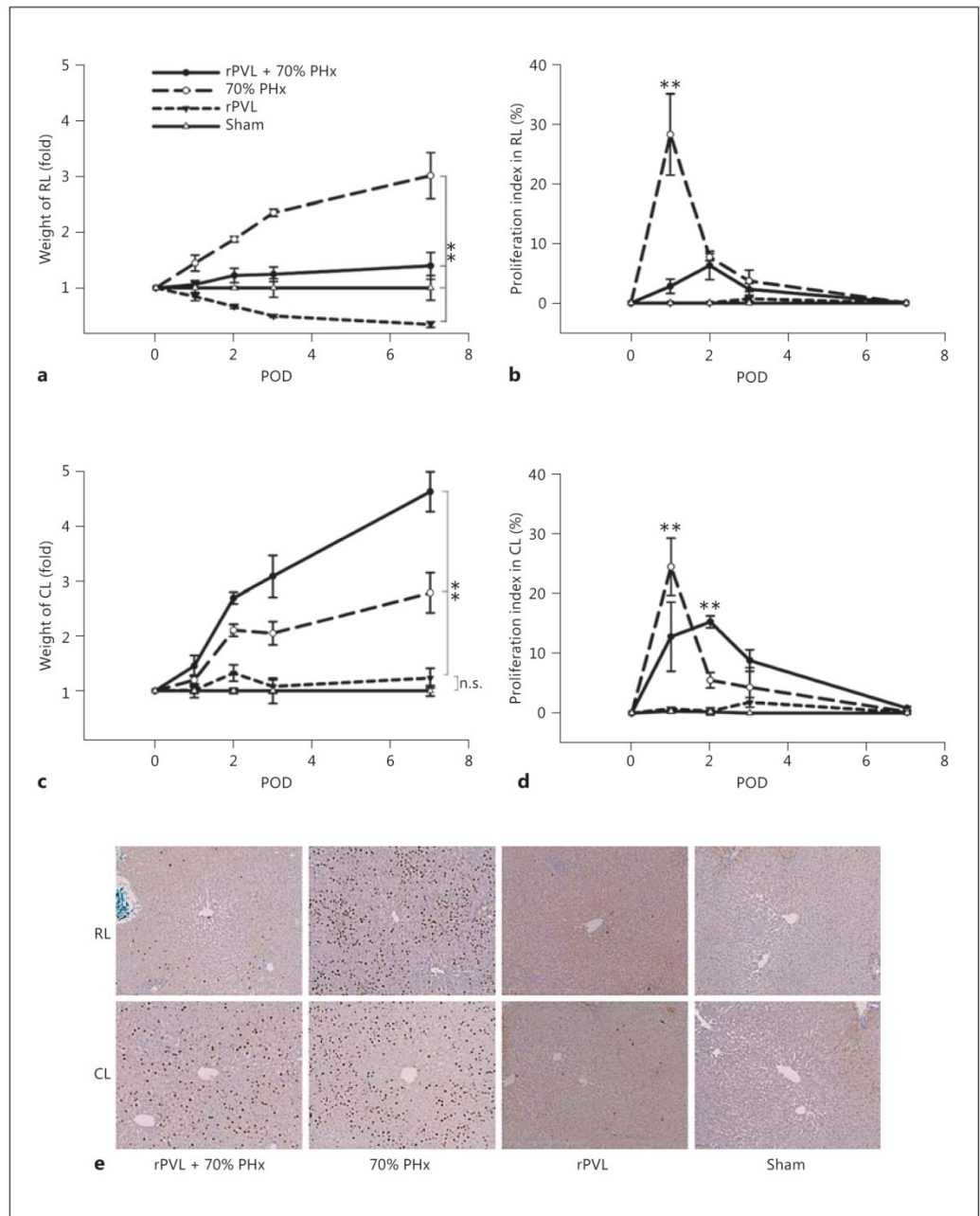
Color version available online

Fig. 3. Relative liver weight adaptation and hepatocyte proliferation in the ligated right lobe (RL; **a**, **b**) and the non-ligated caudate lobe (CL; **c**, **d**). In the rPVL + 70% PHx group, the RL increased slightly but significantly in size instead of presenting obvious shrinkage (**a**). The RL increased significantly in the 70% PHx group and decreased significantly in case of rPVL (** $p < 0.01$; n = 6 animals/group/time point). The CL increased significantly only after rPVL + 70% PHx and 70% PHx on POD 7 (** $p < 0.01$; n = 6 animals/group/time point), but not after rPVL (**c**). Both the RL and the CL had a moderate and prolonged regenerative response in the rPVL + 70% PHx group. The peak of the proliferation index was delayed in case of rPVL + 70% PHx (**b**, **d**). Immunohistochemistry (**e**; Brdu staining; magnification ×100) presents the proliferation index at 24 h. Representative pictures from one of the 6 animals of each group. n.s. = Not significant.
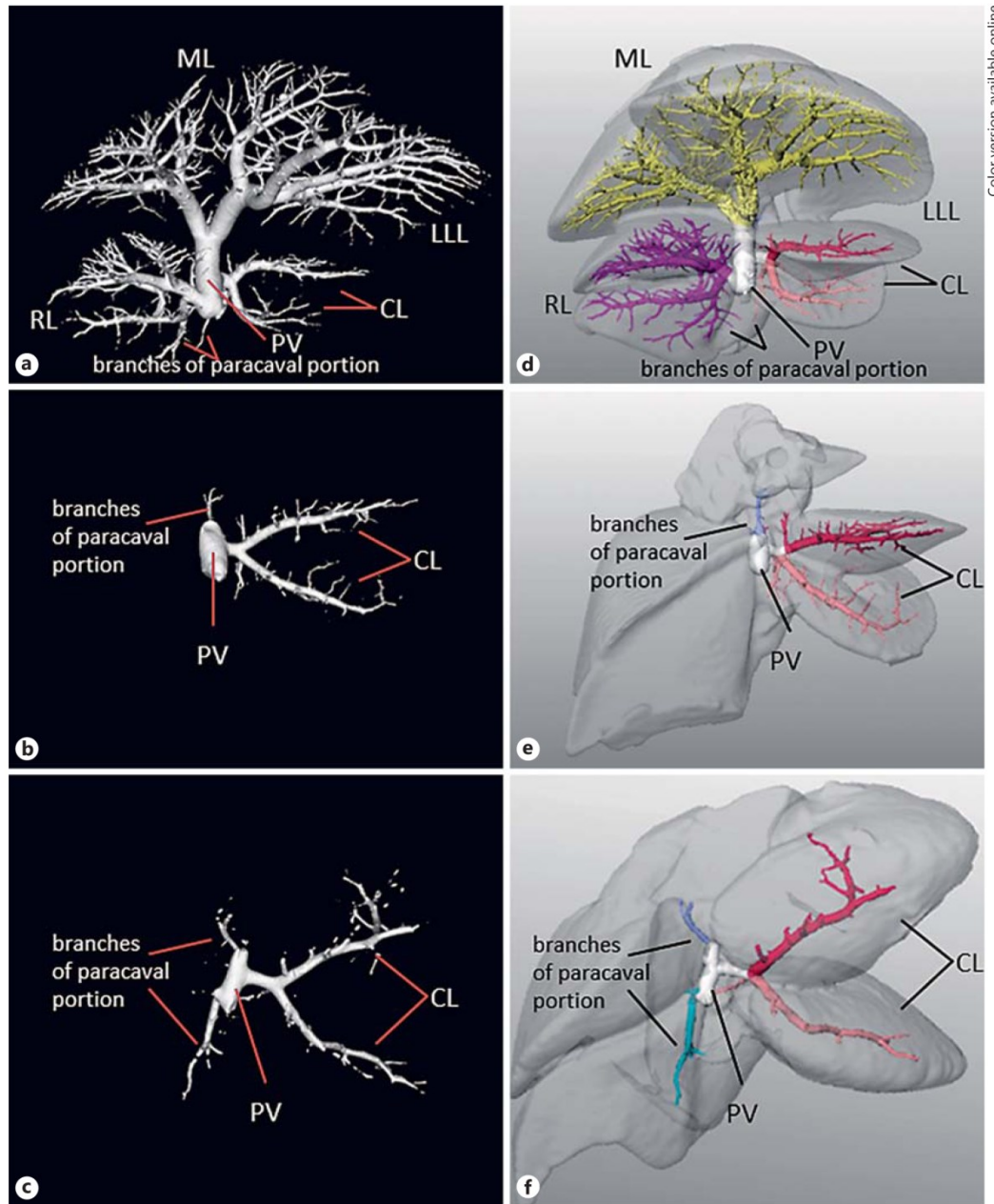
Fig. 4. Visualization of the portal vascular tree before, immediately after, and 7 days after rPVL + 70% PHx. Before operation, the right portal vein (PV) was well perfused (**a**, **d**). Immediately after rPVL + 70% PHx, the right PV was not perfused (**b**, **e**). There was still no portal perfusion in the right lobe after 7 days (**c**, **f**). ML = Median lobe; LLL = left lateral lobe; RL = right lobe; CL = caudate lobe.

Wei et al.: Intrahepatic Size Regulation in a Surgical Model: Liver Resection-Induced
Liver Regeneration Counteracts the Local Atrophy following Simultaneous PVL

Fig. 5. Portal perfusion rate of the caudate lobe in the rPVL + 70% PHx group. Portal inflow perfused only the non-ligated caudate lobe after rPVL + 70% PHx, because of the portal deprivation of the right lobe. The values before and 7 days after the operation were about 2 ml/min/g. The portal perfusion rate was significantly increased on POD 1, POD 2, and POD 3 (** p < 0.01; n = 6 animals/time point). It reached the peak on POD1 and decreased on POD2 and POD3 but maintained a high level.
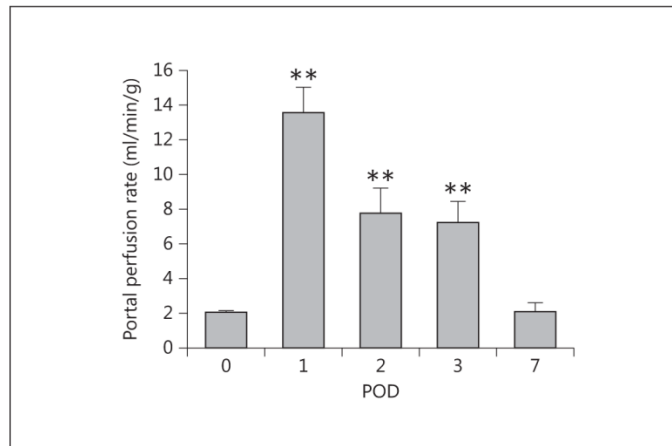
Regeneration in the Portally Supplied Caudate Lobe Was Increased by a Concurrent Atrophic Stimulus to the Deportalized Right Lobe

The caudate lobe tripled its mass after 70% PHx by POD 7 (fig. 3c). No obvious alterations in hepatic morphology were observed – especially no signs of hepatic outflow obstruction (image not shown) – confirming that the 70% PHx had indeed been performed properly. After portal deprivation of an additional 20% of the liver mass by ligating the right portal vein, the liver weight recovery of the caudate lobe increased remarkably to almost 4.6-fold (p < 0.01 vs. control). This increase in liver weight was accompanied by a lower but longer proliferative response compared to simple 70% PHx. The peak of the proliferation index with 15 ± 5% was reached on POD 2, whereas the peak after 70% PHx reached 25 ± 4% and was observed on POD 1 (fig. 3d, e). The proliferative activity remained high with a proliferation index of 10% on POD 3 in the rPVL + 70% PHx group, which was significantly higher than the 5% observed in the 70% PHx group (p < 0.05).

The prolonged proliferative phase during regeneration of the caudate lobe was accompanied by a slow recovery from portal hyperperfusion (fig. 5). Portal hyperperfusion persisted until POD 3, as did hepatocyte proliferation. The maximum of 13.63 ± 1.39 ml/min/g was reached on POD 1; it decreased to 7.79 ± 1.42 ml/min/g on POD 2 and remained within the same range (7.28 ± 1.17 ml/min/g) on POD 3 (p < 0.01). Portal flow returned to normal with a flow rate of about 2 ml/min/g on POD 7 (p > 0.05 vs. before operation).

Discussion

The development of complex surgical strategies in clinical practice, such as two-stage hepatectomy or ALPPS (associating liver partition and PVL for staged hepatectomy), calls for a deep understanding of intrahepatic size regulation. Previous studies regarding liver size regulation were limited to the situation where a given liver lobe was subjected to PVL only, PHx only, or PVL followed by PHx. Therefore, we extended the existing model of PVL by adding a concurrent 70% liver resection. Doing so, we subjected the ligated right lobe to two concurrent signals and the caudate lobe to an augmented regeneration stimulus.

This novel, combined procedure turned out to be suitable to study liver size regulation. The body weight recovery and the level of serum transaminases implied that the animals tolerated all procedures well. rPVL did neither affect body weight recovery nor the release of

135

serum transaminases compared to the sham operation. This indicates that liver function was not impaired after rPVL in our study, as was also reported by Mueller et al. [13]. They stated that the regressive lobe did not lose its functional integrity after portal occlusion. However, Furrer et al. [14] reported a significant elevation of serum AST after 70% PVL. Apparently, the impact of portal deprivation on a small liver lobe is not as noticeable as that on a major liver lobe. Taken together, combining PVL and PHx opens a new avenue to study intrahepatic size regulation.

A Concurrent Regenerative Stimulus Prevents Atrophy in the Portally Deprived Lobe

Atrophy in the ligated right lobe was prevented by simultaneous 70% PHx. Currently, two hypotheses regarding the initiation of liver atrophy and regeneration are discussed: (1) decreased intrahepatic shear stress leads to apoptosis [15], whereas elevated shear stress due to portal hypertension triggers hepatocyte proliferation [16–20], and (2) a decreased metabolic demand imposed on the individual liver lobe leads to atrophy, whereas an increased metabolic load imposed on the residual liver triggers hepatocyte proliferation after PHx or PVL [5, 6].

The novel finding of our study is that hepatic atrophy subsequent to PVL is counteracted. The deportalized right lobe underwent hyperplasia instead, albeit not as pronounced as after 70% PHx. Proliferation in the deportalized lobe was not due to portal supply via pre-existing or newly formed collaterals, since we did not identify any collaterals between the ligated right lobe and the non-ligated lobe. Hence, portal hyperperfusion as a driving force for regeneration of the right lobe could be excluded. This finding suggests that atrophy and hyperplasia interweave in the same lobe. It seems that the slightly increased size of the right liver lobe results from balancing a slight atrophic stimulus and a strong regenerative stimulus.

Portal Flow Is Not Necessary for Liver Regeneration

Portal hyperperfusion is important in initiating liver regeneration, but not necessarily the only and indispensable factor. It was noticeable that the proliferative stimulus induced by the additional 70% PHx resulted in a prolonged but not drastic proliferative response in the portally supplied caudate lobe. Similar results were previously observed after an extended loss of liver mass such as after 90% PHx or 90% PVL [20, 21]. Excessive hyperperfusion of the portal vein was suggested as probably accounting for the lesser degree of regeneration [22]. This observation confirmed that portal hyperperfusion is of importance for liver regeneration, as well as for the initiation and maintenance of hepatocyte proliferation. This observation also supports the hypothesis that a prolonged proliferative response might be required to make up for the extended loss. Even simultaneous division of all hepatocytes in the remaining 10% of the liver would not be sufficient to recover the original liver mass. Therefore, several cell cycles are possibly needed to restore the original liver mass.

Unexpectedly, additional 70% PHx also resulted in a moderate and prolonged proliferative response in the portally deprived right lobe. In this case, the moderate proliferation index in the portally deprived right lobe suggested that portal perfusion cannot be the sole factor for inducing and maintaining liver regeneration. According to the hepatic arterial buffer response, a lack of portal supply leads to an increase in hepatic arterial supply [23, 24]. The increased arterial supply reflected the increased shear stress in the sinusoids and might contribute to the initiation of liver regeneration. Interestingly, the kinetics of regeneration in the portally deprived right lobe after rPVL + 70% PHx was different from the proliferation kinetics after standard 70% PHx, with a sharp peak at 24 h after the operation. The proliferative response of the ligated right lobe followed a different time course, with a delayed maximum at 48 h. This observation could be attributed to the enhanced energy demand of proliferating cells, which cannot be fully met when relying solely on arterial perfusion but

136

lacking the nutrient-rich portal blood. Portal blood is much richer in dissolved nutrients such as glucose than arterial blood. A lack of nutrients from portal blood could alter the proliferative response [25].

Perspective for Future Studies

We hypothesize that regenerating portally deprived lobes receive signals for both atrophy and regeneration, and that they undergo both hepatocyte apoptosis and proliferation. Therefore, we plan to investigate apoptosis using TUNEL and caspase staining in addition to assessing proliferation. We are also planning on providing further elucidation regarding the underlying molecular mechanism. We would like to investigate the cytokine and growth factor network by looking at the balance of gene and protein expression over time in the different liver lobes. We would expect a higher expression of apoptosis-relevant factors in the liver lobes subjected to atrophy only (caspase-2, -3, and -9) and a higher expression of regeneration-relevant factors (TNF-α, IL-6, HGF, and c-Met) in the lobes subjected to regeneration only.

HGF/c-Met signalling is essential for initiating the cell cycle after PHx [26, 27]. The activated HGF/c-Met signalling pathway stimulates hepatocyte DNA synthesis via an endocrine or paracrine mechanism. It was reported that the level of plasma HGF was elevated sharply and reached a peak within 1 h after PHx and stayed at a high level for more than 3 days [28]. In the portally deprived right lobe after rPVL + 70% PVL, which also receives a regeneration stimulus, we would expect a merged gene and protein expression profile.

Conclusions

Our newly established combination of rPVL and 70% PHx represents a suitable model to study the interaction between hepatic atrophy and hepatic regeneration. The systemic regenerative stimulus induced by liver resection counteracted the local atrophic stimulus from PVL. It led to hyperplasia in both portally ligated and portally supplied lobes.

Based on these observations, two conclusions are drawn: (1) lack of portal perfusion and a decreased metabolic load cannot be the key stimulus for hepatic atrophy, since the portally ligated lobe did not decrease in size, and (2) portal hyperperfusion and shear stress cannot be the key mechanism of liver regeneration in the rPVL + 70% PHx model either, since the portally ligated lobe did actually increase in size. Our findings suggest focusing on more mechanistic studies to better understand intrahepatic size regulation.

Acknowledgements

Disclosure Statement

The authors report no conflicts of interest.

References

1 Qiu J, Chen S, Pankaj P, Wu H: Portal vein arterialization as a bridge procedure against acute liver failure after extended hepatectomy for hilar cholangiocarcinoma. Surg Innov 2014;21:372–375.

2 Rous P, Larimore LD: Relation of the portal blood to liver maintenance: a demonstration of liver atrophy conditional on compensation. J Exp Med 1920;31:609–632.

3 Gock M, Eipel C, Linnebacher M, Klar E, Vollmar B: Impact of portal branch ligation on tissue regeneration, microcirculatory response and microarchitecture in portal blood-deprived and undeprived liver tissue. Microvasc Res 2011;81:274–280.

4 Rozga J, Jeppsson B, Bengmark S: Portal branch ligation in the rat. Reevaluation of a model. Am J Pathol 1986; 125:300–308.

5 Schoen JM, Wang HH, Minuk GY, Lautt WW: Shear stress-induced nitric oxide release triggers the liver regeneration cascade. Nitric Oxide 2001;5:453–464.

6 Hohmann N, Weiwei W, Dahmen U, Dirsch O, Deutsch A, Voss-Böhme A: How does a single cell know when the liver has reached its correct size? PLoS One 2014;9:e93207.

7 Donati M, Stavrou GA, Oldhafer KJ: Current position of ALPPS in the surgical landscape of CRLM treatment proposals. World J Gastroenterol 2013;19:6548–6554.

8 Dell RB, Holleran S, Ramakrishnan R: Sample size determination. ILAR J 2002;43:207–213.

9 Madrahimov N, Dirsch O, Broelsch C, Dahmen U: Marginal hepatectomy in the rat: from anatomy to surgery. Ann Surg 2006;244:89–98.

10 Wei W, Zhang T, Zafarnia S, Schenk A, Xie C, Kan C, Dirsch O, Settmacher U, Dahmen U: Establishment of a rat model: associating liver partition with portal vein ligation for staged hepatectomy. Surgery 2016;159:1299–1307.

11 Homeyer A, Schenk A, Arlt J, Dahmen U, Dirsch O, Hahn HK: Fast and accurate identification of fat droplets in histological images. Comput Methods Programs Biomed 2015;121:59–65.

12 Gremse F, Stärk M, Ehling J, Menzel JR, Lammers T, Kiessling F: Imalytics Preclinical: interactive analysis of biomedical volume data. Theranostics 2016;6:328–341.

13 Mueller L, Grotelueschen R, Meyer J, Vashist YK, Abdulgawad A, Wilms C, Hillert C, Rogiers X, Broering DC: Sustained function in atrophying liver tissue after portal branch ligation in the rat. J Surg Res 2003;114:146–155.

14 Furrer K, Tian Y, Pfammatter T, Jochum W, El Badry AM, Graf R, Clavien PA: Selective portal vein embolization and ligation trigger different regenerative responses in the rat liver. Hepatology 2008;47:1615–1623.

15 Sato Y, Tsukada K, Hatakeyama K: Role of shear stress and immune responses in liver regeneration after a partial hepatectomy. Surg Today 1999;29:1–9.

16 Niiya T, Murakami M, Aoki T, Murai N, Shimizu Y, Kusano M: Immediate increase of portal pressure, reflecting sinusoidal shear stress, induced liver regeneration after partial hepatectomy. J Hepatobiliary Pancreat Surg 1999;6:275–280.

17 Abshagen K, Eipel C, Vollmar B: A critical appraisal of the hemodynamic signal driving liver regeneration. Langenbecks Arch Surg 2012;397:579–590.

18 Michalopoulos GK: Liver regeneration after partial hepatectomy: critical analysis of mechanistic dilemmas. Am J Pathol 2010;176:2–13.

19 Fausto N, Campbell JS, Riehle KJ: Liver regeneration. Hepatology 2006;43:S45–S53.

20 Sato Y, Koyama S, Tsukada K, Hatakeyama K: Acute portal hypertension reflecting shear stress as a trigger of liver regeneration following partial hepatectomy. Surg Today 1997;27:518–526.

21 Li K, Qi X, Yang J, Gong J, Tan C, Xia Q, Long J, Wang Z: Losartan supports liver regrowth via distinct boost of portal vein pressure in rodents with 90% portal branch ligation. Dig Dis Sci 2013;58:2205–2211.

22 Schleimer K, Stippel DL, Kasper HU, Tawadros S, Allwissner R, Gaudig C, Greiner T, Hölscher AH, Beckurts KT: Portal hyperperfusion causes disturbance of microcirculation and increased rate of hepatocellular apoptosis: investigations in heterotopic rat liver transplantation with portal vein arterialization. Transplant Proc 2006; 38:725–729.

23 Lautt WW: Regulatory processes interacting to maintain hepatic blood flow constancy: vascular compliance, hepatic arterial buffer response, hepatorenal reflex, liver regeneration, escape from vasoconstriction. Hepatol Res 2007;37:891–903.

24 Rocheleau B, Ethier C, Houle R, Huet PM, Bilodeau M: Hepatic artery buffer response following left portal vein ligation: its role in liver tissue homeostasis. Am J Physiol 1999;277:G1000–G1007.

25 Ding X, Beier JI, Baldauf KJ, Jokinen JD, Zhong H, Arteel GE: Acute ethanol preexposure promotes liver regeneration after partial hepatectomy in mice by activating ALDH2. Am J Physiol Gastrointest Liver Physiol 2014; 306:G37–G47.

26 He Y, Long J, Zhong W, Fu Y, Li Y, Lin S: Sustained endoplasmic reticulum stress inhibits hepatocyte proliferation via downregulation of c-Met expression. Mol Cell Biochem 2014;389:151–158.

27 Michalopoulos GK: Liver regeneration. J Cell Physiol 2007;213:286–300.

28 Michalopoulos GK, DeFrances MC: Liver regeneration. Science 1997;276:60–66.

Manuscript IV

Simultaneous liver resection suppressed hepatic apoptosis after portal vein ligation and determined the size of the deportalized liver lobe in the rat

Weiwei Wei, Tianjiao Zhang, Olaf Dirsch, Felix Gremse, Sara Zafarnia, André Homeyer, Utz Settmacher, Uta Dahmen

Authorship

First author

Authors' Contribution

W.Wei, O.Dirsch and U.Dahmen contributed to conception and design;

W.Wei, T.Zhang and U.Dahmen for analysis and interpretation;

W.Wei, T.Zhang and S.Zafarnia for data collection;

F.Gremse and S.Zafarnia for CT-imaging and 3D reconstruction;

A. Homeyer for providing the analysis tool;

W.Wei and T.Zhang for writing the article;

O.Dirsch, U.Settmacher and U.Dahmen for critical revision of the article;

U.Dahmen and O.Dirsch for obtaining funding.

Abstract

Background: Portal vein ligation (PVL) and atypical resection are usually performed as a first operation of two-stage hepatectomy to cure liver tumors. A large number of patients fail to undergo sufficient hypertrophy of the unligated regenerating lobe and atrophy of the deportalized lobe. However, the role of the additional resection in this complex process of intrahepatic size regulation remains unclear. This study aims for investigating the effects of the additional partial hepatectomy (PHx) on size regulation of the deportalized liver lobe when performing simultaneous PVL+PHx.

Methods: Lewis-rats were subjected to either 20%,70% or 90%PHx respectively PVL as control or to a combined procedure consisting of 20%PVL+70%PHx respectively 70%PVL+20%PHx. Relative weights of liver lobes, proliferation index (PI) and apoptotic density were assessed. Explanted livers were subjected to computer-tomography to investigate formation of collaterals.

Results: After the combined procedure, size of non-ligated liver increased 4-fold(maximal PI>15%). Size of the ligated lobe increased to140% after small ligation+large resection but decreased to75% after large ligation+small resection, whereas maximal PI was similarly low (6.3% versus 3.6%). However, apoptotic density in the portally-deprived lobes was related to the extent of PHx (3cells/mm^2 after 20%PVL+70%PHx compared to14cells/mm^2 after 70%PVL+20%PHx). Here, size regulation was associated with formation of extrahepatic collaterals as also observed after 90%PVL, where size reduction and apoptotic density was less pronounced than after 20% or 70%PVL.

Conclusions: The additional liver resection seemed to counteract the local atrophy in a PHx-extent-dependent way by suppressing hepatic apoptosis, possibly facilitated by the reestablishment of extrahepatic porto-portal collaterals.

Keywords: intrahepatic size regulation, portal vein ligation, partial hepatectomy, hepatocyte proliferation, apoptosis

Summary for surgical relevance

Portal vein ligation (PVL) with simultaneous atypical resection was adopted in selected patients with primarily non-resectable liver tumors. Better understanding of intrahepatic size regulation in case of concurrent PVL and liver resection may help to develop clinical strategies of promoting liver regeneration and avoiding postoperative liver failure.

Our study indicated that interaction of proliferation and apoptosis seemed to regulate the intrahepatic size adjustment. Simultaneous liver resection is not only inducing hepatocyte proliferation in the ligated lobe but also suppressing hepatic apoptosis remarkably leading to a less pronounced atrophy of deportalized lobe. Furthermore, liver regeneration was enhanced after PVL and simultaneous liver resection compared to an extended PVL only.

These observations support that an atypical resection combined with moderate portal vein ligation leads to better tolerance of the liver to extended hepatectomy in comparison to a single major PVL. This could serve as an additional argument of removing more tumor-bearing liver in the first stage-operation.

Introduction:

Liver resection is the best curative strategy to treat liver tumors and metastases[1, 2]. Loss of liver mass due to partial hepatectomy (PHx) is compensated by the regenerative capacity of remnant liver to restore liver volume and function. However, extended hepatectomy may result in insufficient future liver remnant mass, associated with hepatic dysfunction and acute postoperative liver failure. To reduce the risk of fulminant liver failure, portal vein ligation (PVL) of the diseased liver has been established as one optional strategy. After PVL, the portally-supplied future remnant liver lobes undergo compensatory hypertrophy[3], which significantly improves the tolerance to extended hepatectomy[4]. However, the extent of hypertrophy seems to be unpredictable. Previous reports[5, 6] demonstrated that about one third of patients undergoing portal vein occlusion do not proceed to liver resection, mostly due to insufficient liver regeneration.

Insufficient liver regeneration may have several reasons: insufficient size or impaired tissue quality of the future remnant liver and collateral formation between the ligated and the non-ligated liver[7, 8]. The formation of interlobe porto-portal neocollaterals after PVL was postulated to reduce the extent of atrophy in the portally-deprived lobe and to reduce the hypertrophy in the portally-supplied lobe[9, 10]. This leads to an interest in the interaction of liver regeneration and hepatic atrophy.

Recently, some studies focused on liver regeneration not only in terms of proliferation but also in terms of apoptosis. Zhou[11] reported that the balance between hepatocyte proliferation and apoptosis is critical for liver homeostasis during liver regeneration. Köhler[12] investigated hepatocytes proliferation and apoptosis after PHx to assess liver regeneration. It is not clear how the contradictory processes govern the intrahepatic size regulation. Further studies are needed to better understand the regulatory processes. Understanding is not only scientifically interesting, but also important to better modulate liver regeneration to the need of the patient.

We observed previously that loss of liver mass due to PHx represents a proliferation stimulus not only to the portally-supplied lobe but also to the portally-deprived lobe[13]. We questioned to which extent the additional PHx might exert a regenerative effect on the portally-deprived lobe. To investigate this question, we extended our previous study of concurrent PVL and PHx. We designed an experiment to elucidate the effects of two concurrent stimuli of different extent on the size regulation of the portally-deprived lobe. Furthermore, explanted

livers injected with contrast polymer were subjected to computer-tomography imaging to investigate collateral formation.

Methods:

Animals

Animal experiments were performed in inbred male Lewis Rats (Charles River, Sulzfeld, Germany) aged 9-10 weeks (body weight 250-300g). Rats were fed a laboratory diet with water and rat chow ad libitum until harvest and were kept under constant environmental conditions with a 12h light–dark cycle in a conventional animal facility until harvest.

Ethics statement

All procedures and housing of the animals were performed according to current German regulations and guidelines for animal welfare and the ARRIVE Guidelines for Reporting Animal Research [14]. The Thüringer Landesamt für Verbraucherschutz, Thuringia, Germany approved the protocols (Approval-Number: 02-024/13).

Experimental design

Seventy-two male Lewis rats were enrolled randomly into 3 groups with partial hepatectomy (PHx). Liver resections of different extent (20%PHx, 70%PHx and 90%PHx) were performed to determine the strength of regenerative stimulus on the size regulation of the remnant liver. Another 72 rats were subjected to 20%PVL, 70%PVL and 90%PVL to determine the correlation between the extent of ligation and atrophy. Additional 48 rats were allocated into two groups to further investigate the effect of the two concurrent stimuli on the size regulation: **(i) 20%PVL+70%PHx**: ligation of right portal vein in combination with resection of left lateral and median lobes; **(ii) 70%PVL+20%PHx**: ligation of left portal vein in combination with liver resection of right lobe (Supplemental Figure 1).

Operative procedures and postoperative management

Surgical procedures were performed under inhalation of 3% isoflurane mixed with pure oxygen at a flow rate of 0.5L/min (isoflurane vaporizer, Sigma Delta, UK). Laparotomy was carried out via a transverse upper abdominal incision. PHx was performed using a modified technique from the precise vessel-oriented technique[15]. The portal vein, hepatic artery and bile duct of the respective lobe were ligated before resection to minimize the proliferation of the ischemic tissue in the stump. Resection of right lobe represented removal of 20% of the liver

mass, resection of left lateral lobe and median lobe represented 70%PHx. Both together represented 90%PHx. PVL was performed carefully under an operating microscope (Zeiss, magnification 10-25×, Germany). Ligation of right portal vein represented 20%PVL; ligation of left portal vein represented 70%PVL, while ligation of both right and left portal vein represented 90%PVL. All animals received analgesic treatment with buprenorphine in a dose of 0.05 mg/kg body weight (Temgesic, Essex Pharma GmbH, Germany). Daily assessment of activity was carried out. Animals in each group were harvested at four observation time points (postoperative day (POD) 1, 2, 3 and 7, n=6/group/time points). One hour before harvest, 5-bromo-2-deoxyuridine (BrdU, SIGMA-ALDRICH, St. Louis, USA) was injected via penile vein in a dose of 50 mg/kg body weight for revealing hepatocellular proliferation.

Liver enzymes

Blood was collected for measurement of serum aspartate aminotransferase (AST) and alanine aminotransferase (ALT) by using the AEROSET System (Abbott Laboratories, Wiesbaden, Germany) according to the instructions of the manufacturers.

Liver explantation, liver weight determination

Livers were mobilized for liver explantation and photodocumentation (Supplemental Figure 2). Individual liver lobes were weighed to calculate the liver weight/body weight ratio using the following formula: liver weight of individual lobe (g)/ body weight (g)*100%. Six additional rats were subjected to laparotomy to obtain normal values of liver weights and normal range of liver enzymes.

Immunohistochemistry (IHC)

Liver sections were cut after formalin fixation and paraffin embedding. BrdU-staining was performed using a monoclonal anti-BrdU antibody (Dako, Hamburg, Germany) following the protocol described previously[16]. The terminal deoxynucleotidyltransferase-mediated UTP end labeling (TUNEL) staining was performed using an Apoptag peroxidase in-situ apoptosis-detection kit (Intergen, Purchase, NY) according to the manufacturer's instructions.

Assessment of proliferation and apoptosis

The analysis of proliferation index (PI) was performed with a histological image analysis tool "Histokat" (Fraunhofer MEVIS, Bremen, Germany) as described previously[13]. The result was expressed as the fraction of proliferating hepatocyte nuclei to the total number of hepatocyte

nuclei (accurate to 0.1%). In contrast , apoptosis density was assessed manually by counting the number of TUNEL-positive cells per observation area (magnification 400-fold) in 10 fields per animal (given as cells/mm^2)[17]. PI was defined as high when it was more than 20%; PI was defined as moderate when it was less than 20% but more than 10%; PI was defined as low when it was less than 10%.

Visualization of portal blood supply

Additional 11 rats were subjected to portal vascular anatomy study using imaging technique. The portal blood supply of the remnant liver was visualized using an imaging approach before (n=1) as well as immediately and 7 days after operation (N=10). The imaging work flow followed the same protocol as described before[18]. Briefly, contrasting the vascular tree was achieved by injecting a silicone radiopaque contrast agent (Microfil; Flow Tech, Inc., Carver, Mass., USA) into the portal vein. Subsequently, the explanted liver were subjected to formalin fixation, and the specimens were scanned using the scan protocol HQD-6565-390-90 during one full rotation with a scanning time of 90s per subscan (TomoScope Duo CT; CT Imaging GmbH, Erlangen, Germany). Three-dimensional reconstruction of the vascular tree was performed using "Imalytics Preclinical" (Philips Research, Aachen, Germany).

Statistical analysis

The data, expressed as mean ±standard deviation (SD), were analyzed using SigmaPlot 13.0 (Statcon, Witzenhausen, Germany). Differences between paired groups were analyzed using the two-tailed paired samples Student's t-test and multiple groups were compared using the one way independent ANOVA test. Differences were considered statistically significant if p-values were less than 0.050.

Results:

Combination of small and moderate PVL and PHx caused less liver damage than extended 90%PHx.

All animals tolerated the surgical procedure well in respect to the severity of surgical stress (See Supplemental Table 1, displaying the levels of liver enzymes in relation to the surgical procedure). As expected, a small 20% PVL caused minor hepatic injury defined as ALT<250 IU/L and AST<500IU/L. In contrast, removal of 20% of the liver mass respectively ligating 70% or 90% of the liver mass caused moderate liver injury (250IU/L<ALT<750IU/L and 500IU/L<AST<1000IU/L). Removing 70% or 90% of the liver mass caused major hepatic

injury (ALT>750IU/L, AST>1000IU/L). In the combination groups the extent of resection determined the severity of the procedure.   Irrespectively of the surgical procedure, animals experienced maximal hepatic damage on POD 1 which recovered within 7 days.

Total liver weight recovery time correlated to the extent of PHx.

Partial hepatectomy: Total remnant liver weight and its recovery time correlated with the extent of PHx **(Figure 1A)**. The total liver/body weight ratio was 3.3% in unresected control animals. The remnant liver started to regain its weight from POD 1. Total liver weight recovered fully within 7 days after 20%PHx (vs. control, p=0.390) and almost fully after 70%PHx (vs. control, p =0.019).   In contrast 90%PHx, total liver weight did not recover fully comparing with the control liver weight after 7 days (vs. control, p<0.001).

Portal vein ligation: Total liver weight was maintained after 20% and 70%PVL by the timely balance of hepatic atrophy and hypertrophy, but not after 90%PVL. After 90%PVL, the total liver weight to body weight ratio decreased during the first 3 postoperative days, but recovered within 7 days (**Figure 1B**).   In this case, the ligated liver mass underwent severe atrophy at a faster pace than the regeneration of the small non-ligated lobe, leading to a decrease of relative total liver weight during three postoperative days.

Combination group: Total liver weight and its recovery correlated to the extent of PHx (**Figure 1C**). The recovery was slower comparing with the recovery after PHx only. This finding is in line with the transient loss of liver mass observed after 90%PVL.

The ligated liver lobes adjusted their size according to extent of PHx.

Portal vein ligation: The relative weight of ligated lobes decreased comparably to about 1/3 of the original liver weight after 20%PVL and 70%PVL only (see Figure 2A). In contrast, after 90%PVL atrophy was less pronounced. Atrophy of the left and median lobe reached 46% of the original liver whereas the right liver lobe only lost very little of its mass reaching 95% of the original liver weight (p<0.001).

Combination group: In contrast, the **ligated right lobe** in 20%PVL+70%PHx group did not decrease in weight, but increased steadily to almost 140% of the starting weight on POD 7 (see also previous study[13]) , which was significantly higher than the 95% relative liver weight observed after 90%PVL (p<0.001) (**Figure 2A**). In contrast, in case of 70%PVL+20%PHx, the relative weight of **ligated left lateral lobe (LLL) and median lobe (ML)** only decreased to 75% of the original value on POD 7, which was significantly less than the decrease to 46%

observed in the 90%PVL (p<0.001) **(Figure 2B)**. Therefore it seems that the weight adaptation of the ligated lobes may be related to the extent of resection: with a large resection leading to an overall increase in liver weight and a small resection leading to an overall decrease in liver weight, but less pronounced than after ligation only.

Hepatocyte proliferation in the ligated lobe was induced in case of additional PHx.

Partial hepatectomy: Hepatocyte proliferation occurred after hepatectomy and was related to the extent of liver resection (**Figure 3A).** The PI reached its peak on POD 1 with a maximum of 3%, 25% and 28% after 20%PHx, 70%PHx and 90%PHx respectively.

Portal vein ligation: As expected, the PI of the non-ligated caudate lobe was related to the extent of ligation (**Figure 3B**). 20%PVL only induced a maximal PI of 2%, whereas 70%PVL induced a maximal PI of 8% and 90%PVL induced an even higher PI of 12.2%. Only few proliferating hepatocyte were observed in the ligated lobe after PVL only, irrespectively of the extent of ligation (**Figure 3D**).

Combination group: In the ***non-ligated caudate lobe,*** moderate PI (about15%) without a defined peak was observed on POD 1 and POD 2 (**Figure 3C**). There was no significant difference of PI in the non-ligated lobes between the two combination groups (p>0.050). However, the PI was significantly higher on POD 2 and POD 3 after additional PHx than after 90%PVL only (p<0.001), accompanied by an enhanced liver weight recovery of the non-ligated caudate lobe on POD 7 (p=0.001and p=0.035) (Supplemental Figure 3).

Hepatocyte proliferation did occur also in the ***ligated lobes*** after additional liver resection with the peak on POD 2 (PI of 6.3% and 3.6% respectively) (**Figure 3D, F**). Notably, the PI of ligated lobes in both combination groups were more than 10-fold higher comparing with PI in PVL only groups (PI of 0.3%, p<0.001). Both observations together confirmed the induction of a proliferative response in the ligated lobes in case of the additional resection.

Apoptosis density in the ligated lobe was remarkably reduced in case of additional PHx.

Partial hepatectomy: Apoptosis was not observed after hepatectomy only (data not shown).

Portal vein ligation: Apoptosis was observed in the deportalized lobes after PVL only and reached a maximum on POD3. The apoptotic density was not clearly related to the extent of ligation. High apoptotic density (>26 cells/mm²) was observed in the right lobe after 20%PVL and on LLL after 70%PVL. However, 90%PVL resulted in a significantly lower apoptotic

density (3cells/mm^2 in RL and 14 cells/mm² in LLL, p<0.001) (**Figure 4A, B, C**). Rare single apoptotic cells were also observed in the non-ligated lobes (data not shown).

Combination group: Interestingly, we observed a reduced apoptotic density with a maximum on POD 3 on the ligated liver lobes. Reduction of apoptosis was very pronounced in right lobe after 20%PVL+70%PHx and reached only a maximum of 3 cells/mm², significantly lower comparing with 20%PVL group (27 cells/mm²; p<0.001) (**Figure 4A, C**).Similarly, reduction of apoptosis was also observed, but less pronounced in LLL after 70%PVL+20%PHx (14 cells/mm²), significantly lower comparing with 70%PVL group (31 cells/mm^2; p<0.001) (**Figure 4B, C**).

Taken together, the size increase or decrease of the portally-ligated lobe after the combined procedure seemed to be related to the extent of the additional liver resection. This was apparently not due to an induction of hepatocyte proliferation but rather a reduction of apoptosis in the ligated lobes. Since apoptosis is strongly influenced by the formation of porto-portal collaterals, we wanted to investigate collateral formation as reason for the reduced suppression of apoptosis, in other words the higher apoptosis rate, in case of the 20%PHx+70%PVL.

Formation of extrahepatic porto-portal collaterals was associated with prevention of atrophy of deportalized liver.

The visualization of the portal perfusion immediately after operation indicated that the portal vein ligation was well-performed, since no portal perfusion in the portally-ligated lobes was visible (data not shown). As expected, the visualization of portal perfusion on POD7 revealed that no obvious portal revascularization did occur in the normal liver and between the portal stem and the ligated portal branches after 20%PVL and 70%PVL (**Figure 5A, B, C**). Interestingly, 90%PVL seemed to induce extra-hepatic revascularization as indicated by a dense network of small collaterals (**Figure 5D**) and the clearly visible right portal vein tree respectively left portal vein tree supplying the LLL and the ML. However, formation of this dense network did not occur after performing a 20%PVL and simultaneous 70%PHx, leaving the right portal vein invisible (**Figure 5E**). However, collaterals between the stem of the portal vein and the LLL and the ML with the subsequent perfusion of the respective lobar portal vein became clearly visible after performing a 70%PVL and simultaneous 20%PHx (**Figure 5F**).

These findings suggest that on the one hand a large PVL can induce formation of collaterals and subsequent suppression of hepatic apoptosis. On the other hand, we observed that apoptosis can also be suppressed in case of an additional large resection even without formation of collaterals.

Discussion:

Intrahepatic liver size regulation is gaining attention from basic scientists as well as clinicians.

PHx and PVL have been adopted to treat liver tumors and metastases in clinic. Thus, understanding intrahepatic size regulation after liver resection and PVL is of high clinical relevance. Techniques to selectively control liver and liver lobe size could provide new chances for extended resection operations[19].

This study explores intrahepatic size regulation using a newly developed surgical model.

We asked the question how a given liver lobe may regulate its size when subjected to two concurrent stimuli of two different strength: Strong regeneration stimulus induced by performing a 70% PHx combined with weak atrophy stimulus induced by 20% PVL, respectively weak regeneration stimulus induced by 20% PHx combined with strong atrophy stimulus induced by 70% PVL.

We hypothesized that hepatocytes in the liver lobe receiving both signals may undergo either proliferation or apoptosis. The net balance would determine liver size in a stimulus dependent manner, since the control of proliferation and the regulation of cell death seems to be tightly connected[20].

Our results were in support of the hypotheses. We observed three phenomena: (1) The strong systemic regeneration stimulus counteracting the weak local atrophy stimulus caused an increase in liver lobe size. (2) In contrast, the weak regeneration stimulus counteracting the strong local atrophy stimulus resulted in a lower extent of liver size decrease. (3) Furthermore, the reduced atrophy of the deportalized lobe seemed to be related to the formation of extrahepatic collaterals.

Proliferation: These observations prompted speculations regarding an unknown sensing mechanism in the liver governing intrahepatic size regulation. After PHx the portal inflow to the remnant liver increases, accompanied by an increased metabolic load imposed on the remnant liver. We speculate that hepatocytes may possibly "sense" the metabolic overload,

resulting consequently in increased energy demand of the remnant liver. Nakatani described already in 1981 that PHx greatly increases demand for energy[21]. A similar study was performed by Ngala Kenda and colleagues [22]. In their study, the decrease in hepatic ATP energy charge, reflecting the increased energy demand, has been suggested to account for the early events involved in the initiation of DNA synthesis after PHx.

Apoptosis: Similarly we speculate that lack of nutrients and hormones from portal blood may be sensed as atrophy stimulus triggering hepatic apoptosis. It has been reported that the lack of insulin from the portal blood may contribute to hepatic apoptosis. The anti-apoptotic effects of insulin on normal hepatocytes were shown in vitro and in vivo by Bilodeau and colleagues[23]. In their in-vitro experiment, they applied insulin to transforming growth factor-beta-treated hepatocyte cultures and observed a decrease in apoptosis by 43%. In their in-vivo experiment, they applied insulin to the deportalized liver lobe and observed a five-fold decrease in the apoptotic index resulting in a higher liver weight of the atrophying liver lobe in comparison to control animals.

Collaterals: In consequence, the prevention of apoptosis indicated by the reduced apoptosis density may be related to formation of collaterals. The presence of extrahepatic collateral formation may explain the moderately reduced apoptosis density observed after 90%PVL and 20%PHx+70%PVL compared to the high apoptosis density observed after 20% and 70%PVL. Here apoptosis may have been prevented by the incomplete lack of nutrients. Our results demonstrated that extrahepatic collateral formation resembled collateral formation in case of extrahepatic portal hypertension[24]. Extrahepatic collateral formation was accompanied by a lower level of atrophy in deportalized liver. This indicated that collateral formation is not only reducing liver regeneration but also reducing hepatic atrophy.

Autophagy: However, in the absence of collateral formation, another mechanism must cause the suppression of apoptosis. In case of concurrent signals induced by large PHx and small PVL, the sustained proliferation in non-ligated as well as the low proliferation in the ligated lobe may not be sufficient to meet the metabolic need. We speculated that in this case a "rescue"-mechanism might kick in, which reduced hepatic apoptosis. It is well known that nutrient deprivation, in other words starvation, is inducing autophagy[25]. Therefore we wondered whether nutrient deprivation in the ligated lobe is inducing autophagy thereby preventing apoptosis.

The liver is essential for the maintenance of nutrients metabolism and energy homeostasis. After extended simultaneous PVL+PHx, the small remnant liver may not meet the energy demand. Particularly the portally-deprived liver lobe suffering from nutrient deprivation may have a reduced metabolic capacity due to starvation. Lack of nutrients may cause amino acid deprivation, adenosine triphosphate depletion and endoplasmic reticulum stress and may lead to starvation-induced autophagy in the ligated liver lobe[26].

Autophagy is a cellular protein degradation process that enables cells to recycle cytoplasmic components through degradation within lysosomes[27]. Autophagy protects tissues and cells against various types of cytotoxic stresses by inhibition of cellular apoptosis. Evidence is increasing that autophagy can cross-inhibit apoptosis[28]. Apoptosis is suggested to account for the atrophy of the portal blood-deprived liver lobes by activation of the mitochondrial and death receptor-mediated pathways[29]. Autophagy can also attenuate apoptosis inhibition by the extrinsic pathway of apoptosis[30].

Perspectives

Although sound and novel findings were observed in the present study, our study calls for consequent investigations of the underlying mechanism.

For further elucidation whether collateral formation is decisive for intrahepatic liver lobe size regulation, we propose a complementary experiment of 70%PV-embolization +20%PHx and 90% PV-embolization. PV-embolization will prevent formation of collaterals, observed in the present study, so that it can be used to investigate the role of collateral formation in balancing different signals as a controlled study.

For further elucidation regarding the role of autophagy in intrahepatic size regulation, we propose to investigate the autophagic activity in the regenerating and the atrophying lobe as a next step.

In conclusion, in case of concurrent PVL and PHx, the liver adjusted the size of the portally deprived lobe by the balance of liver regeneration and liver atrophy stimulus. The size of portally-deprived lobes was dependent on the extent of the additional regenerative stimulus. However, the additional hepatectomy induced a similar proliferative response of the portally ligated lobe, irrespectively of the extent of resection, but modulated apoptosis differently.

In case of minor PHx, apoptosis was suppressed to a lower extent thereby not leading to hypertrophy but to a mild atrophy of the portally deprived lobe. In case of additional major

PHx apoptosis was strongly suppressed causing mild hypertrophy of deportalized lobes, even in the absence of collateral formation.

Acknowledgments

Authors' Contribution

W.Wei, O.Dirsch and U.Dahmen contributed to conception and design; W.Wei, T.Zhang and U.Dahmen for analysis and interpretation; W.Wei, T.Zhang and S.Zafarnia for data collection; S.Zafarnia and F.Gremse for µCT-imaging and 3D-reconstruction; A.Homeyer for providing the histological analysis tool; W.Wei and T.Zhang for writing the article; O.Dirsch, U.Settmacher and U.Dahmen for critical revision of the article.

References

1. Dong J, Yang S, Zeng J, Cai S, Ji W, Duan W, Zhang A, Ren W, Xu Y, Tan J, Bu X, Zhang N, Wang X, Wang X, Meng X, Jiang K, Gu W, Huang Z. Precision in liver surgery. *SeminLiver Dis* 2013;**33**(3): 189-203.

2. Pulitano C, Castillo F, Aldrighetti L, Bodingbauer M, Parks RW, Ferla G, Wigmore SJ, Garden OJ. What defines 'cure' after liver resection for colorectal metastases? Results after 10 years of follow-up. *HPB (Oxford)* 2010;**12**(4): 244-249.

3. Wilms C, Mueller L, Lenk C, Wittkugel O, Helmke K, Krupski-Berdien G, Rogiers X, Broering DC. Comparative study of portal vein embolization versus portal vein ligation for induction of hypertrophy of the future liver remnant using a mini-pig model. *AnnSurg* 2008;**247**(5): 825-834.

4. Nagano Y, Nagahori K, Kamiyama M, Fujii Y, Kubota T, Endo I, Togo S, Shimada H. Improved functional reserve of hypertrophied contra lateral liver after portal vein ligation in rats. *JHepatol* 2002;**37**(1): 72-77.

5. Elias D, Ouellet JF, De Baere T, Lasser P, Roche A. Preoperative selective portal vein embolization before hepatectomy for liver metastases: long-term results and impact on survival. *Surgery* 2002;**131**(3): 294-299.

6. Tschuor C, Croome KP, Sergeant G, Cano V, Schadde E, Ardiles V, Slankamenac K, Claria RS, de Santibanes E, Hernandez-Alejandro R, Clavien PA. Salvage parenchymal liver transection for patients with insufficient volume increase after portal vein occlusion -- an extension of the ALPPS approach. *EurJSurgOncol* 2013;**39**(11): 1230-1235.

7. de Graaf W, van den Esschert JW, van Lienden KP, van Gulik TM. Induction of tumor growth after preoperative portal vein embolization: is it a real problem? *AnnSurgOncol* 2009;**16**(2): 423-430.

8. Serenari M, Cescon M, Cucchetti A, Pinna AD. Liver function impairment in liver transplantation and after extended hepatectomy. *World JGastroenterol* 2013;**19**(44): 7922-7929.

9. Stavrou GA, Donati M, Ringe KI, Peitgen HO, Oldhafer KJ. Liver remnant hypertrophy induction--how often do we really use it in the time of computer assisted surgery? *AdvMedSci* 2012;**57**(2): 251-258.

10. van Lienden KP, Hoekstra LT, Bennink RJ, van Gulik TM. Intrahepatic left to right portoportal venous collateral vascular formation in patients undergoing right portal vein ligation. *CardiovascInterventRadiol* 2013;**36**(6): 1572-1579.

11. Zhou Y, Xu JC, Jia YF, Xu CS. Role of death receptors in the regulation of hepatocyte proliferation and apoptosis during rat liver regeneration. *GenetMolRes* 2015;**14**(4): 14066-14075.

12. Kohler UA, Kurinna S, Schwitter D, Marti A, Schafer M, Hellerbrand C, Speicher T, Werner S. Activated Nrf2 impairs liver regeneration in mice by activation of genes involved in cell-cycle control and apoptosis. *Hepatology* 2014;**60**(2): 670-678.

13. Wei W, Zhang T, Fang H, Dirsch O, Schenk A, Homeyer A, Gremse F, Zafarnia S, Settmacher U, Dahmen U. Intrahepatic Size Regulation in a Surgical Model: Liver Resection-Induced Liver Regeneration Counteracts the Local Atrophy following Simultaneous Portal Vein Ligation. *EurSurgRes* 2016;**57**(1-2): 125-137.

14. Kilkenny C, Browne WJ, Cuthill IC, Emerson M, Altman DG. Improving bioscience research reporting: the ARRIVE guidelines for reporting animal research. *PLoSBiol* 2010;**8**(6): e1000412.

15.   Madrahimov N, Dirsch O, Broelsch C, Dahmen U. Marginal hepatectomy in the rat: from anatomy to surgery. *AnnSurg* 2006;**244**(1): 89-98.

16.   Wei W, Zhang T, Zafarnia S, Schenk A, Xie C, Kan C, Dirsch O, Settmacher U, Dahmen U. Establishment of a rat model: Associating liver partition with portal vein ligation for staged hepatectomy. *Surgery* 2016;**159**(5): 1299-1307.

17.   Eipel C, Hirschmann M, Abshagen K, Menger MD, Vollmar B. Local interaction of apoptotic hepatocytes and Kupffer cells in a rat model of systemic endotoxemia. *HepatolRes* 2007;**37**(10): 863-871.

18.   Gremse F, Doleschel D, Zafarnia S, Babler A, Jahnen-Dechent W, Lammers T, Lederle W, Kiessling F. Hybrid microCT-FMT imaging and image analysis. *JVisExp* 2015(100): e52770.

19.   Hohmann N, Weiwei W, Dahmen U, Dirsch O, Deutsch A, Voss-Bohme A. How does a single cell know when the liver has reached its correct size? *PLoSOne* 2014;**9**(4): e93207.

20.   Lauschke VM, Mkrtchian S, Ingelman-Sundberg M. The role of microRNAs in liver injury at the crossroad between hepatic cell death and regeneration. *BiochemBiophysResCommun* 2016.

21.   Nakatani T, Ozawa K, Asano M, Ukikusa M, Kamiyama Y, Tobe T. Differences in predominant energy substrate in relation to the resected hepatic mass in the phase immediately after hepatectomy. *JLab ClinMed* 1981;**97**(6): 887-898.

22.   Ngala Kenda JF, de Hemptinne B, Lambotte L. Role of metabolic overload in the initiation of DNA synthesis following partial hepatectomy in the rat. *EurSurgRes* 1984;**16**(5): 294-302.

23.   Bilodeau M, Tousignant J, Ethier C, Rocheleau B, Raymond VA, Lapointe R. Anti-apoptotic effect of insulin on normal hepatocytes in vitro and in vivo. *Apoptosis* 2004;**9**(5): 609-617.

24.   Sharma M, Rameshbabu CS. Collateral pathways in portal hypertension. *JClinExpHepatol* 2012;**2**(4): 338-352.

25.   Takagi A, Kume S, Kondo M, Nakazawa J, Chin-Kanasaki M, Araki H, Araki S, Koya D, Haneda M, Chano T, Matsusaka T, Nagao K, Adachi Y, Chan L, Maegawa H, Uzu T. Mammalian autophagy is essential for hepatic and renal ketogenesis during starvation. *SciRep* 2016;**6**: 18944.

26.   Russell RC, Yuan HX, Guan KL. Autophagy regulation by nutrient signaling. *Cell Res* 2014;**24**(1): 42-57.

27.   Mizushima N, Komatsu M. Autophagy: renovation of cells and tissues. *Cell* 2011;**147**(4): 728-741.

28.   Zhang L, Wang K, Lei Y, Li Q, Nice EC, Huang C. Redox signaling: Potential arbitrator of autophagy and apoptosis in therapeutic response. *Free RadicBiolMed* 2015;**89**: 452-465.

29.   Picard C, Starkel P, Sempoux C, Saliez A, Lebrun V, Horsmans Y. Molecular mechanisms of apoptosis in the liver of rats after portal branch ligation with and without retrorsine. *Lab Invest* 2004;**84**(5): 618-628.

30.   Marino G, Niso-Santano M, Baehrecke EH, Kroemer G. Self-consumption: the interplay of autophagy and apoptosis. *NatRevMolCell Biol* 2014;**15**(2): 81-94.
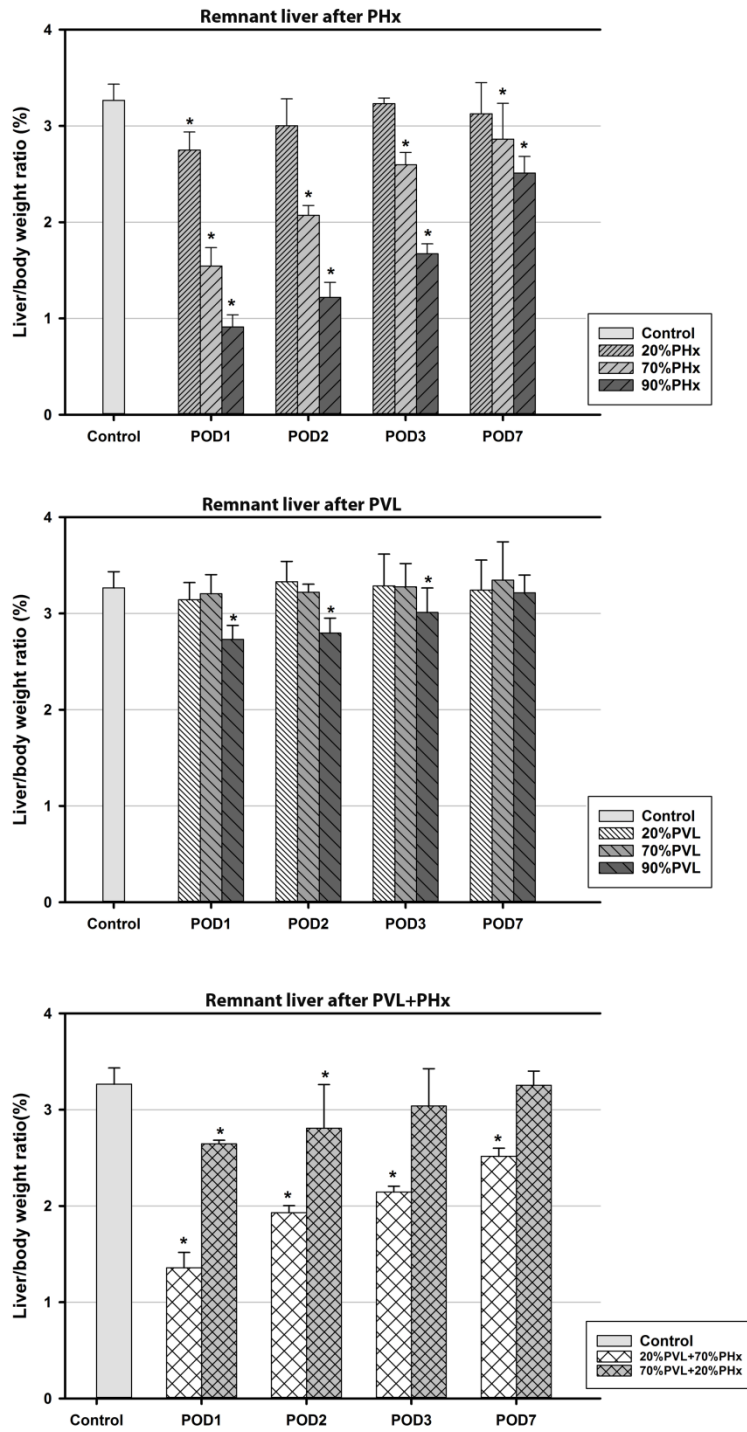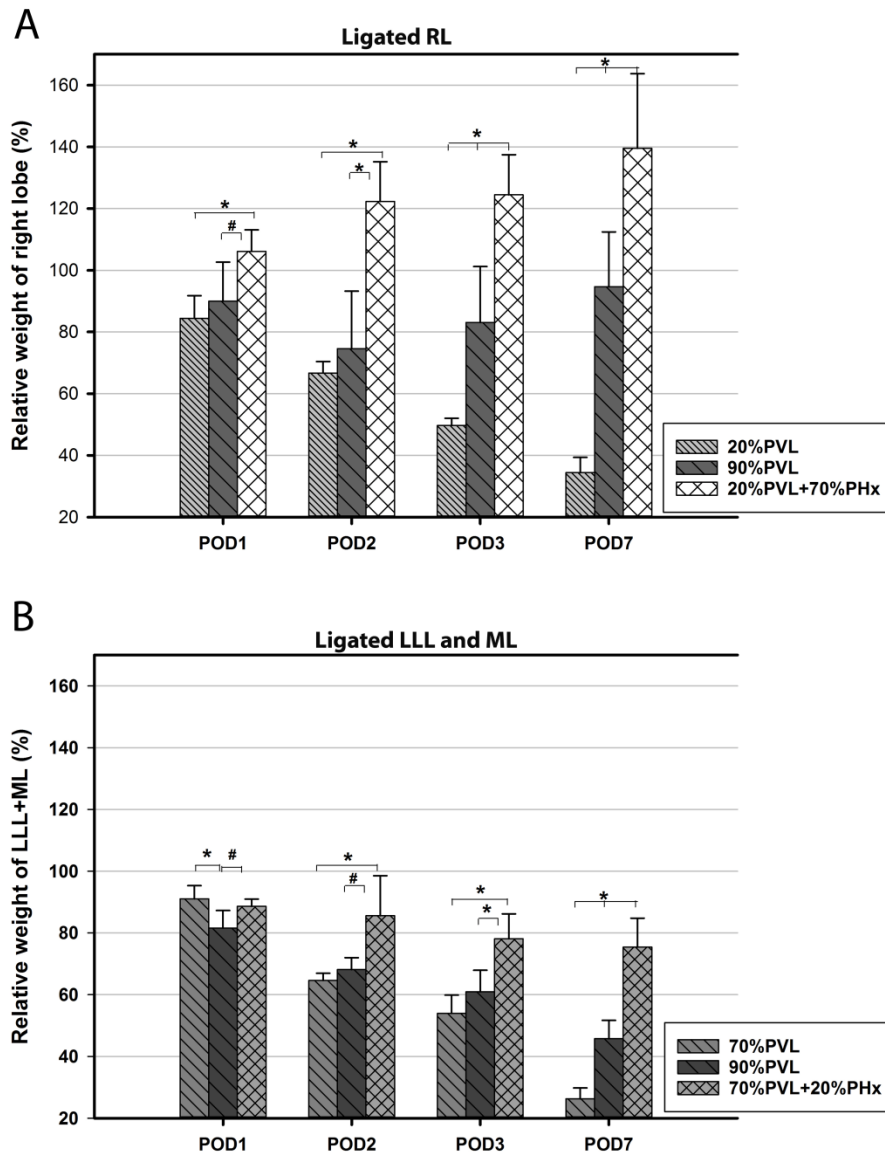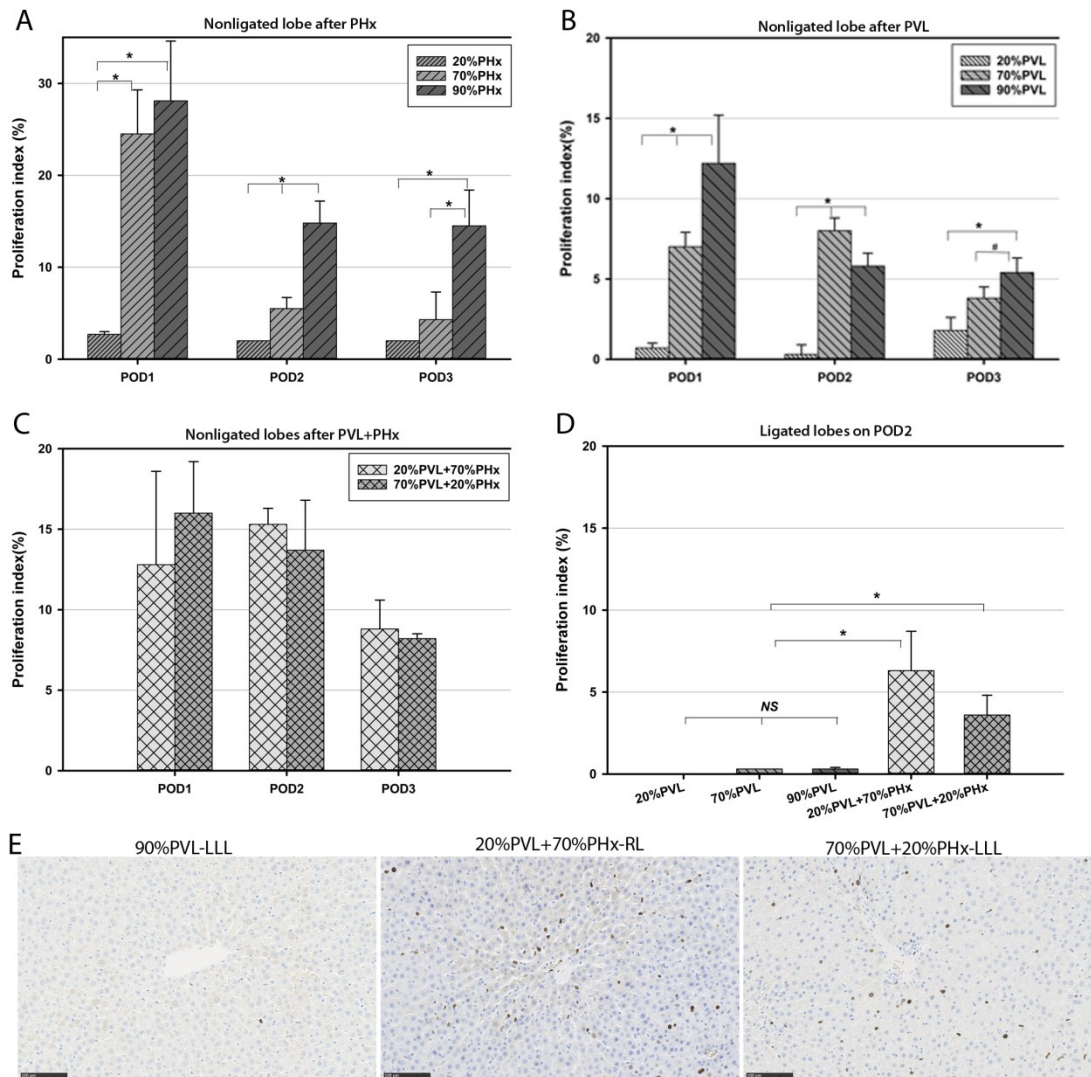
Figure 1

Figure 2

Figure 3

Figure 4
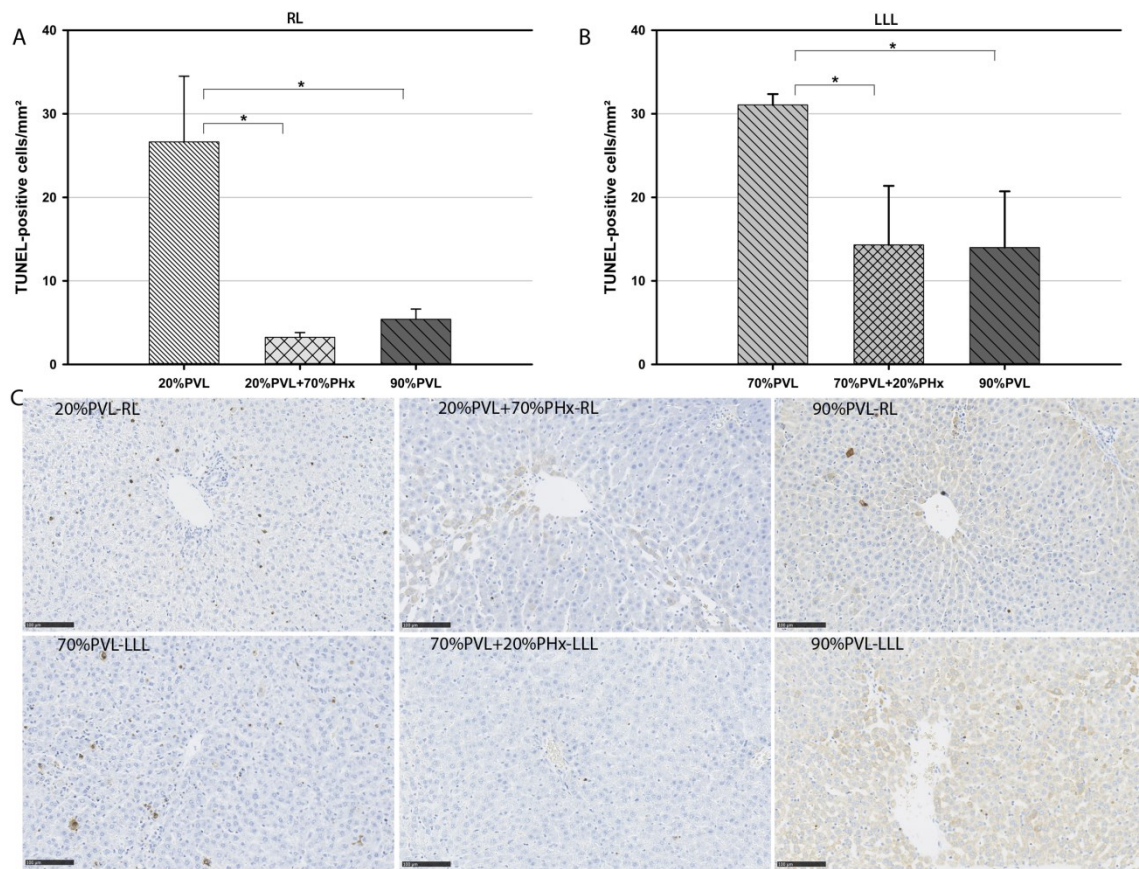
Figure 5

Supplemental Figure 1

normal

20%PVL+70%PHx

70%PVL+20%PHx

20%PHx

70%PHx

90%PHx

20%PVL

70%PVL

90%PVL
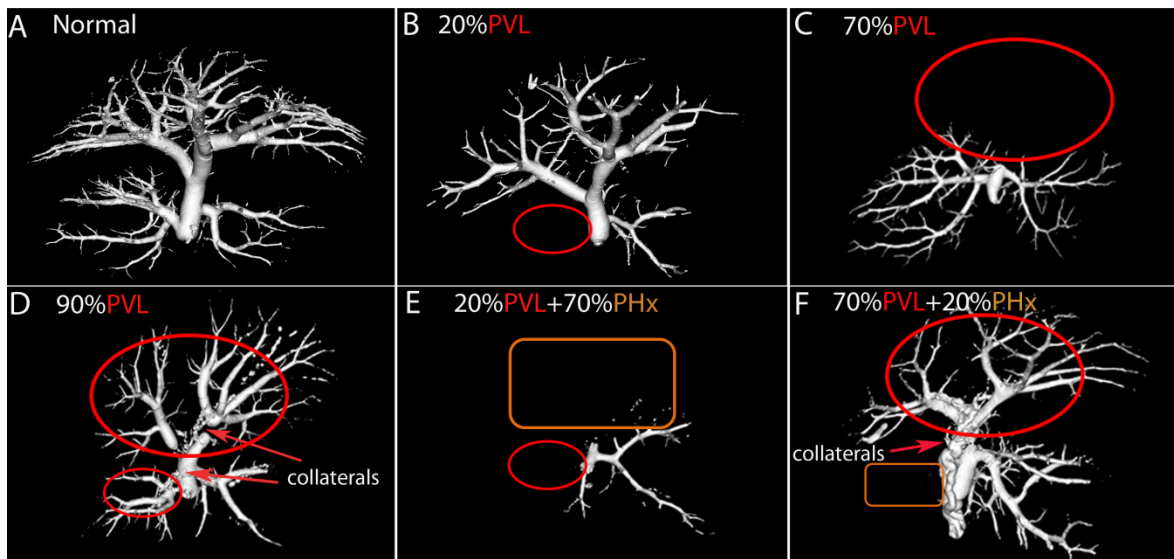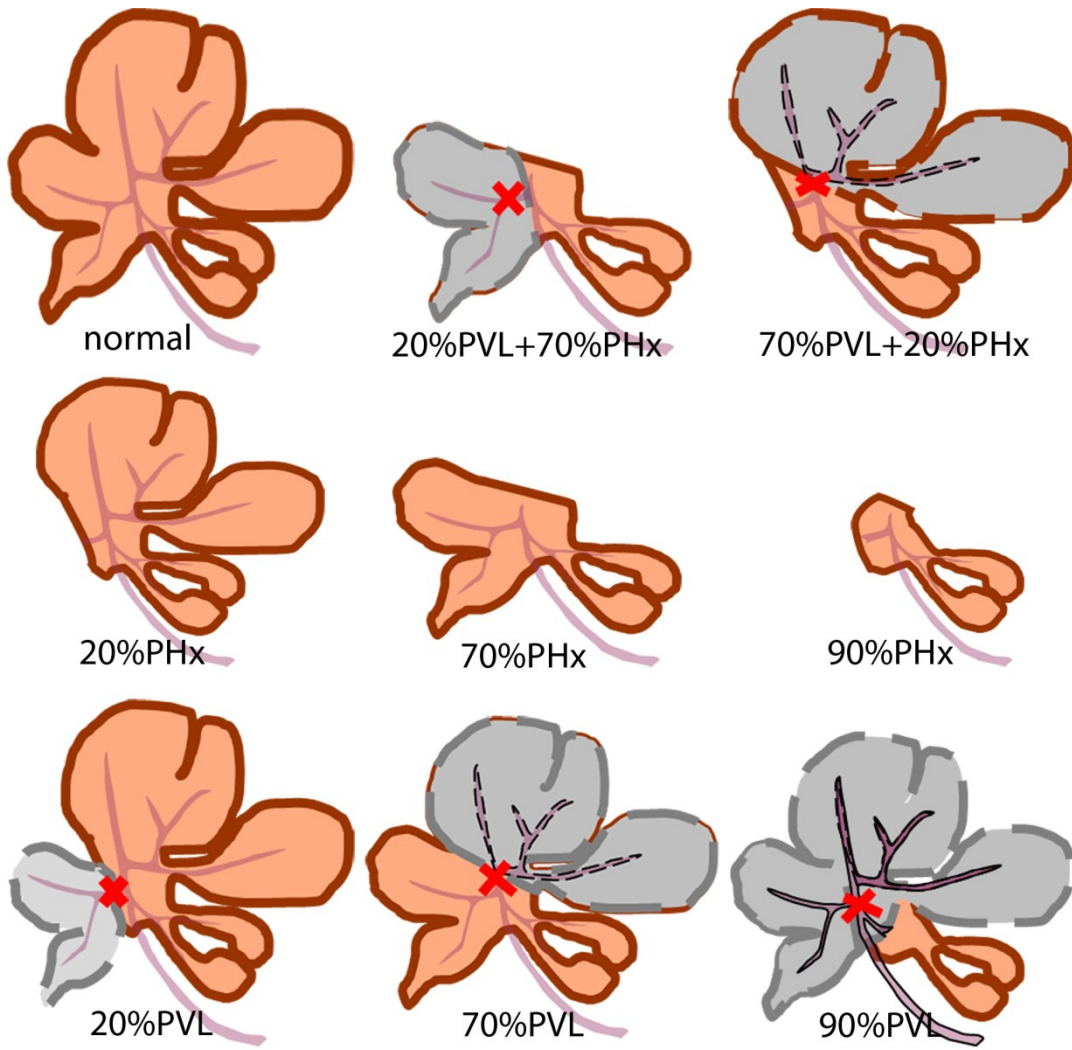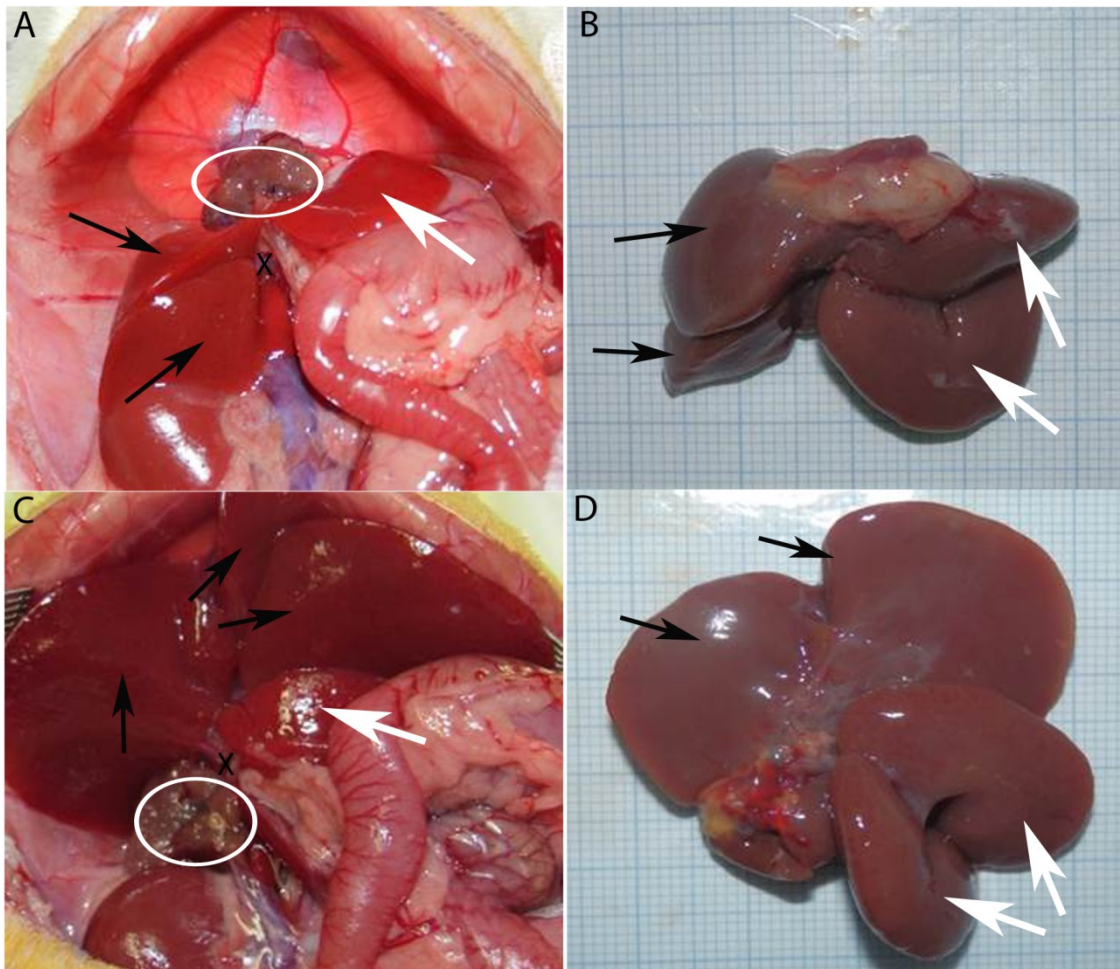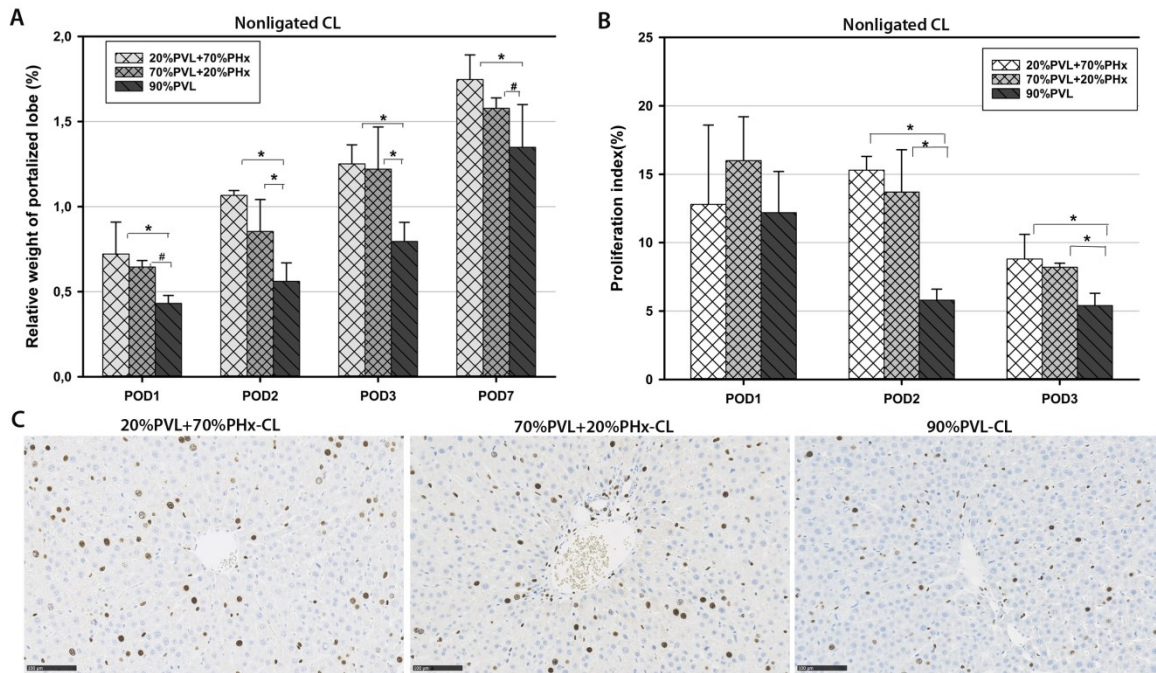
Supplemental Figure 2

Supplemental Figure 3

Supplemental Table 1

Supplemental Table 1. Level of surgical stress as indicated by the release of transaminases

Severity	Surgery	ALT (IU/L)				AST (IU/L)			
		POD 1	POD 2	POD 3	POD 7	POD 1	POD 2	POD 3	POD 7
Minor	20%PVL	106.8	68.8	52.0	42.8	429.4	129.4	100.6	90.6
Moderate	70%PVL	611.6	499.6	243.0	62.2	823.8	609.6	300.5	93.2
	90%PVL	745.0	164.0	257.4	85.6	963.1	274.7	330.0	114.4
	20%PHx	499.8	131.2	57.4	65.8	692.6	185.9	106.6	69.2
Major	70%PHx	1225.8	260.6	60.8	42.1	1360.3	377.6	102.0	73.8
	90%PHx	1422.9	896.7	260.2	72	2565.2	1310.2	484.0	102.0
	20%PVL+70%PHx	1383.4	334.0	112.6	40.1	1723.7	495.0	192.6	83.0
	70%PVL+20%PHx	934.6	522.9	123.1	49.2	1505.9	580.6	167.2	77.6

AST: alanine aminotransferase; AST: aspartate aminotransferase; Minor: ALT<250 IU/L and AST<500IU/L; Moderate: 250IU/L<ALT<750IU/L and 500IU/L<AST<1000IU/L; Major: ALT>750IU/L, AST>1000IU/L; Values: mean values.

Legends

Figure 1: Regulation of total liver/body weight ratio after partial hepatectomy (PHx) only, portal vein ligation (PVL) only and combined PVL+PHx. (**A**) The recovery time of total liver /body weight ratio was related to the extent of PHx. It was restored on POD 2 after 20%PHx, whereas it was not fully recovered on POD 7 after 70%PHx and 90%PHx (p<0.001). (**B**) The total liver /body weight ratio did not change after 20%PVL and 70%PVL. In contrast, it significantly decreased during the first 3 postoperative days after 90%PVL and recovered thereafter. There was no significant difference between 90%PVL and control value on POD 7 (p=0.627). (**C**) The recovery time of total liver /body weight ratio was also related to the extent of PHx. After 70%PVL+20%PHx the relative total liver weight was fully recovered on POD 3 (p=0.217). In contrast, the total liver weight after 20%PVL+70%PHx was not fully recovered even on POD 7 (p<0.001).

Figure 2: Liver size regulation of ligated liver lobes after portal vein ligation (PVL) only and combined PVL+PHx. The extent of atrophy on POD 7 was related to the extent of ligation and the extent of additional resection. (A) The ligated right lobe decreased to 34% after 20%PVL, whereas it increased to 140% after 20%PVL+70%PHx (p<0.001). (B) The ligated left lateral and median lobes decreased to 26%, and 46% of the original volume after 70%PVL and 90%PVL respectively. However, after the combined 70%PVL+20%PHx size of LLL+MLdecreased only to 75% of the original liver mass (p<0.001). (*:p<0.001, #:p<0.05)

Figure 3: Proliferation index (PI) after partial hepatectomy (PHx) only, portal vein ligation (PVL) only and combined PVL+PHx. (**A**) **PI of non-ligated lobes after PHx only:** After PHx, PI of the remnant liver peaked on POD 1 and reached a maximum of 3%, 25% and 28% after 20%PHx, 70%PHx and 90%PHx respectively; (**B**) **PI of non-ligated lobe after PVL only**: After 20%PVL the PI remained low (<2%) without a defined peak throughout the first three postoperative days. In contrast, after 70%PVL the peak of proliferation occured on POD 2 and reached a considerable maximal level of about 8%. Furthermore, after 90%PVL, the kinetic of proliferation was again different; the peak of proliferation occurred on POD 1 and reached a maximum of 12.2%; (**C**) **PI of non-ligated lobes in combination groups:** In both combination groups, there were no defined peaks of proliferation, but maximal PI ranging between 10% and 16% were observed on the first two postoperative days. (**D**) **PI of the ligated liver lobes after PVL only respectively in the combination**

groups: After PVL only, proliferation was absent after small 20% PVL and very low after 70% and 90%PVL (maximum PI of 0.3% on POD 2). In contrast, in both combination groups where an additional resection was performed, the PI of ligated lobe was more than 10-fold higher (4%-6% on POD 2) comparing with PI after PVL only. (*:p<0.001, #:p<0.050, NS: not significant). **(E) BrdU-staining of *ligated* right** or left lateral lobe (RL or LLL) on POD 2 after 90%PVL, 20%PVL+70%PHx and 70%PVL+20%PHx (scale marker:100μm, magnification:200×). Despite portal deprivation, proliferating cells were clearly visible in the ligated RL after 20%PVL+70%PHx respectively the LLL after 70%PVL+20%PHx.

Figure 4: Density of apoptotic cells in deportalized lobe on POD3. **After small to moderate PVL only,** density of apoptotic cells was high and ranged between 25-35 cells/mm^2 in left lateral (20%PVL, **A**) and right lobe (70% PVL, **B**). In contrast, **after large 90% PVL only**, density of apoptotic cells was significantly lower in the ligated lobes with 5 cells/mm^2 in RL respectively 14 cells/mm^2 in LLL (p<0.001); possibly due to the formation of collaterals as shown in Figure 5D. **In both combination groups**, density of apoptotic cells was as low as after 90%PVL, and seemed to be related to the extent of the additional resection. Density of apoptotic cells was very low in the ligated RL with 3 cells/mm^2 after small ligation and large resection (20%PVL+70%PHx). However, in this case no collaterals were abserved, see Figure 5E. Density of apoptotic cells was significantly higher and reached 14 cells/mm^2 in the LLL+ML after large ligation and small resection (70%PVL+20%PHx) (p<0.001). Here, collateral formation was clearly visible, see Figure 5F. **(C) TUNEL-staining** of deportalized right lobe (RL, upper panel) after 20%PVL, 20%PVL+70%PHx and 90%PVL, and TUNEL-staining of deportalized left lateral lobe (LLL, lower panel) after 70%PVL, 70%PVL+20%PHx and 90%PVL. After PVL only (left panel), abundant apoptotic cells were clearly visible, whereas after the combined procedure, only signal TUNEL-positive cells were visible (middle and right panel) (scale marker:100μm, magnification:200×)

Figure 5: Visualization of portal venous tree on POD7. (A) Normal portal venous tree. (**B, C**) After 20%PVL and 70%PVL no collaterals between portal stem and ligated lobar portal veins were observed. (**D**) However, after 90%PVL the ligated liver lobes were portally-perfused and extrahepatic portal collateral formation between portal stem and lobar portal veins was observed; (**E**) After 20%PVL+70%PHx the ligated right lobes were not portally-perfused indicating there was no formation of collaterals; (**F**) In

contrast, after 70%PVL+20%PHx obvious collateral formation was noticed and the ligated liver lobes were portally-perfused. (red arrow indicates collateral; red circle indicates portally-ligated lobe; orange rectangle indicates resected liver lobes)

Legends for Supplemental Figures

Supplemental Figure 1: Sketches of experimental groups. (red cross: portal vein ligation; grey colored lobes: deportalized lobes; orange colored lobes: portalized lobes)

Supplemental Figure 2: **Intraoperative images after combined portal vein ligation (PVL) and partial hepatectomy (PHx) of different extent** (**A, C**) and images of explanted livers on POD 7 to illustrate liver lobe size adjustment (**B, D**). (**A**) **Intraoperative situs after 20%PVL+70%PHx:** depicting portally deprived right lobes (black arrows) with darker red color after PVL (black cross) and stumps of left lateral and median lobes (white circle) after resection, and remnant caudate lobes with fresh red color (white arrow);(**B**) **Explanted liver after 20%PVL+70%PH on POD7:** demonstrating the **discrete hypertrophy** of the deportalized right lobe (black arrows) and the substantial 4-fold increase in size of the regenerating caudate lobes (white arrows); (**C**) **Intraoperative situs after 70%PVL+20%PHx:** depicting portally deprived left lateral and median lobes (black arrows) with darker red color after PVL (black cross) and stumps of right lobes (white circle), and remnant caudate lobes with fresh red color (white arrow); (**D**) **Explanted liver after 70%PVL+20%PHx on POD7**: demonstrating **discrete atrophy** of left lateral and median lobes (black arrows) and the substantial 4-fold increase in size of the regenerating caudate lobes (white arrows)

Supplemental Figure 3: **Size regulation of portalized caudate lobe** (**A**) At all observation time points the **relative weight of portalized lobe** was significantly higher after both combined procedures compared to 90%PVL only. (**B**) **Proliferation index** (PI) ranging between 13% and 16% was observed on POD 1 in all three groups ($p > 0.050$). Thereafter (POD 2 and 3), the PI in both combination groups remained significantly higher as after 90%PVL only, ($p < 0.001$). Both observations together suggest an increased regenerative response in case of the additional resection. (*:$p < 0.001$, #:$p < 0.05$). (**C**) **BrdU-staining of *non-ligated* caudate lobe** (CL) on POD2 after 20%PVL+70%PHx, 70%PVL+20%PHx and 90%PVL. Density of Brdu-marked proliferating cells in both combination groups (left and middle image) much higher than after 90%PVL only (right image). (scale marker:100μm, magnification:200×).

Discussion

Liver regeneration has been and is being studied using various experimental models. Partial hepatectomy (PHx) is the most frequently used surgical model to study liver regeneration. The small liver remnant undergoes full volume and functional regeneration within 7-14 days. However, in clinical routine, extended liver resection is not always possible due to a presumingly insufficient size of the future liver remnant. Therefore, PVL was developed to enhance regeneration prior to extended resection.

However, this concept does not always lead to success; the future liver remnant does not always undergo sufficient volume and functional regeneration. Up to now, it is not well explored how liver regeneration is regulated, especially not how the individual liver lobes adjust their size after resection or portal vein ligation. Further research is needed to better understand this process of intrahepatic size regulation.

We investigated two interrelated factors influencing intrahepatic size regulation: the effect of vascular remodeling in terms of collateral formation and the effect of simultaneously applied concurrent signals.

First we gained an overview about current techniques to explore liver regeneration, especially the imaging techniques to demonstrate the hepatic vascular system (Manuscript I, published). We generated an ALPPS model and confirmed that prevention of collateral formation by parenchymal transection accelerated liver regeneration (Manuscript II, published). We observed that the PHx induced regeneration stimulus prevented hepatic atrophy of deportalized liver lobe by inducing hepatocyte proliferation (Manuscript III, published). We learned that inhibition of atrophy in the deportalized liver lobe was associated with down-regulation of hepatic apoptosis, which was inversely correlated to the strength of the regenerative stimulus induced by PHx (Manuscript IV, submitted).

Modern technologies enable visualization of collaterals

Contrasting the vascular tree was achieved by injecting a silicone radiopaque contrast agent (Microfil; Flow Tech, Inc.) into the portal vein. The explanted liver was subjected to Micro-CT (TomoScope Duo CT; CT Imaging GmbH). The data from micro-CT was subjected to 3D reconstruction using "Imalytics preclinic" (Philips Research) and "HepaVison" (Fraunhofer Institute for Medical Image Computing MEVIS).

Both programs allow the visualization of the topographic vascular anatomy of the liver. Imalytics preclinic and HepaVision enable free rotation of the vascular tree and optimal demonstration of the intrahepatic and extrahepatic collateral formation after PVL. In addition, HepaVison allows determination of hepatic volume and volume of territories of lobes, visualization of collaterals and determination of vascular parameter and therefore vascular growth in liver regeneration (Xie et al. 2016).

However, there are still limitations when using the imaging technologies: one being the low resolution of the µCT imaging device (70µm) which renders visualization of very small vessels like the sinusoidal network of the remnant liver impossible; the other being the need for applying the silicone polymer for contrasting the vessels. This contrast medium crystallizes in the vessels and can only be used in explanted livers, rendering the repetitive imaging of the vascular tree within the same animal impossible.

Development of novel contrast media allowing in-vivo imaging of the rat liver at high resolution is needed to overcome these limitations.

Role of collaterals in size regulation: Prevention of collateral formation accelerates liver regeneration

Formation of interlobe porto-portal neocollaterals after PVL is considered to be one of major factors reducing the extent of hypertrophy in the FLR (Riehle et al. 2011). This prompted the development of the ALPPS-procedure to prevent the formation of porto-portal collaterals. The key step of this procedure is the trans-section of hepatic parenchyma after ligating the portal vein. Prevention of PV-collateralization is achieved by placing a mechanical barrier between the transected liver lobes (Tanaka et al. 2015).
In addition to preventing formation of collaterals, liver transection also causes a traumatic stimulus, which may contribute to the accelerated hypertrophy of FLR (Gall et al. 2015). Schlegel came up with the speculation of a circulating growth factor induced by surgical injury. In their study, surgical injuries to spleen, kidney or lung induced comparable liver regeneration after PVL like ALPPS (Schlegel et al. 2014). The authors therefore concluded that a systemic growth factor rather than preventing the formation of porto-portal collaterals was essential for the observed accelerated liver regeneration after ALPPS. Unfortunately, they did not investigate size development of the deportalized lobe after ALPPS procedure.

Our study questioned this point of view. It seems unlikely that the postulated systemic growth factor induces accelerated hypertrophy of the portalized lobe and augmented atrophy of deportalized lobe at the same time. In our study, prevention of porto-portal collateral formation after ALPPS led to enhanced hypertrophy of FLR and enhanced atrophy of the ligated lobe compared to that after PVL without liver transection. Our study did not address the role of eventual systemic growth factors. However, the key role of preventing collateral formation cannot be denied.

It is also tempting to consider the controversially discussed role of hypoxia for accelerated regeneration. On the one hand, hypoxia after PVL is considered to act as stimulus for regeneration. On the other hand, increasing oxygen supply via arterialization of PV after hepatectomy is apparently enhancing regeneration.

In ALPPS model with 70%PVL, the parenchymal transection prevents collateral formation between portalized lobe and deportalized lobe leading to hyperperfusion of the regenerating lobe. In response to portal hyperperfusion, hepatic arterial flow to the regenerating lobe should decrease accordingly to maintain the constant hepatic sinusoidal inflow (Lautt 2007, Lautt 1985). Schadde observed that the decreased arterial flow was causing hypoxia (indicated by pimonidazole staining) in the regenerating liver; the hypoxia subsequently accelerated liver regeneration after portal deprivation (Schadde et al. 2016). The observation of Kron supported this view (Kron et al. 2016). He observed significant hypoxia during liver regeneration, also indicated by Pimonidazol staining. They further demonstrated that hypoxia-driven Hif2a activation promoted hepatocytes mitosis.

In contrast to these observations, other studies suggest that the reduced oxygen supply would be detrimental to liver regeneration, albeit after 70%PHx (Eipel et al. 2010). Nardo reported that portal vein arterialization increased O2 partial pressure and oxygen saturation in the portal vein and enhanced the BrdU-proliferation rate by 3-fold. (Nardo et al. 2006). Li also demonstrated that portal vein arterialization promoted liver regeneration after extended hepatectomy in a rat model (Li et al. 2015).

This debate requires further experiments to define the role of oxygen and hypoxia for accelerating or decreasing live regeneration, possibly by exploring the role of portal vein arterialization in intrahepatic size regulation after the ALPPS procedure. These experiments would improve our understanding of liver regeneration and contribute to the optimized performance of ALPPS.

Regeneration stimulus prevents the hepatic atrophy of deportalized liver lobe by inducing hepatocyte proliferation.

Portal vein blood is considered to be essential for liver regeneration (van Lienden et al. 2013). Currently two mechanisms regarding the relevance of portal vein blood are discussed. The hemodynamic theory suggests that the increased portal blood flow resulting in an elevated shear stress is the driving force for liver regeneration after PHx and PVL (Um et al. 1994, Schoen et al. 2001). Furthermore, PHx and portal vein occlusion results to metabolic overload as well as an increased hormonal supply from the gut to the non-deprived remnant liver lobe, both leading to the hypertrophy of the portalized lobe (Wilms et al. 2008). However, our study regarding intrahepatic size regulation rejects the essential role of portal inflow for liver regeneration.

Our results demonstrated that liver regeneration can be induced in portally-deprived liver lobes within the first week, albeit following a different kinetics. This was in line with Kollmar's finding. He also observed cell proliferation in the portal blood-deprived liver tissue, but only in the late phase. In his study the expression of PCNA was detected on day 14 after PVL (Kollmar et al. 2007).

Without any evidence of porto-portal collateral formation, we could speculate about the role of arterial flow to the deprived lobe in priming hepatocyte proliferation.

Portal hypertension after PHx is considered to reduce hepatic arterial inflow to the remnant liver because of the hepatic arterial buffer response (**HABR),** described by Lautt in 1985 (Lautt 1985). A controversial finding has been reported by Dold who observed that portal hyperperfusion after PHx (30%, 70% and 90%PHx) did not induce an adaptive hepatic arterial constriction because of nitric oxide release (Dold et al. 2015). However, the author also emphasized that "the lack of HABR after major hepatectomy despite portal hyperperfusion may not necessarily disprove the HABR theory". The nitric oxide release may counteract the HABR by dilating the hepatic artery (Macedo und Lautt 1998).

The HABR was also investigated after 70%PVL (Gock et al. 2011). Gock reported an unchanged sinusoidal blood flow in the sinusoids, although the liver underwent portal deprivation. This observation implied an elevated arterial inflow to the deportalized lobes. Applying those studies to the analysis of our observations, one might speculate that arterial inflow to the deprived right lobes may increase massively because of the additional liver resection. However, we did not yet provide experimental evidence. The

increased arterial flow due to the additional resection may cause a substantially elevated shear stress, possibly triggering liver regeneration, even in the deportalized lobe.

However, liver regeneration followed a different time course with a delayed peak occurring only at 48h. The prolonged course of regeneration in the portally deprived liver lobe is possibly related to the lack of nutrients normally supplied by the portal blood, needed to meet the energy demand of the proliferating hepatocytes.

Further elucidation of the underlying mechanism would call for additional experiments with a detailed examination if hepatic hemodynamics on the level of the remnant liver, but also on the level of the lobar vessels. However, this is technically currently unfeasible due to the lack of required very small sensors to measure lobar inflow directly (Schadde et al. 2016).

The regenerative stimulus governs the size regulation of the deportalized liver by determining hepatic apoptosis.

PHx induces hepatocyte proliferation leading to hypertrophy the liver remnant, whereas PVL-induced apoptosis leads to atrophy of the deportalized liver (Zhou et al. 2015). The control of cell proliferation and the regulation of cell death are tightly connected (Lauschke et al. 2016). We wondered how size regulation was affected when applying the two concurrent stimuli of varying strength.

Our study results revealed that the net balance of the two stimuli determined liver lobe size and directed the lobe to undergo either hypertrophy or atrophy or to keep its size. The strong systemic regeneration stimulus counteracted the local atrophy stimulus strongly leading to an increase in liver lobe size. In contrast, the moderate regeneration stimulus counteracted against the local atrophy stimulus only moderately leading to a lower decrease of liver size compared to PVL only.

We reported as **key finding** that hepatic apoptosis was dramatically reduced in the deportalized lobe, when it was subjected to an additional liver resection representing a regeneration stimulus. Extent of reduction was related to the resected liver mass, in other words to the "strength" of the regeneration stimulus. This may be essential for the size regulation of the deportalized lobes and important for intrahepatic size regulation of the whole liver.

Our study revealed that the hepatic apoptosis seemed to be counteracted by extrahepatic collateral formation. Our results demonstrated that the extrahepatic collateral formation was similar to collateral formation during portal hypertension (Sharma und Rameshbabu 2012, Kamel et al. 2004). It was noteworthy that the formation of collaterals was accompanied by a lower level of atrophy in deportalized liver when compared to the situation without collateral formation. This indicated that collateral formation was determining hepatic atrophy also in this situation, possibly due to suppression of hepatic apoptosis. Collateral formation could contribute to redistribution of hepatic inflow blood after PVL. Redistribution of blood flow may normalize the nutrient distribution and oxidative homeostasis in the deprived lobe leading to a partial restoration of metabolic capacity and modulating apoptosis related pathway (mitochondrial and death receptor-mediated pathways) (Lee et al. 1999).

For further elucidation whether the extrahepatic collateral formation is decisive for intrahepatic liver lobe size regulation, we propose a complementary experiment of 70% portal vein embolization (PVE) combined with 20%PHx, respectively a 90% PVE. PVE will prevent formation of intra- and extrahepatic collateral formation, so that it can be used to investigate the role of collateral formation in balancing different signals as a controlled study.

However, when performing small ligation together with a large resection, we did not observe collateral formation. In this case we speculated that another mechanism must be responsible for the observed reduction in apoptosis. In the case of concurrent signals induced by large PHx and small PVL, the sustained proliferation in non-ligated as well as the low proliferation in the ligated lobe may not be sufficient to meet the metabolic need. Particularly the portally-deprived liver lobe suffering from nutrient deprivation may have a reduced metabolic capacity, partly due to the lack of nutrients provided by the portal blood leading to starvation. Nutrient starvation may cause amino acid deprivation, ATP depletion and endoplasmic reticulum stress and may lead to starvation-induced autophagy in the deprived liver lobe. Evidence is increasing that autophagy influences recycling of mitochondria and can thus modulate hepatic apoptosis in mitochondrial pathway (Wang 2014). **Autophagy** can also attenuate apoptosis by selectively reducing cytoplasmic pro-apoptotic proteins in death receptor-mediated pathways (Marino et al. 2014).

For further elucidation regarding the role of autophagy in intrahepatic size regulation, we propose to investigate the autophagic activity in the regenerating and the atrophying lobe as a next step.

In conclusion, our studies provide novel and interesting surgical findings regarding intrahepatic size regulation. Our results challenge the widely assumed paradigm that portal deprivation leads to hepatic atrophy and prevents liver regeneration. Further work is needed to understand the underlying molecular mechanisms.

References

Abdalla EK, Barnett CC, Doherty D, Curley SA, Vauthey JN. 2002. Extended hepatectomy in patients with hepatobiliary malignancies with and without preoperative portal vein embolization. ArchSurg, 137 (6):675-680.

Abulkhir A, Limongelli P, Healey AJ, Damrah O, Tait P, Jackson J, Habib N, Jiao LR. 2008. Preoperative portal vein embolization for major liver resection: a meta-analysis. AnnSurg, 247 (1):49-57.

Asencio JM, Garcia Sabrido JL, Olmedilla L. 2014. How to expand the safe limits in hepatic resections? JHepatobiliaryPancreatSci, 21 (6):399-404.

Dahm F, Georgiev P, Clavien PA. 2005. Small-for-size syndrome after partial liver transplantation: definition, mechanisms of disease and clinical implications. AmJTransplant, 5 (11):2605-2610.

de Graaf W, van den Esschert JW, van Lienden KP, van Gulik TM. 2009. Induction of tumor growth after preoperative portal vein embolization: is it a real problem? AnnSurgOncol, 16 (2):423-430.

Denys AL, Abehsera M, Sauvanet A, Sibert A, Belghiti J, Menu Y. 1999. Failure of right portal vein ligation to induce left lobe hypertrophy due to intrahepatic portoportal collaterals: successful treatment with portal vein embolization. AJR AmJRoentgenol, 173 (3):633-635.

Dimitroulis D, Tsaparas P, Valsami S, Mantas D, Spartalis E, Markakis C, Kouraklis G. 2014. Indications, limitations and maneuvers to enable extended hepatectomy: current trends. World JGastroenterol, 20 (24):7887-7893.

Dold S, Richter S, Kollmar O, von Heesen M, Scheuer C, Laschke MW, Vollmar B, Schilling MK, Menger MD. 2015. Portal Hyperperfusion after Extended Hepatectomy Does Not Induce a Hepatic Arterial Buffer Response (HABR) but Impairs Mitochondrial Redox State and Hepatocellular Oxygenation. PLoSOne, 10 (11):e0141877.

Eipel C, Abshagen K, Vollmar B. 2010. Regulation of hepatic blood flow: the hepatic arterial buffer response revisited. World JGastroenterol, 16 (48):6046-6057.

Fausto N, Campbell JS, Riehle KJ. 2006. Liver regeneration. Hepatology, 43 (2 Suppl 1):S45-S53.

Gall TM, Sodergren MH, Frampton AE, Fan R, Spalding DR, Habib NA, Pai M, Jackson JE, Tait P, Jiao LR. 2015. Radio-frequency-assisted Liver Partition with Portal vein ligation (RALPP) for liver regeneration. AnnSurg, 261 (2):e45-e46.

Giglio MC, Giakoustidis A, Draz A, Jawad ZA, Pai M, Habib NA, Tait P, Frampton AE, Jiao LR. 2016. Oncological Outcomes of Major Liver Resection Following Portal Vein Embolization: A Systematic Review and Meta-analysis. AnnSurgOncol.

Glantzounis GK, Tokidis E, Basourakos SP, Ntzani EE, Lianos GD, Pentheroudakis G. 2016. The role of portal vein embolization in the surgical management of primary hepatobiliary cancers. A systematic review. EurJSurgOncol.

Gock M, Eipel C, Linnebacher M, Klar E, Vollmar B. 2011. Impact of portal branch ligation on tissue regeneration, microcirculatory response and microarchitecture in portal blood-deprived and undeprived liver tissue. MicrovascRes, 81 (3):274-280.

Hayashi S, Baba Y, Ueno K, Nakajo M, Kubo F, Ueno S, Aikou T, Komokata T, Nakamura N, Sakata R. 2007. Acceleration of primary liver tumor growth rate in embolized hepatic lobe after portal vein embolization. Acta Radiol, 48 (7):721-727.

Higgins GM. 1931. Experimental pathology of the liver. Arch Pathol, 12:186-202.

Hoekstra LT, van Lienden KP, Doets A, Busch OR, Gouma DJ, van Gulik TM. 2012. Tumor progression after preoperative portal vein embolization. AnnSurg, 256 (5):812-817.

Kamel IR, Lawler LP, Corl FM, Fishman EK. 2004. Patterns of collateral pathways in extrahepatic portal hypertension as demonstrated by multidetector row computed tomography and advanced image processing. JComputAssistTomogr, 28 (4):469-477.

Kollmar O, Corsten M, Scheuer C, Vollmar B, Schilling MK, Menger MD. 2007. Portal branch ligation induces a hepatic arterial buffer response, microvascular remodeling, normoxygenation, and cell proliferation in portal blood-deprived liver tissue. AmJPhysiol GastrointestLiver Physiol, 292 (6):G1534-G1542.

Kron P, Linecker M, Limani P, Schlegel A, Kambakamba P, Lehn JM, Nicolau C, Graf R, Humar B, Clavien PA. 2016. Hypoxia-driven Hif2a coordinates mouse liver regeneration by coupling parenchymal growth to vascular expansion. Hepatology, 64 (6):2198-2209.

Lam VW, Laurence JM, Johnston E, Hollands MJ, Pleass HC, Richardson AJ. 2013. A systematic review of two-stage hepatectomy in patients with initially unresectable colorectal liver metastases. HPB (Oxford), 15 (7):483-491.

Lauschke VM, Mkrtchian S, Ingelman-Sundberg M. 2016. The role of microRNAs in liver injury at the crossroad between hepatic cell death and regeneration. BiochemBiophysResCommun.

Lautt WW. 1985. Mechanism and role of intrinsic regulation of hepatic arterial blood flow: hepatic arterial buffer response. AmJPhysiol, 249 (5 Pt 1):G549-G556.

Lautt WW. 2007. Regulatory processes interacting to maintain hepatic blood flow constancy: Vascular compliance, hepatic arterial buffer response, hepatorenal reflex, liver regeneration, escape from vasoconstriction. HepatolRes, 37 (11):891-903.

Lee FY, Li Y, Zhu H, Yang S, Lin HZ, Trush M, Diehl AM. 1999. Tumor necrosis factor increases mitochondrial oxidant production and induces expression of uncoupling protein-2 in the regenerating rat liver. Hepatology, 29 (3):677-687.

Li J, Cai C, Guo H, Guan X, Yang L, Li Y, Zhu Y, Li P, Liu X, Zhang B. 2015. Portal vein arterialization promotes liver regeneration after extended partial hepatectomy in a rat model. JBiomedRes, 29 (1):69-75.

Macedo MP, Lautt WW. 1998. Shear-induced modulation of vasoconstriction in the hepatic artery and portal vein by nitric oxide. AmJPhysiol, 274 (2 Pt 1):G253-G260.

Mailey B, Truong C, Artinyan A, Khalili J, Sanchez-Luege N, Denitz J, Marx H, Wagman LD, Kim J. 2009. Surgical resection of primary and metastatic hepatic malignancies following portal vein embolization. JSurgOncol, 100 (3):184-190.

Makuuchi M, Thai BL, Takayasu K, Takayama T, Kosuge T, Gunven P, Yamazaki S, Hasegawa H, Ozaki H. 1990. Preoperative portal embolization to increase safety of major hepatectomy for hilar bile duct carcinoma: a preliminary report. Surgery, 107 (5):521-527.

Marino G, Niso-Santano M, Baehrecke EH, Kroemer G. 2014. Self-consumption: the interplay of autophagy and apoptosis. NatRevMolCell Biol, 15 (2):81-94.

Michalopoulos GK. 2007. Liver regeneration. JCell Physiol, 213 (2):286-300.

Michalopoulos GK, DeFrances MC. 1997. Liver regeneration. Science, 276 (5309):60-66.

Mueller L, Grotelueschen R, Meyer J, Vashist YK, Abdulgawad A, Wilms C, Hillert C, Rogiers X, Broering DC. 2003. Sustained function in atrophying liver tissue after portal branch ligation in the rat. JSurgRes, 114 (2):146-155.

Nardo B, Puviani L, Caraceni P, Pacile V, Bertelli R, Beltempo P, Cavallari G, Chieco P, Pariali M, Pertosa AM, Angiolini G, Domenicali M, Neri F, Prezzi D, Tsivian M, Bernardi M,

Cavallari A. 2006. Portal vein arterialization for the treatment of post resection acute liver failure in the rat. TransplantProc, 38 (4):1185-1186.

Riehle KJ, Dan YY, Campbell JS, Fausto N. 2011. New concepts in liver regeneration. JGastroenterolHepatol, 26 Suppl 1:203-212.

Schadde E, Tsatsaris C, Swiderska-Syn M, Breitenstein S, Urner M, Schimmer R, Booy C, Z'graggen BR, Wenger RH, Spahn DR, Hertl M, Knechtle S, Diehl AM, Schlapfer M, Beck-Schimmer B. 2016. Hypoxia of the growing liver accelerates regeneration. Surgery.

Schlegel A, Lesurtel M, Melloul E, Limani P, Tschuor C, Graf R, Humar B, Clavien PA. 2014. ALPPS: From Human to Mice Highlighting Accelerated and Novel Mechanisms of Liver Regeneration. AnnSurg, 260 (5):839-847.

Schleimer K, Stippel DL, Kasper HU, Tawadros S, Allwissner R, Gaudig C, Greiner T, Holscher AH, Beckurts KT. 2006. Portal hyperperfusion causes disturbance of microcirculation and increased rate of hepatocellular apoptosis: investigations in heterotopic rat liver transplantation with portal vein arterialization. TransplantProc, 38 (3):725-729.

Schnitzbauer AA, Lang SA, Goessmann H, Nadalin S, Baumgart J, Farkas SA, Fichtner-Feigl S, Lorf T, Goralcyk A, Horbelt R, Kroemer A, Loss M, Rummele P, Scherer MN, Padberg W, Konigsrainer A, Lang H, Obed A, Schlitt HJ. 2012. Right portal vein ligation combined with in situ splitting induces rapid left lateral liver lobe hypertrophy enabling 2-staged extended right hepatic resection in small-for-size settings. AnnSurg, 255 (3):405-414.

Schoen JM, Wang HH, Minuk GY, Lautt WW. 2001. Shear stress-induced nitric oxide release triggers the liver regeneration cascade. NitricOxide, 5 (5):453-464.

Serenari M, Cescon M, Cucchetti A, Pinna AD. 2013. Liver function impairment in liver transplantation and after extended hepatectomy. World JGastroenterol, 19 (44):7922-7929.

Sharma M, Rameshbabu CS. 2012. Collateral pathways in portal hypertension. JClinExpHepatol, 2 (4):338-352.

Stavrou GA, Donati M, Ringe KI, Peitgen HO, Oldhafer KJ. 2012. Liver remnant hypertrophy induction--how often do we really use it in the time of computer assisted surgery? AdvMedSci, 57 (2):251-258.

Tanaka K, Matsuo K, Murakami T, Kawaguchi D, Hiroshima Y, Koda K, Endo I, Ichikawa Y, Taguri M, Tanabe M. 2015. Associating liver partition and portal vein ligation for staged hepatectomy (ALPPS): short-term outcome, functional changes in the future liver remnant, and tumor growth activity. EurJSurgOncol, 41 (4):506-512.

Um SH, Nishida O, Tokubayashi M, Kimura F, Takimoto Y, Yoshioka H, Inque R, Kita T. 1994. Hemodynamic changes after ligation of a major branch of the portal vein in rats: comparison with rats with portal vein constriction. Hepatology, 19 (1):202-209.

van Lienden KP, Hoekstra LT, Bennink RJ, van Gulik TM. 2013. Intrahepatic left to right portoportal venous collateral vascular formation in patients undergoing right portal vein ligation. CardiovascInterventRadiol, 36 (6):1572-1579.

Wang K. 2014. Molecular mechanisms of hepatic apoptosis. Cell DeathDis, 5:e996.

Wilms C, Mueller L, Lenk C, Wittkugel O, Helmke K, Krupski-Berdien G, Rogiers X, Broering DC. 2008. Comparative study of portal vein embolization versus portal vein ligation for induction of hypertrophy of the future liver remnant using a mini-pig model. AnnSurg, 247 (5):825-834.

Xie C, Schwen LO, Wei W, Schenk A, Zafarnia S, Gremse F, Dahmen U. 2016. Quantification of Hepatic Vascular and Parenchymal Regeneration in Mice. PLoSOne, 11 (8):e0160581.

Xu X, Man K, Zheng SS, Liang TB, Lee TK, Ng KT, Fan ST, Lo CM. 2006. Attenuation of acute phase shear stress by somatostatin improves small-for-size liver graft survival. Liver Transpl, 12 (4):621-627.

Zhou Y, Xu JC, Jia YF, Xu CS. 2015. Role of death receptors in the regulation of hepatocyte proliferation and apoptosis during rat liver regeneration. GenetMolRes, 14 (4):14066-14075.

Acknowledgment

Sincerely thanks **Anding Liu**, my dear colleague from "Experimental Medicine Center, Tongji Hospital, Tongji Medical College of Huazhong University of Science and Technology", for his constructive comments at the beginning of the project, also for the warm help in the living here. It was really important for me.

Sincerely thanks my kind colleagues **Isabel Jank** for manuscript revision and ordering, **Kathrin Schulz and Stephanie Lange for histological staining**, **Dr.Claudia Schindler** and **Bianca Göhrig** for animal-related work, **Juliana Neumann** and **Ulrike Vetterling** for measurement of clinical chemistry, **Janine Arlt** for assisting operating the software for analysis, **Dr. Franziska Mußbach** and **Elke Oswald** for their comments on sample collection. Their valuable help and technique support were important throughout the years. I would not have finished my work without their warm help in the past few years.

Last but not least, I would like to thank my lovely wife and colleague **Tianjiao Zhang** for her great support and assistance both in living and work. I would never be successful without her love and encouragement. She has also supported me in data collection, in analysis of the results and the interpretation, in manuscript writing and revision during the past two years.

Ehrenwörtliche Erklärung

Hiermit erkläre ich, dass mir die Promotionsordnung der Medizinischen Fakultät der Friedrich-Schiller-Universität bekannt ist,

ich die Dissertation selbst angefertigt habe und alle von mir benutzten Hilfsmittel, persönlichen Mitteilungen und Quellen in meiner Arbeit angegeben sind,

mich folgende Personen bei der Auswahl und Auswertung des Materials sowie bei der Herstellung des Manuskripts unterstützt haben: Tianjiao Zhang, Haoshu Fang, Andrea Schenk, André Homeyer, Anna Lawson Mclean, Chichi Xie, Chunyi Kan, Felix Gremse, Michael Schwier, Olaf Dirsch, Sara Zafarnia, Uta Dahmen und Utz Settmacher

die Hilfe eines Promotionsberaters nicht in Anspruch genommen wurde und dass Dritte weder unmittelbar noch mittelbar geldwerte Leistungen von mir für Arbeiten erhalten haben, die im Zusammenhang mit dem Inhalt der vorgelegten Dissertation stehen,

dass ich die Dissertation noch nicht als Prüfungsarbeit für eine staatliche oder andere wissenschaftliche Prüfung eingereicht habe und

dass ich die gleiche, eine in wesentlichen Teilen ähnliche oder eine andere Abhandlung nicht bei einer anderen Hochschule als Dissertation eingereicht habe.

Ort, Datum Unterschrift des Verfassers

Scientific Achievement

Publikationen:

1. Zhang T, <u>Wei W</u>, Dirsch O, Krüger T, Kan C, Xie C, Kniemeyer O, Fang H, Settmacher U, Dahmen U. Identification of Proteins Interacting with Cytoplasmic High-Mobility Group Box 1 during the Hepatocellular Response to Ischemia Reperfusion Injury. Int J Mol Sci. 2017 Jan 16;18(1). IF:3.226

2. Xie C, Schwen LO, <u>Wei W</u>, Schenk A, Zafarnia S, Gremse F, Dahmen U. Quantification of Hepatic Vascular and Parenchymal Regeneration in Mice. PLoS One. 2016 Aug 5;11(8). IF:2.806

3. Xie C, <u>Wei W</u>, Schenk A, Schwen LO, Zafarnia S, Schwier M, Gremse F, Jank I, Dirsch O, Dahmen U. Visualization of Vascular and Parenchymal Regeneration after 70% Partial Hepatectomy in Normal Mice. J Vis Exp. 2016 Sep 13;(115). IF:1.2319

4. <u>Wei W</u>, Zhang T, Fang H, Dirsch O, Schenk A, Homeyer A, Gremse F, Zafarnia S, Settmacher U, Dahmen U. Intrahepatic Size Regulation in a Surgical Model: Liver Resection-Induced Liver Regeneration Counteracts the Local Atrophy following Simultaneous Portal Vein Ligation. Eur Surg Res. 2016 Jun 17;57(1-2):125-137. IF:1.154

5. <u>Wei W</u>, Zhang T, Zafarnia S, Schenk A, Xie C, Kan C, Dirsch O, Settmacher U, Dahmen U. Establishment of a rat model: Associating liver partition with portal vein ligation for staged hepatectomy. Surgery. 2016 May;159(5):1299-307. IF:3.38

6. Sänger C, Schenk A, Schwen LO, Wang L, Gremse F, Zafarnia S, Kiessling F, Xie C, <u>Wei W</u>, Richter B, Dirsch O, Dahmen U. Intrahepatic Vascular Anatomy in Rats and Mice-Variations and Surgical Implications. PLoS One. 2015 Nov 30;10(11):e0141798. IF:3.057

7. <u>Wei W</u>, Dirsch O, Lawson Mclean A, Zafarnia S, Schwier M, Dahmen U, Rodent Models and Imaging Techniques to Study Liver Regeneration. Eur Surg Res 2015;54:97-113. IF:2.474

8. Schwen LO, <u>Wei W</u>, Gremse F, Ehling J, Wang L, Dahmen U, Preusser T. Algorithmically generated rodent hepatic vascular trees in arbitrary detail. J Theor Biol. 2015 Jan 21;365:289-300. IF:2.049

9. Liu A, Fang H, <u>Wei W</u>, Dirsch O, Dahmen U. Ischemic Preconditioning Protects Against Liver Ischemia/Reperfusion Injury via Heme Oxygenase-1-Mediated Autophagy. Crit Care Med. 2014 Dec;42(12):e762-71. IF:6.312

10. Xie C, <u>Wei W</u>, Zhang T, Dirsch O, Dahmen U. Monitoring of systemic and hepatic hemodynamic parameters in mice. J Vis Exp. 2014 Oct 4;(92). IF:1.325

11. Liu A, Fang H, <u>Wei W</u>, Kan C, Xie C, Dahmen U, Dirsch O. G-CSF pretreatment aggravates LPS-associated microcirculatory dysfunction and acute liver injury after partial hepatectomy in rats. Histochem Cell Biol. 2014 Jul 25. IF:3.054

12. Hohmann N, <u>Wei W</u>, Dahmen U, Dirsch O, Deutsch A, Voss-Böhme A. How does a single

cell know when the liver has reached its correct size? PLoS One. 2014 Apr 1;9(4). IF:3.232

13. Dahmen U, Sänger C, Wurst C, Arlt J, <u>Wei W</u>, Dondorf F, Richter B, Settmacher U, Dirsch O. Video-based self-control in surgical teaching. A new tool in a new concept. Chirurg. 2013 Oct;84(10):851-8.

14. Wei WW, Wu JH, Cao ZX. [Effect of closed high-pressure suction drainage on primary healing of perineal wound after abdominoperineal resection for rectal cancer]. Zhonghua Wei Chang Wai Ke Za Zhi. 2012 Apr;15(4):367-9.

Vorträge:

1. Personal experiences with new training concept in establishment of rat liver transplantation. Amsterdan, ESSR 2017, 52th Congress of the European Society for Surgical Research

2. Establishment of ALPPS model in rats. Prague, ESSR 2016, 51th Congress of the European Society for Surgical Research

3. Glucose metabolism during intrahepatic size regulation after simultaneous portal vein ligation and liver resection. Liverpool, ESSR 2015, 50th Golden Anniversary Congress of the European Society for Surgical Research

4. Establishment of Portal vein ligation + In situ splitting model in rat. Wien, ESSL 2015, (50th)The International Liver Congress

5. How to increase the size of the future remnant liver: Lessons learnt from animal models of portal vein ligation. Munich, DGCH 2015, 132.Kongress Deutsche Gesellschaft für Chirurgie

6. Reevaluation of Rats' Hepatic Vascular Anatomy – Getting Ready for ALLPS model. Mannheim, DTG 2014, 23.Jahrestagung der Deutschen Transplantationsgesellschaft

7. Regulation of liver lobe size with contradictory signals. Budapest, ESSR2014, The 49th Congress of the European Society for Surgical Research

8. Regulation of liver lobe size in case of concurrent contradictory signals. Frankfurt, DTG2013, 22.Jahrestagung der Deutschen Transplantationsgesellschaft